VYSOKÉ UČENÍ TECHNICKÉ V BRNĚ

BRNO UNIVERSITY OF TECHNOLOGY

FAKULTA STROJNÍHO INŽENÝRSTVÍ
ENERGETICKÝ ÚSTAV

FACULTY OF MECHANICAL ENGINEERING
ENERGY INSTITUTE

MODERN DENITRIFICATION METHODS OF COAL FIRED BOILERS

MODERNÍ METODY DENITRIFIKACE UHELNÝCH KOTLŮ

DIPLOMOVÁ PRÁCE
MASTER'S THESIS

AUTOR PRÁCE — Bc. JIŘÍ NÁROVEC
AUTHOR

VEDOUCÍ PRÁCE — doc. Ing. ZDENĚK SKÁLA, CSc.
SUPERVISOR

BRNO 2015

Vysoké učení technické v Brně, Fakulta strojního inženýrství

Energetický ústav
Akademický rok: 2014/15

ZADÁNÍ DIPLOMOVÉ PRÁCE

student(ka): Bc. Jiří Nárovec

který/která studuje v **magisterském studijním programu**

obor: **Energetické inženýrství (2301T035)**

Ředitel ústavu Vám v souladu se zákonem č. 111/1998 o vysokých školách a se Studijním a zkušebním řádem VUT v Brně určuje následující téma diplomové práce:

Moderní metody denitrifikace uhelných kotlů

v anglickém jazyce:

Modern denitrification methods of coal fired boilers

Stručná charakteristika problematiky úkolu:

Uhelné elektrárny patří k významným producentům elektrické energie v České republice a v Evropské unii. Vzhledem k nové evropské legislativě platné od 1. ledna 2016 je nutné, aby všechny jednotky splňovaly nové emisní limity. Největších změn dosahují emisní limity oxidů dusíku (NOx). Z tohoto důvodu je tato práce zaměřena na denitrifikaci uhelných kotlů.

Cíle diplomové práce:

Cílem této práce je denitrifikace hnědouhelného kotle PG 640 provozovaného ve 200MW bloku elektrárny Počerady. Jednotlivé cíle práce jsou následující:
- Zpracovat odbornou rešerši moderních metod denitrifikace uhelných kotlů.
- Pro zadání konkrétní jednotky uhelného kotle dále zpracovat:
o Ekonomickou rozvahu investičních nákladů sekundárních metod SNCR, SCR.
o Dle investičních nákladů, dispozice a možností instalace stanovit vhodnou sekundární denitrifikační metodu.
o Na základě zadání připravit podklady pro technickou specifikaci poptávky příslušné denitrifikační metody.
- Na závěr srovnat výše uvedené denitrifikační metody z hlediska investičních nákladů, složitosti instalace a dosažitelné účinnosti denitrifikace. Na základě srovnání stanovit obecnou vhodnost instalace SNCR a SCR ve stávajících uhelných jednotkách.

Seznam odborné literatury:

BUDAJ, Florian. Parní kotle: Podklady pro tepelný výpočet. 4. vydání. Brno: Nakladatelství VUT Brno, 1992. 200 s. ISBN 80-214-0426-4.

BASU, P.,C. KEFA a L. JESTIN. Boilers and Burners: Design and Theory. New York: Springer –Verlag New York, 2000. 563 s. ISBN 0-387-98703-7.
SPLIETHOFF, Hartmut. Power Generation from Solid Fuels. Springer-Verlag Berlin Heidelberg 2010. 672 s. ISBN 978-3-642-02855-7.
SEIKAN, Ishigai. Steam Power Engineering: Thermal and hydraulic design principles. Cambridge University Press, 1999. 349 s. ISBN 978-0-521-62635-4.

Vedoucí diplomové práce: doc. Ing. Zdeněk Skála, CSc.

Termín odevzdání diplomové práce je stanoven časovým plánem akademického roku 2014/15.

V Brně dne 10. 3. 2015

L.S.

VYSOKÉ UČENÍ TECHNICKÉ V BRNĚ
FAKULTA STROJNÍHO INŽENÝRSTVÍ
DĚKANÁT

doc. Ing. Jiří Pospíšil, Ph.D.
ředitel ústavu

doc. Ing. Jaroslav Katolický, Ph.D.
děkan

ABSTRAKT

V současnosti musí velké energetické podniky k dodržení emisních předpisů, zejména pak vyžadovaných limitů NO_x, uplatňovat denitrifikační metody. Tématem předkládané diplomové práce jsou moderních denitrifikační metody a jejich praktické uplatnění v lokálních poměrech uhelného kotle s parním výkonem 640 $t.h^{-1}$ v elektrárně Počerady. Práce obsahuje rešerši moderních denitrifikačních metod používaných velkými uhelnými kotli se zaměřením zejména na sekundární denitrifikační metody. Jsou uvažovány dvě možné varianty denitrifikace – varianta 1 využívá selektivní katalytickou redukci (SCR) a varianta 2 selektivní nekatalytickou redukci (SNCR) společně s nízkoemisními hořáky a stupňovaným přívodem spalovacího vzduchu. Pro výběr vhodné denitrifikační metody jsou studovány investiční náklady jednotlivých variant – nižší investiční náklady (o 19.4%) slibuje varianta 2. Při srovnávání SCR se SNCR vyšlo najevo, že investiční náklady metody SNCR jsou 5krát nižší než metody SCR. V souladu s investičními náklady, s dispozicí kotle a se složitostí jeho instalace je pro navazující studium problematiky využita varianta 2. Stěžejní část práce se zabývá stanovením optimálního tzv. teplotního okna pro konkrétní metodu SNCR. Těžištěm práce je tepelný výpočet ohniště a části deskového přehříváku pro stanovený rozsah paliv a výkon kotle v rozmezí 60-100%. S uvažováním výsledků z výpočtu jsou navrženy dvě vstřikovací roviny, které mají zaručit vysokou efektivitu denitrifikačního procesu při uvažovaných provozních podmínkách kotle. Diplomová práce rovněž diskutuje obecnou vhodnost instalace SNCR a SCR ve stávajících uhelných kotlích.

ABSTRACT

To fulfil strict NO_x emission limits for large combustion plants it is nowadays necessary to equip existing boilers with denitrification techniques. This master's thesis deals with denitrification of the existing 640 $t \cdot h^{-1}$ coal-fired boiler in Počerady power plant. The thesis contains background research of modern denitrification methods focused especially on secondary denitrification methods. Two variants for denitrification of the boiler are studied – variant 1 uses selective catalytic reduction (SCR) and variant 2 selective non-catalytic reduction (SNCR) supported by low NO_x burners and over-fire air technology. An economic analysis of investment costs is carried out to find the suitable variant – variant 2 promises lower investment costs (by 19.4%). When comparing only SCR with SNCR, the SNCR method has 5 times lower investment costs. In accordance with investment costs, boiler dispositions and the difficulty of the installation, the second variant is chosen for further study. The next fundamental part of the thesis comprises the determination of suitable position for SNCR process. The determination contains a thermal calculation of the furnace and platen superheater for the fuel range within the load range of 60-100% of boiler maximum continuous rating (BMCR). According to the results of the calculation, two injecting levels of reagent were designed to ensure high effectiveness of the process within the considered boiler conditions. The last part of the thesis compares general applicability of SCR and SNCR installation in existing coal-fired boilers.

KLÍČOVÁ SLOVA

- denitrifikace, selektivní katalytická redukce (SCR), selektivní nekatalytická redukce (SNCR)

KEY WORDS

- denitrification, selective catalytic reduction (SCR), selective non-catalytic reduction (SNCR)

BIBLIOGRAPHIC CITATION

NÁROVEC, J. *Modern denitrification methods of coal fired boilers.* Brno: Brno University of Technology, Faculty of Mechanical Engineering, 2015. (78 pages). Supervisor doc. Ing. Zdeněk Skála, CSc.

DECLARATION

I declare that I have written the master's thesis *Modern denitrification methods of coal fired boilers* on my own according to advices of my master's thesis supervisor doc. Ing. Zdeněk Skála, CSc. and external expert Ing. Milan Houdek, and using the sources listed in references.

Brno, 25th May 2015 ……..

Jiří Nárovec

ACKNOWLEDGMENTS

I would like to express thanks to my master's thesis supervisor doc. Ing. Zdeněk Skála, CSc. and external expert Ing. Milan Houdek for numerous comments and valuable suggestions on improving my thesis.

Jiří Nárovec

CONTENTS

1 INTRODUCTION

Nowadays electricity is a daily part of our modern society. Energy needs are growing fast in many parts of the world. When countries want to improve their economy (i.e., increase their gross domestic product) it is usually connected with a simultaneous increase in energy demand. The International Energy Agency (IEA) predicts that global energy demands will rise 37% by 2040. In much of Europe, Japan, Korea and North America is it foreseen that energy demands will stagnate, while energy consumption of other regions will rise. (1)

The energy mix[1] of countries depends on many factors such as geographical location, accessible energy sources, economy, technology etc. Coal-fired power plants belong and in future decades (1) will still belong among mainly used electricity producers. In the last decades there has been significant pressure toward reduction of greenhouse-gas emissions (due to the 1997 Kyoto Protocol), which are emitted in large scale by coal-fired power plants. In spite of the fact that many countries are looking for more environmentally friendly energy sources, coal-fired power plants will still be widely used in the following years. Due to these facts the European Union requires adherence to regulations, which are being more restrictive. These regulations force the power plants to implement new technologies to meet strict emission limits. One of the limitations is the emission level of nitrogen oxides (NO_x). Denitrification methods have to be applied in coal-fired power plants to decrease the amount of emitted NO_x. (2)

This master's thesis deals with modern denitrification methods of coal-fired boilers and focuses on denitrification of 640 $t \cdot h^{-1}$ coal-fired boiler located in the 5×200 MW Počerady power plant, Czech Republic. The main part of the work is classified into the four following major sections, namely, denitrification of coal-fired boilers (chapter 3.1); considered variants for boiler denitrification (chapter 3.2); a detailed design of the chosen denitrification method (chapter 3.3); and comparison of SCR and SNCR methods (chapter 3.4). A suitable denitrification method for the above-mentioned boiler is selected in accordance with investment costs, disposition and installation possibilities. The principal part of the thesis is a thermal calculation of the furnace and platen superheater to determine a proper position for the denitrification process. A general applicability of installation of secondary denitrification methods in existing coal-fired power plants is discussed at the end of the work.

[1] The energy mix can be defined according to Alain Grandjean (48) as "*the distribution of primary energy sources consumed to produce various types of energy used in a given country*".

2 AIMS OF WORK

The main objective of this thesis is denitrification of the Počerady power plant's lignite coal-fired boiler PG 640 (640 $t \cdot h^{-1}$). The particular tasks are as follows:

1) Develop a background research of modern denitrification methods of coal-fired boilers.
2) For the above-stated unit:
    - Assess investment costs of secondary denitrification methods (selective non-catalytic reduction (SNCR) and selective catalytic reduction (SCR)).
    - Determine a suitable secondary denitrification method according to the investment costs, disposition and installation possibilities.
    - Prepare process data for technical specification of selected denitrification method.
3) Compare the above-mentioned denitrification methods in terms of investment costs, installation possibilities and achievable denitrification effectivity. On the basis of the comparison determine general applicability of SNCR/SCR installation in existing coal-fired boilers.

Further detailed data for the calculation are described in Appendix A.

3 DESCRIPTION OF CURRENT STUDY

3.1 Denitrification of coal-fired boilers

3.1.1 Nitrogen oxides

3.1.1.1 Origin of NO_x in air

When talking about NO_x, we usually mean nitrogen monoxide (NO) and nitrogen dioxide (NO_2). We can also classify other substances such as N_2O, N_2O_3 and N_2O_5 as NO_x, but these substances are usually present in minor quantities (3 p. 100). NO_2 is mainly formed by oxidation of NO in the atmosphere. The oxidation process occurs when the flue gas is cooled in the atmosphere. NO is mainly emitted from combustion processes, where the rate of NO emission is about 90-95% of NO_x (5-10% belongs to NO_2). Exceptions are diesel engines, which emit higher portion of NO_2 (up to 70% of NO_x refers to NO_2) (4). The rate of NO_x emissions among different sectors in Europe in 2011 expresses Figure 3.1.1-1. Nowadays thermal power stations and industrial plants use significant amount of fossil fuels (coal, gas, oil). From these fuels the boiler outlet NO_x level of coal-fired boilers is higher than of gas or oil fired boilers, because coal contains more organic nitrogen.

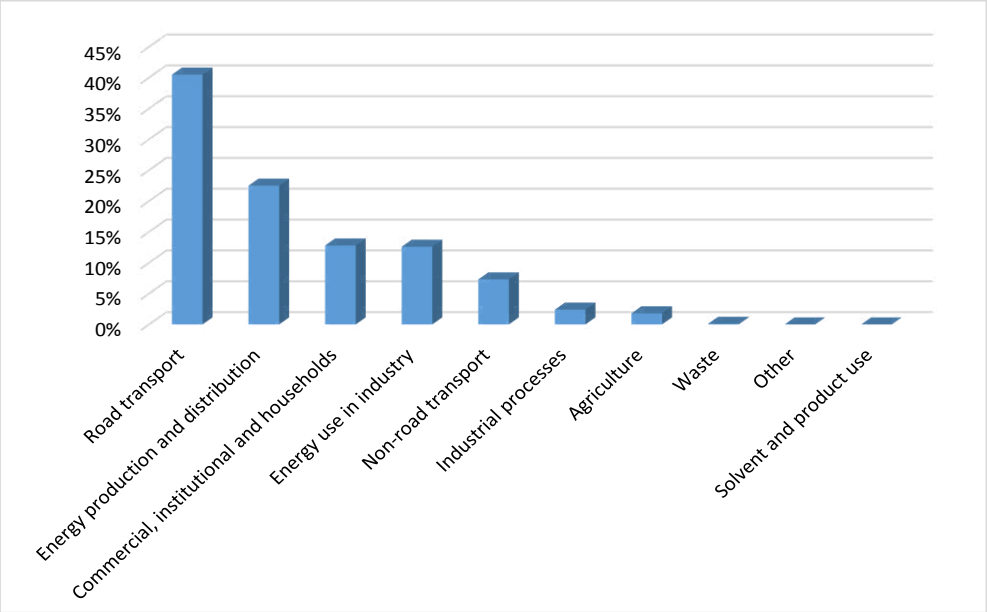

Figure 3.1.1-1 NO_x emissions emitted by various sectors in Europe in 2011 (5)

3.1.1.2 Effects of NO_x

Nitrogen compounds have an unfavorable impact on public health and the environment and additionally contribute to climate changes. The most harmful effect from NO_x is nitrogen dioxide (NO_2), which is formed by the reaction of nitric oxide (NO) with oxygen (O_2). High concentration of NO_2 in the air can cause serious health problems such as airways damage and other respiratory troubles. NO_x contributes to the acidification and eutrophication[1] of soil and

[1] Eutrophication is the ecosystem response to an excess of artificial or natural substances in water or soil. This can cause biodiversity through abnormal growth of some species, which are nowadays considered as a part of a lower-nutrient environment. (2)

water. The NO_2 reacts in the atmosphere with sunlight and hydrocarbon radicals which leads to formation of acid rain and to increase of ground level ozone which causes forest damages and climate changes. (4) (6) (7)

3.1.1.3 Formation of NO_x

Formation of NO_x during combustion processes is caused by nitrogen content in fossil fuels and also by other reactions which use atmospheric nitrogen for forming NO_x (8). The main producers of NO_x are transport (passenger cars, trucks etc.) and the energy sector (power plants and heating plants). Coal-fired combustion processes produce both NO and NO_2 but major part of emissions contains NO (8). Due to the fact that the thesis deals with coal-fired boilers, the following text is focused only on the formation of NO.

There are three NO formation mechanisms. The first mechanism concerns the thermal fixation of atmospheric nitrogen (thermal NO). The second mechanism deals with the oxidation of intermediate compounds such as NH, CN and HCN, converted from hydrocarbons contained in the fuel (prompt NO) (9). The third mechanism includes the conversion of nitrogen which is chemically fixed in the fuel (fuel NO). All these mechanisms depend on the temperature as is shown in Figure 3.1.1-2. The three formation mechanisms create:

- Thermal NO
- Prompt NO
- Fuel NO

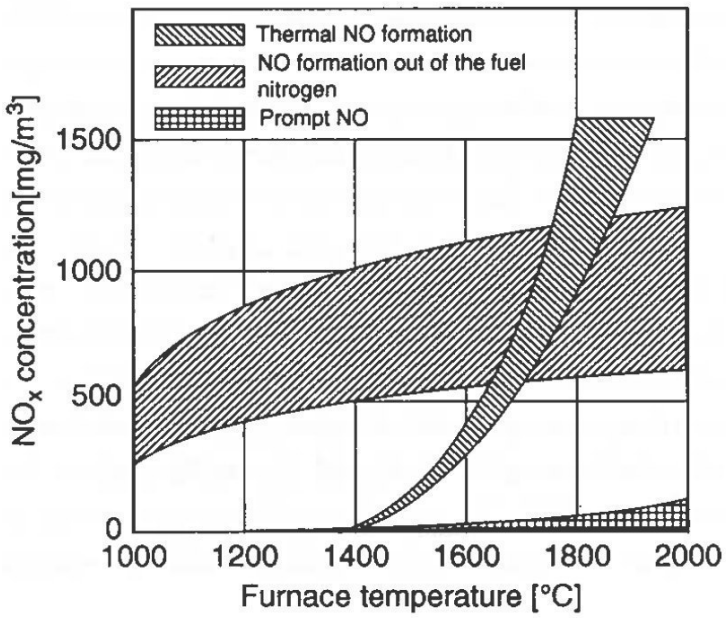

Figure 3.1.1-2 NO_x emissions in dependence on temperature in coal combustion (10 p. 235)

According to the Figure 3.1.1-2 it is possible to postulate that the formation of NO can be controlled by the conditions of the reaction process, especially by the temperature to avoid thermal and prompt NO formation.

The formation process of thermal NO was first postulated by Zeldovich in 1947 (8). The process takes place in the combustion zone where the temperature is very high (more than 1 300°C) (6 p. 13). Thermal NO is formed in the oxygen-rich area by reactions of nitrogen molecules and free oxygen atoms which are in the firing zone (8). The formation of thermal

NO is increased by higher combustion temperature, longer residence time of flue gas in the area with maximal temperature and higher concentration of oxygen in the flue gas stream. Zeldovich described the mechanism using Equation 3.1.1-1 (oxygen-rich zone), Equation 3.1.1-2 (oxygen-rich zone) and Equation 3.1.1-3 (fuel-rich zone). (6) (3)

$$O + N_2 \rightleftarrows NO + N$$ *Equation 3.1.1-1*

$$N + O_2 \rightleftarrows NO + O$$ *Equation 3.1.1-2*

$$N + OH \rightleftarrows NO + H$$ *Equation 3.1.1-3*

Prompt NO is created upstream a region near the burner by a mechanism described by C. P. Fenimore in 1971 (8). The mechanism utilizes nitrogen, as well as thermal NO, from air but occurs at lower temperatures, fuel-rich conditions and short residence times (8). In the flame there are many hydrocarbons which react with molecular nitrogen to produce HCN, NH and CN which can be easily oxidized to NO. The amount of prompt NO (in comparison with thermal NO and fuel NO) is relatively small (3). The process can be described using Equation 3.1.1-4, Equation 3.1.1-5, Equation 3.1.1-6, Equation 3.1.1-7 and Equation 3.1.1-8 (6).

$$CH + N_2 \rightleftarrows HCN + N$$ *Equation 3.1.1-4*

$$C + N_2 \rightleftarrows CN + N$$ *Equation 3.1.1-5*

$$CN + H_2 \rightleftarrows HCN + H$$ *Equation 3.1.1-6*

$$CN + H_2O \rightleftarrows HCN + OH$$ *Equation 3.1.1-7*

$$HCN + O \rightleftarrows NO + R$$ *Equation 3.1.1-8*
$(R = \text{"the rest of organic compound"})$

Fuel NO is created from organically-bonded nitrogen in fuel. Coal typically contains of 1.2 to 1.6% of nitrogen (8). The process of fuel NO formation can be divided into two steps. In the first step the chemically fixed nitrogen in the fuel is thermally decomposed to NH, CN, HCN and/or atomic nitrogen. The second step is a reaction of these substances with oxygen compounds to create NO or a reaction with nitrogen compounds to create N_2. The process is schematically described in Figure 3.1.1-3. The amount of nitrogen formed depends on the composition of nitrogen compounds in the fuel and volatile nitrogen compounds (6). (3 pp. 101-102) (9)

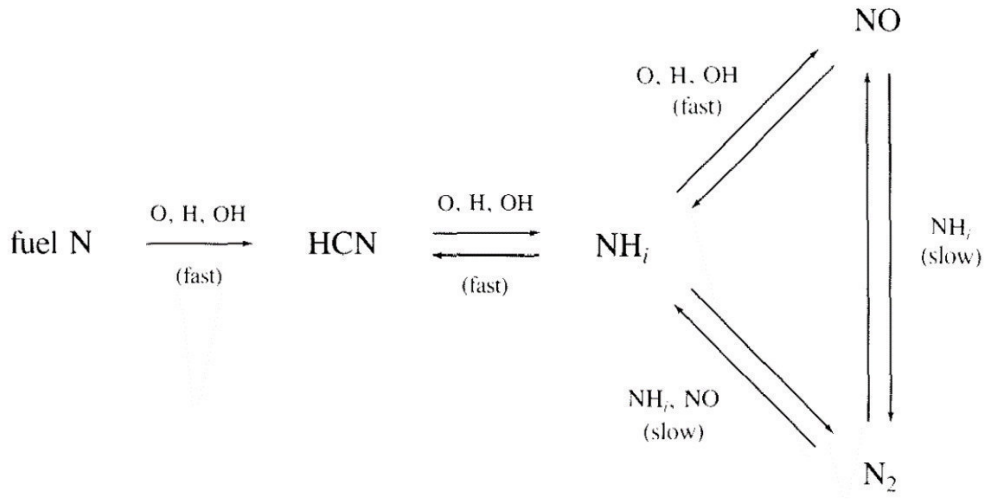

Figure 3.1.1-3 Fuel nitrogen reactions (8)

3.1.1.4 NO_x emission limits for coal-fired power plants in the Czech Republic

Large combustion plants produce significant amount of pollutants. Some of the pollutants are controlled by laws and regulations. In the Czech Republic there were milestones concerning the emission limits decrease. Due to these restrictions the amount of the most dangerous pollutants decreased because all significant polluters had to fulfill required emission limits. The most important milestones in the Czech Republic were the adoptions of laws in 1991, 2002 and 2012. The amount of pollutants emitted from large combustion plants decreases over the years – some of the emitted pollutants are shown in Figure 3.1.1-4.

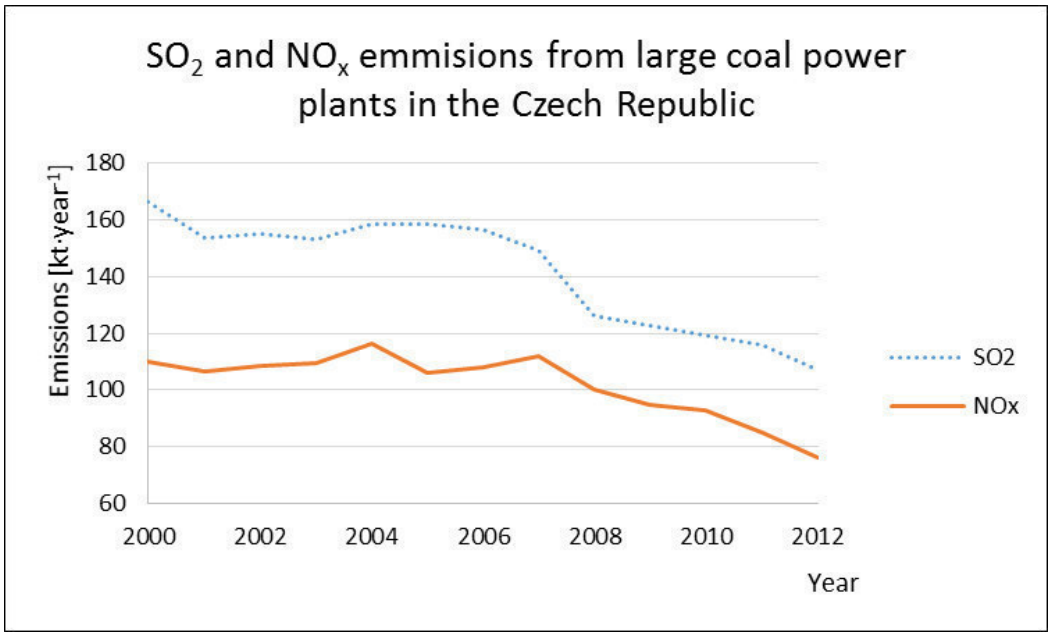

Figure 3.1.1-4 SO_2 and NO_x emissions from large coal-fired power plants emitted in the Czech Republic (11)

The first tendency to protect the environment in the Czech Republic was the adoption of Act No. 309/1991 Coll. This law specified emission limits for air polluters which had to be kept from 1998 onwards. The law followed by Act No. 389/1991 Coll., which determined emission charges. The emission limits started to be valid later (in 1998) to give some time to the polluters for technology improvement. Many polluters modernized their technologies and some of them had to reduce or completely shut down their plants. This led to the boiler modernization and, in the case of coal-fired boilers, equipping them with desulfurization technologies. (12)

In connection with joining the EU, the Czech Republic created Act No. 86/2002 Coll. in accordance with Directive 2001/81/EC of the European Parliament and the Council on National Emission Ceilings for certain pollutant. By this the emission limits of SO_2, NO_x, Volatile Organic Compounds (VOC) and NH_3 were created. These limits are described in Government Regulation No. 352/2002 Coll. The limits shown in Table 3.1.1-1 became valid in 2010.

Table 3.1.1-1 NO_x emissions limits for coal-fired boilers according to the Government Regulation No. 352/2002 Coll. (13)

Total rated thermal input	**Limit value of NO_x emissions [mg·Nm^{-3}]**		
	Date of construction approval		
	< 1.7. 1987	1.7. 1987 - 31.12. 2002	> 1.1.2003
50 -100 MW_{th}	650	600	400
100 -300 MW_{th}	650	600	200
300 -500 MW_{th}	650	600	200
≥ 500 MW_{th}	650	500	200

Nowadays in the Czech Republic the emission limits are regulated by the Act No. 201/2012 Coll. on Clean Air Protection. Detailed limitations are directed by the Decree No. 415/2012 Coll. from 21st November 2012. These laws were created in accordance with Directive 2010/75/EU of the European Parliament and of the Council of 24 November 2010 on industrial emissions (integrated pollution prevention and control). As previously, the laws give some time to the polluters to fulfill the stricter requirements. The validity of the new emission limits is from 1st January 2016. The limits vary in dependence of the boiler (plant) capacity, fuel type, boiler type, age of the boiler (plant) and year working hours. Actual NO_x emission limitations for coal-fired boilers are shown in Table 3.1.1-2.

Table 3.1.1-2 Actual NO_x emissions limits for coal-fired boilers according to the Decree No. 415/2012 Coll. (14)

Total rated thermal input	**Limit value of NO_x emissions [mg·Nm^{-3}]**			
	Valid till 31.12.2015		**Valid from 1.1.2016**	
	Date of putting into service		Date of putting into service	
	< 27.11. 2003	27.11.2003 - 7.1.2014	< 7.1.2014	> 7.1.2014
50 -100 MW_{th}	600	400	300	300 (400[1])
100 -300 MW_{th}	600	200	200	200
300 -500 MW_{th}	600	200	200	150 (200[1])
≥ 500 MW_{th}	500	200	200	150 (200[1])

[1] Value valid for boilers which use pulverized coal

3.1.2 Modern denitrification methods for coal-fired boilers

There are many methods for the denitrification of coal-fired boilers. Generally we divide these methods into two groups – primary denitrification methods and secondary denitrification methods. Primary denitrification methods are applied to decrease NO_x formation during the combustion process. Secondary denitrification methods transform NO_x generated from the combustion process into molecular nitrogen (N_2) and water vapor. For denitrification of newly-built boilers, it is often enough to use just primary denitrification methods. Secondary denitrification methods are used for retrofitting of existing (old) boilers to meet new strict NO_x emission limits. For the retrofitting it is usually used just SCR method or SNCR method supported by using of primary deNO_x methods.

3.1.2.1 Primary denitrification methods

Primary denitrification methods are usually applied during the combustion process. Their aim is to decrease amount of NO_x formed during the fuel combustion by using several different principles. These principles include decrease of maximal combustion temperature, decrease of residence time in areas with maximal temperature, creating zones with different stoichiometric conditions, proper mixing of the fuel with combustion air, etc. The main primary denitrification methods applied for coal-fired boilers are low excess air firing (LEA), air staging, fuel staging, exhaust gas recirculation (EGR) and using of low-NO_x burners.

Low excess air firing

To assure complete fuel combustion it is important to burn the fuel with an excess of air. The amount of extra air is described by the excess-air coefficient. For example, a typical value of excess-air coefficient for boilers using beater wheel mills is 1.22 – 1.25 (15 p. 48). High air excess entering the combustion zone increases formation of thermal NO_x because of the extra nitrogen and oxygen entering the combustion zone. An appropriate solution is to use as low air excess as necessary for complete combustion. This process is called low excess air firing. If the amount of air is insufficient, unburned carbon in the ash and formation of CO and soot increase. (16)

Air staging and fuel staging

The way that air is delivered to the combustion zone has an important effect on the combustion process and also on NO_x formation. A proven combustion engineering technique is air staging. Air staging usually divides combustion into three zones (sometimes only two): primary zone, reburning zone and burnout zone. This technique was primarily developed to make the combustion slower (which decreases combustion temperature). The primary zone (also called fuel rich zone) is the lowest-lying zone where air delivery is restricted. This air restriction results in incomplete combustion because the amount of air admitted to the burners is less than the amount theoretically needed for complete burning of the coal (substoichiometric firing). This also results in lower NO_x formation due to the limited oxygen availability for NO_x formation. Further in the furnace CO reacts with thermally unstable NO_x to produce elementary nitrogen (also termed as NO_x destruction) (17). Lower combustion temperature also leads to decrease of NO_x formation. Additional air is supplied to the burnout zone (also called oxygen rich zone). This additional air is often called over-fire air (OFA). The unreacted fuel and also CO react with the over-fire air above the primary zone. The position of the over-fire air injection nozzles and the mixing of the air with unreacted fuel are critical to maintaining high combustion efficiency. (9) (10)

Beside air supply control it is possible to control fuel supply. The method which uses divided fuel supply is called fuel staging. The aim of this technique is the same as for the air staging – create fuel-rich and fuel-lean zones in order to burn the fuel completely. This lowers flame temperature, which leads to decrease of NO formation. Fuel is often fed to primary and reburning zone (can be seen in Figure 3.1.2-1). The fuel fed into the reburning zone (typically 10-30% of the total heat input) can be mixed with recirculated flue gas which is then used as a carrier. Some boilers use secondary fuel for burnout zone. Most widely used fuel for this purpose is natural gas which provides proper mixing with flue gas in the reburning zone. Natural gas is expensive fuel nowadays, so it is rarely used for this purpose. It becomes useful when there is some other source of flammable gas from an industrial process which can be used as a fuel for the burnout zone with none or low aditional costs . (10) (9)

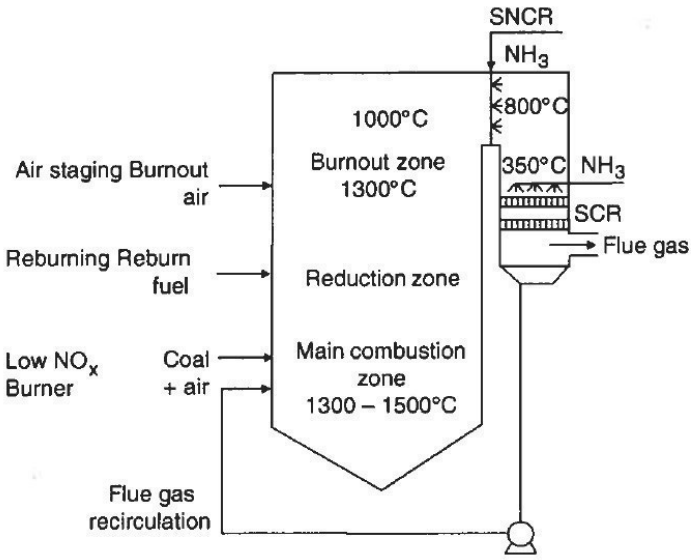

Figure 3.1.2-1 Methods of NO_x reduction (10 p. 279)

The previously mentioned techniques (air staging and fuel staging) can be both used in the furnace and also at the individual burner. For furnace usage the furnace is divided into zones with different stoichiometric parameters. The zones can be seen in Figure 3.1.2-1. In each of these zones there are different NO formation and reduction mechanisms. Possible reactions of pulverized fuel as the primary fuel and gas as the reburn fuel are shown in Figure 3.1.2-2. It is obvious that in the primary zone NO is formed especially from nitrogen content in the coal. In the reduction zone NO formed in the primary zone are reduced. This reduction is caused by the presence of hydrocarbon radicals formed from reburn fuel. The hydrocarbon radicals cause NO transformation into hydrogen cyanide (HCN) which is then converted into ammonia radicals (NH_i). Ammonia radicals can be then oxidized to NO or decomposed to N_2. In the burnout zone NO, HCN and NH_i are oxidized to NO. (10)

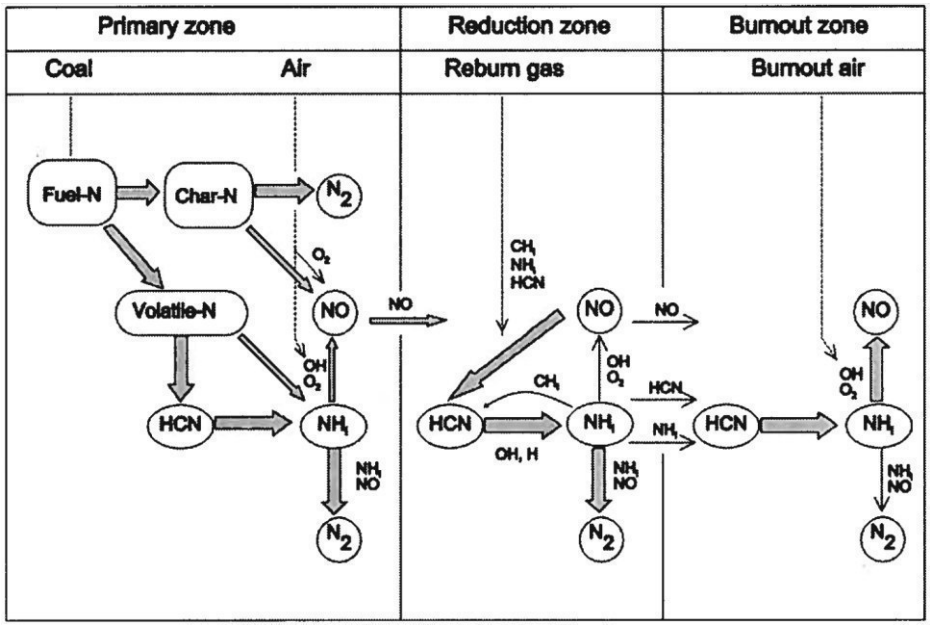

Figure 3.1.2-2 Reactions in fuel staging with pulverized fuel (10 p. 281)

Exhaust gas recirculation

Exhaust Gas Recirculation (EGR) is also used as a tool for slowing down combustion velocity which has an impact on decreasing of the combustion temperature. The method uses part of the exhaust gas which is then recirculated to the furnace combustion zone or mixed with the combustion air. The flue gas is usually taken downstream economizer. This method is often used for retrofits to existing coal-fired boilers. (10) (9)

Low NO_x burners

An appropriate field of research is focused on burner innovation. Current burners control fuel and air mixing in order to enlarge flames and improve flame structure (18). These modern burners are called low-NO_x burners. The principal aim of low-NO_x burners is to divide fuel mixing with primary and secondary air to reduce formation of NO_x and to supply tertiary air to create staged combustion in the burner zone (9). Various burners using different methods have been invented during the last two decades. They can be divided according to their principle of operation into two main groups (with additional categorization) (19):

- Swirl types
- Jet types

Swirl burners use swirling motion of combustion air to create different combustion zones (fuel-rich and fuel-lean zones). Swirling technology improves flame stability and mixing process of fuel with combustion air. These burners are often used for front and opposite fired boilers. According to the burner design and used swirling technology the burners can be furthermore divided into three additional categories: axial vane burners, volute burners and tangential vane burners.

Swirling technology is used in HT-NR (Hitachi NO_x reduction) burner series. One of these burners is HT-NR3 burner invented by Babcock-Hitachi Company which uses a combustion mechanism called “in-flame NO_x reduction” (20). The burner is illustrated in Figure 3.1.2-3.

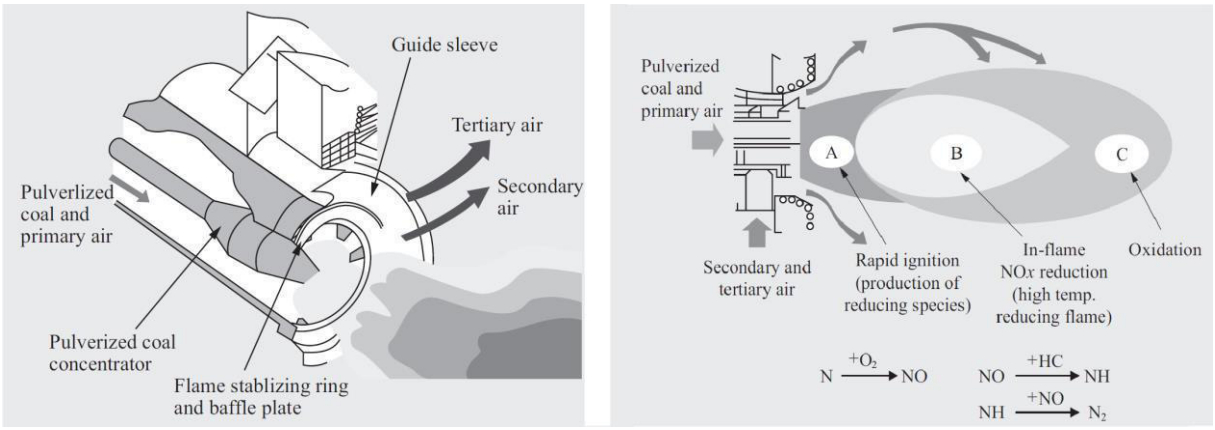

Figure 3.1.2-3 Design of HT-NR3 burner and its in-flame NO_x reduction mechanism (20)

On the left side of the figure we can see a model of the burner with components which create the swirling motion. On the right side of the figure there is a drawing of the different combustion zones (A, B and C) which allow NO_x formation control. Immediately after the fuel nozzle exit (zone A) the mixture is ignited to create a stable flame. This zone is also called the high temperature-fuel rich devolatilization zone, and there the reducing species are created. Zone B is called the NO_x decomposition zone. Zone C is called the char oxidizing zone and there the secondary air enters the combustion process. (19)

Jet burners do not use the swirling motion. These burners are usually placed in furnace corners and are tangentially positioned to an imaginary circle in the center of the furnace (19). The difference between jet burners and swirl burners is shown in Figure 3.1.2-4.

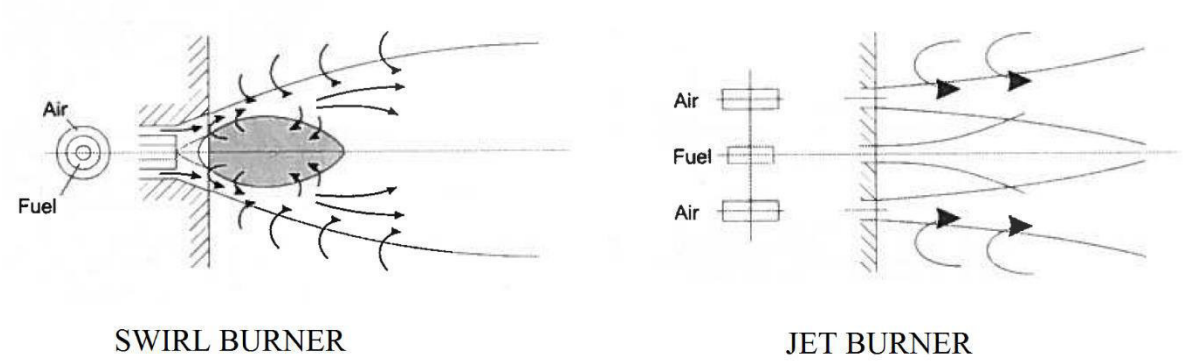

Figure 3.1.2-4 Flow fields of a swirl burner and a jet burner (modified from (10 p. 254))

Further developed burners are often called second-generation low-NO_x burners. These burners utilize modern fluid dynamic principles to develop intensive mixing of fuel with air. These burners used improved design to increase combustion efficiency by modifying the structure of the flame. (18) (10) (9)

Besides above mentioned typical primary de-NO_x methods, there are also other methods aiming to decrease NO_x emissions. One of these methods is called Gas-Fired Coal Preheating (GFCP) and thus method is focused on fuel preparation. The principle of GFCP is that pulverized coal is heated before entering the burners to initiate devolatilization. This allows the release of coal volatiles and also fuel-bound nitrogen compounds into an oxygen-lean atmosphere where it is easier to convert these particles into N_2. (21)

3.1.2.2 Secondary denitrification methods

Secondary denitrification methods are applied downstream of the combustion chamber, where NO_x has already formed. The mostly used methods are selective catalytic reduction (SCR) and selective non-catalytic reduction (SNCR). The basic principle of these methods is using a reagent (usually aqueous NH_3 or urea) for conversion of NO_x in the flue gas into N_2 and water vapor. These methods differ especially in the temperature range where they work, denitrification effectiveness and investments costs. The SCR method needs an additional catalytic bed (catalytic reactor) which usually results in installation of separate steel duct structures, etc. These methods are usually used individually but they can be also used simultaneously for better denitrification effectiveness and lower ammonia slip. In this case SNCR method is used supported by catalyst which is placed in the area with low temperature. In this case the catalyst is called SCR slip killer.

Selective catalytic reduction

SCR is a proven technology using NH_3 or urea as a reagent to reduce nitrogen oxides (NO_x) emitted from stationary combustion sources. The reagent is injected into flue gas and then reacts with nitrogen oxides to convert them to N_2 and water vapor. The technology has been used commercially since 1980 in Japan and since 1986 in Germany (10 p. 306). Nowadays the SCR is used world-wide for the reduction of NO_x emissions formed in stationary combustion sources mainly because of its high efficiency, selectivity and economics (22). Typical applications of this method are in coal-, oil- and gas-fired power plants, chemical plants, and stationary diesel and gas engines. Recently the method is also used for truck and passenger cars (22). By using only this method for denitrification it is possible to reduce more than 75% of NO_x emitted from stationary combustion sources (23 p. 2). The final removal efficiency reaches its maximum around 94% (23 p. 2) (10 p. 305).

SCR is usually located downstream of the economizer (upstream of the air heater) to ensure the optimal temperature range for NO_x reduction (this is called a high-dust configuration (10)). It is also possible to place the SCR after an electrostatic precipitator (EP). In such a case it is called low-dust configuration. Another possibility is to place the SCR after EP (or other equipment for particulate matter (PM) removal) and a desulfurization device – usually reheating of flue gas may be required. Possible positions of SCR are shown in Figure 3.1.2-5. The temperature range for SCR reactor, for coal-fired steam generators, lies between 320 and 400°C (10). The upper limiting temperature is recommended to eliminate of the threat of surface sintering (10 p. 304). The lower limit temperature is determined due to the risk of fouling and corrosion of ducts and technology downstream SCR (catalyst, air heater etc.).

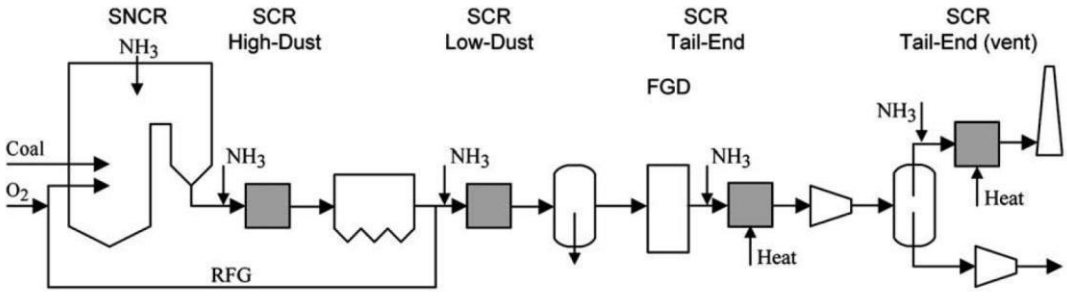

Figure 3.1.2-5 Position for SCR and system in the oxy-fuel process (24)

The reagent injection takes place in the duct upstream the SCR reactor to ensure an adequate mixing of reagent with flue gas. Proper distribution of reagent is necessary for high performance of the process. To achieve a uniform distribution, the reagent is sprayed into the duct through multiple lances with adjustable single flows (10 p. 304). The reagent predominantly used is aqueous ammonia (NH_3-SCR), but hydrocarbons (HC-SCR) have also been used as an alternative solution (mostly for truck diesel engines). Most recently using H_2 as the reagent has attracted some attention. (23 pp. 3-4). HC-SCR is extensively studied but further work must be done to make this method commercially feasible (25 p. 688). The most used types of regents used for coal-fired boilers are:

- anhydrous ammonia (liquid ammonia)
- aqueous ammonia (25-30% of NH_3)
- urea

Anhydrous ammonia is an extremely toxic substance, so it is necessary to design a suitable storage/injecting system. The advantage of this variant is that there is no need for conversion of the substance. Before spraying the anhydrous ammonia into the piping it is essential to vaporize it and then mix with air (26). According to (27) anhydrous ammonia is the least expensive variant for SCR and SNCR methods.

Aqueous ammonia (NH_4OH) is not as toxic as anhydrous ammonia – consisting about 25-30% of NH_3. This dilution of the ammonia gives advantages regarding handling and transportation. To be fed into the injection system the aqueous ammonia is atomized and mixed with air (26).

Urea (NH_2 CO NH_2) is easy to transport and handle, so that it is not necessary to observe as demanding requirements as for anhydrous ammonia (28). The freezing point of urea is about - 11°C, so it is important to protect the substance against freezing. According to Fisher (27), using urea as the reagent for the SRC method is a safe, reliable and cost effective solution and the operating costs are lower than for aqueous ammonia and in contrast with anhydrous ammonia, the risk of toxic accidents is minimal.

The chemical process of the NH_3-SCR is considered selective and consists of several reactions whereas the denitrification procedure mostly involves reaction of NH_3 with NO_x that results in forming of elementary nitrogen (N_2) and water vapor. The dominant reactions of NH_3-SCR are (22):

$$4NH_3 + 4NO + O_2 \rightarrow 4N_2 + 6H_2O$$ *Equation 3.1.2-1*

$$2NH_3 + NO + NO_2 \rightarrow 2N_2 + 3H_2O$$ *Equation 3.1.2-2*

$$8NH_3 + 6NO_2 \rightarrow 7N_2 + 12H_2O$$ *Equation 3.1.2-3*

The design of the catalytic bed and also the proper selection of the catalyst material has a huge impact on the overall efficiency of the denitrification process (see Figure 3.1.2-6). The selection of the catalytic bed and catalyst material depends on many other factors such as operating temperatures, catalyst regeneration, composition of flue gas etc. Common materials for catalyst used in NH_3-SRC are usually metal or metal oxides supported on SiO_2, TiO_2, carbon-based materials or zeolites (29). Extensive researches of catalyst materials, suitable for HC-SCR, also promise successful results (25 p. 688). The geometry of catalyst must ensure a large surface area for adsorption. Generally, a honeycomb, plat-type or corrugated geometry is used. Due to the presence of sulfur in the flue gas the catalyst can be deactivated due to poisoning and plugging the catalyst cells (23).

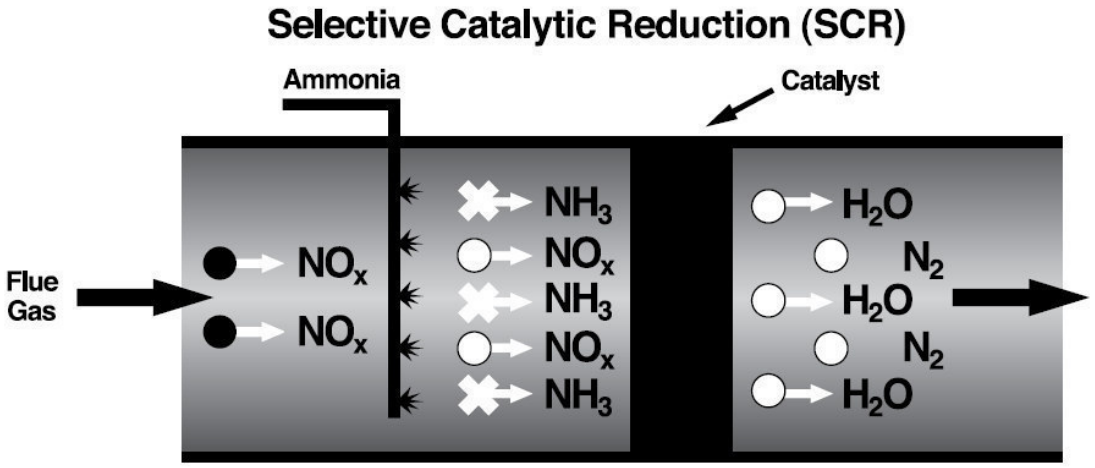

Figure 3.1.2-6 Selective Catalytic Reduction method (16)

Selection of proper material for the catalyst has to take into account the conditions of the denitrification process. The catalyst should be from porous material and provide a large surface area for adsorption and good resistance against sulfur oxides. Almost all metals and their combinations have been studied in order to determine the activity of denitrification for each of them (23). The materials for catalyst can be divided into four groups:

- noble metals (alloy steel)
- metal oxides
- carbon-based materials
- zeolites

Noble metals are used especially for low temperature applications and applications using natural gas. Noble metals offer a good selective reduction of NO_x, but at the same time actively oxidize NH_3 (22) (23). Metal oxides (pure vanadium, iron, copper, chromium and manganese) and metal oxides supported by aluminum, silica, zirconia and titanium have been examined. In conventional SCR applications metal oxides are usually used instead of noble metals (22). The advantage of zeolites is that it is possible for them to work under high temperatures (maximum of 600°C) (22). Among the favorite zeolite materials are Cu/ZSM-5 and Fe/ZSM-5 (23). Ceramic materials such as TiO_2 and Al_2O_3 are often used for creating the element body of the catalytic bed. The body is then coated with a thin layer of catalyst metal such as V_2O_5 or WO_3 (9).

Studies of SCR installations observed increased removal efficiency of mercury (Hg) from flue gas. Coal-fired power plants are major mercury polluters: nearly half of mercury emissions comes from combustion of fossil fuel (mainly from Asia) (30 p. 2494). Mercury deposition depends mainly on coal composition, but also on type and age of the catalyst (31). Especially TiO_2 and V_2O_5 catalyst may promote the formation of oxidized mercury (32).

Nowadays two types of catalyst geometry are usually used – honeycomb and plate-type (see Figure 3.1.2-7). The cell size depends on the process conditions and varies from 3 to 8 mm (26). Smaller diameter of the cell increases the area for adsorption but also increases the risk of cell fouling. Typical mesh size for coal-fired boiler is about 7 mm to avoid plugging and fouling of the catalyst (9). Honey-comb catalysts are smaller than plate-type catalysts and less expensive, but cause higher pressure drop and are more susceptible to plugging (33).

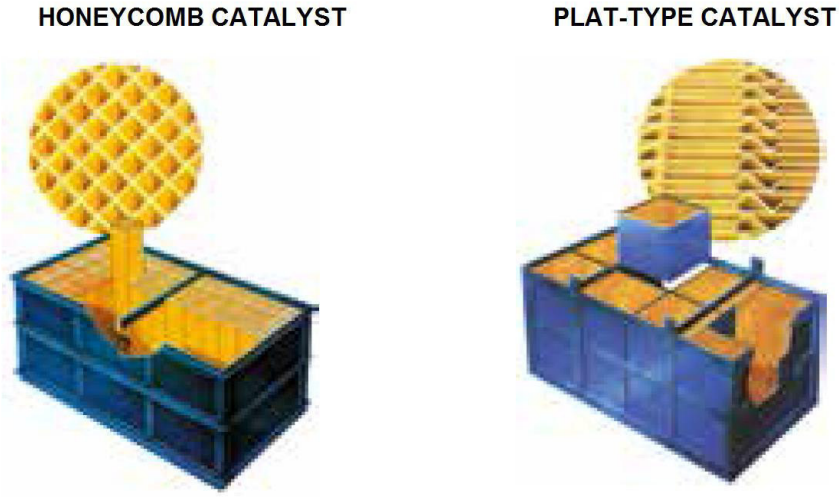

Figure 3.1.2-7 Different types of catalyst design (34)

Catalyst deactivation is caused by presence of sulfur in flue gas. At lower temperatures the catalyst is poisoned by SO_2 and SO_3. SO_3 has higher deactivation potential (23). Deactivation is also caused by thermal sintering of active sites caused by high temperatures flue gas. Ammonia-sulfur salts and PM cause blinding, plugging and fouling of the catalyst. Also erosion of the catalyst material can become a serious problem when flue gas has high velocity and high fly ash content (35). Soot blowers and sonic horns are installed into the catalytic bed to prevent catalyst from plugging.

The catalyst fouling is caused by the undesired presence of SO_2, with minor amount of SO_3, in flue gas and formation of ammonium sulfates. SO_2 can be oxidized to SO_3 (22) (see Equation 3.1.2-4). SO_3 reacts with water and unreacted ammonia to form NH_4HSO_4 (see Equation 3.1.2-5 (23)) and $(NH_4)_2SO_4$ (see Equation 3.1.2-6) which can deposit the catalyst (22). Moreover V_2O_5 (as a catalyst) increases the process of forming SO_3 (36).

$$SO_2 + \frac{1}{2} O_2 \rightarrow SO_3$$ *Equation 3.1.2-4*

$$NH_3 + SO_3 + H_2O \rightarrow NH_4HSO_4$$ *Equation 3.1.2-5*

$$2NH_3 + SO_3 + H_2O \rightarrow (NH_4)_2SO_4$$ *Equation 3.1.2-6*

In lignite fired power plants the presence of ash in flue gas causes the catalyst fouling and plugging. There are two main processes of depositing catalyst (37 p. 159). The first process is caused by low-temperature sodium-calcium-magnesium sulfates, phosphates and carbonates which may plug the catalyst cells. The second process is caused by the carriage of deposit fragments or fly ash, which results in deposition on the top of the SCR catalyst. This increases the pressure drop and decreases the efficiency of the SCR by reducing the catalyst active surface (32 p. 1). It was also discovered that alkali elements are able to migrate through the catalyst material (due to its water-soluble form) and cause deactivation of active cells (37 p. 159). Figure 3.1.2-8 shows pictures of the ash material deposited on the catalyst inlet after 2 months of operation.

Figure 3.1.2-8 Pictures of catalyst inlet after 2 months of testing (32 p. 589)

Using of SCR method leads to presence of NH_3 in flue gas which is called ammonia slip (NH_3 slip). Ammonia slip is the amount of unreacted NH_3 in flue gas after the denitrification process. NH_3 has an unfavorable effect on the environment (unpleasant smell and toxicity) and also on the components of the power plant (especially due to fouling problems) as is mentioned in the previous text. The excess of ammonia has to be kept as low as possible, so sufficient amount of ammonia (with regard to the amount of NO_x) should be injected at proper positions in the flue gas duct. NH_3 slip also increases with deactivation of the catalyst in case of low temperatures (too cold for ammonia to react) (10) (9). Usually ammonia slip should not be higher than 2 ppm (1.4 mg/Nm^3) (10). Static mixing blades inside the piping together with precisely designed lances and pipes for ammonia injection ensure proper mixing of ammonia with flue gas. Figure 3.1.2-9 shows the newest type of static mixers and ammonium injection lances for SCR technology developed by Alstom.

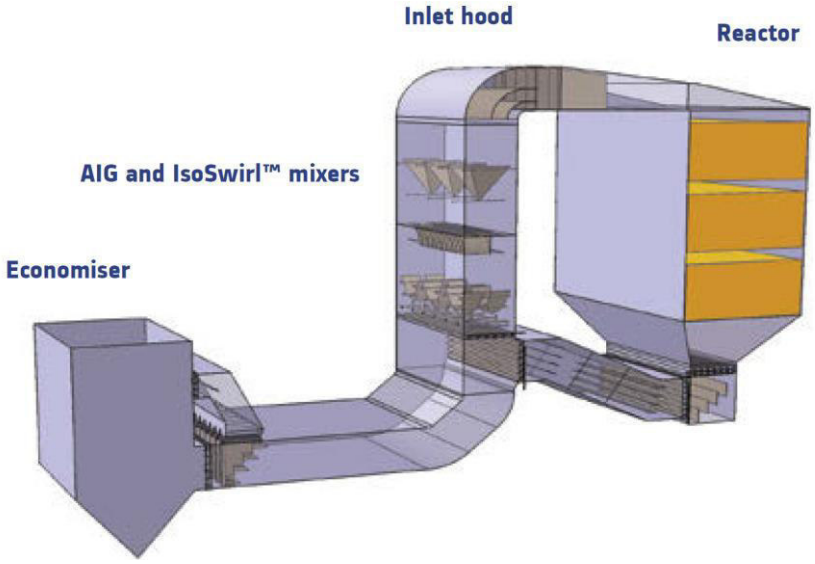

Figure 3.1.2-9 IsoSwirl^{TM} mixer technology and ammonium injection grid (AIG) developed by Alstom (38)

SCR offers the highest NO_x reduction compared to the other methods. The catalyst is situated in lower temperatures, so it is possible to use the SCR method in different position (see Figure 3.1.2-5). Installation of SCR does not require the modification of combustion process. SCR installation into an existing plant can be difficult and costly, due to usually limited space for SCR unit. For denitrification it is necessary to use large volume of catalyst. The excess of the reagent must be kept to minimum, so proper mixing of the reagent with flue gas is required. The investment costs of SCR are higher.

Selective non-catalytic reduction

SNCR (also called Thermal DeNO$_x$) is, as well as SCR, a technology for NO$_x$ reduction in stationary combustion sources of NO$_x$. The technology uses injection of a reagent (ammonia or urea) into flue gas to reduce NO$_x$ to NO$_2$ and water (see Figure 3.1.2-10). The technology was invented by a company called Exxon in the USA and was first applied in 1974 in Japan (25). The first usage of SCR in coal-fired power plant was in 1980 (10). This technology is popular especially for waste incineration plants (36).

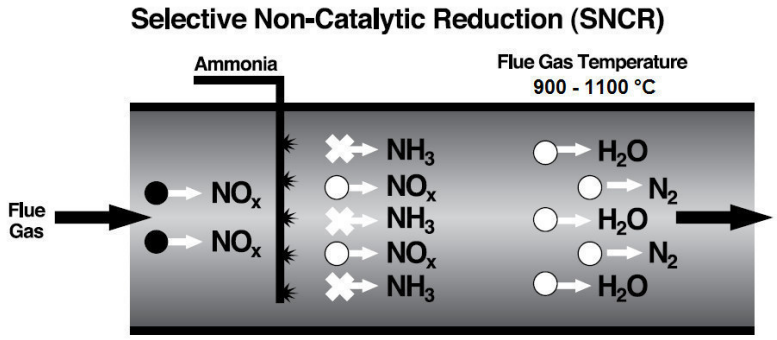

Figure 3.1.2-10 Selective Non-Catalytic Reduction (SNCR) (16)

The main difference compared to SCR is that SNCR works at higher temperature range without the need for a catalyst. SNCR is able to achieve a NO$_x$ removal efficiency about 30–50% (sometimes even higher) (10) (35). Nowadays it is necessary for large coal-fired boilers to achieve NO$_x$ values below 500 mg/Nm^3 (22). Values below 200 mg/Nm^3 will be required from 1.1.2016. SNCR is not as efficient in NO$_x$ reduction as SCR but the investment costs are lower. A basic schema of SNCR method shows Figure 3.1.2-12.

The optimal temperature range for SCR is usually 870-1150°C (35) (another source (10 p. 278) determines the optimal range as 900-1100°C). Figure 3.1.2-11 shows the dependence of the NO$_x$ reduction on temperature. The highest temperature is limited by oxidizing of NH$_3$ to form NO$_x$ (36) (39 p. 492). Oxidation of NH$_3$ depends on the amount of O$_2$ and the temperature in the reaction zone. Equation 3.1.2-7 (39 p. 492) shows the NH$_3$ oxidation.

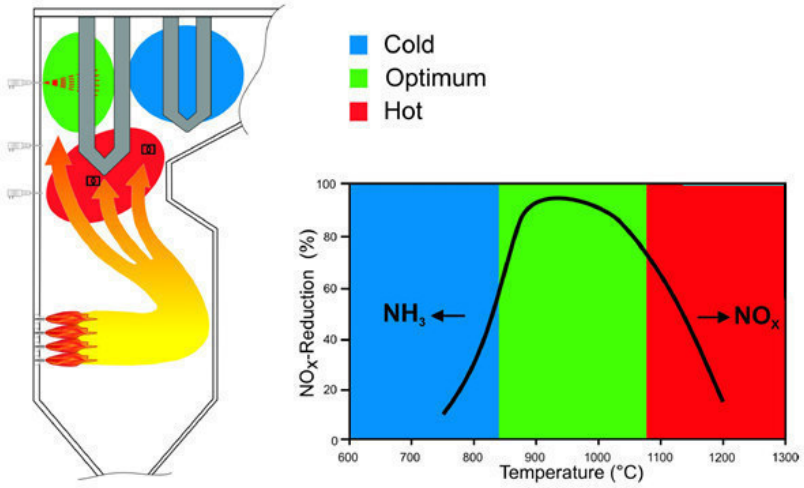

Figure 3.1.2-11 Optimal temperature range for SNCR – modified from (40 p. 2)

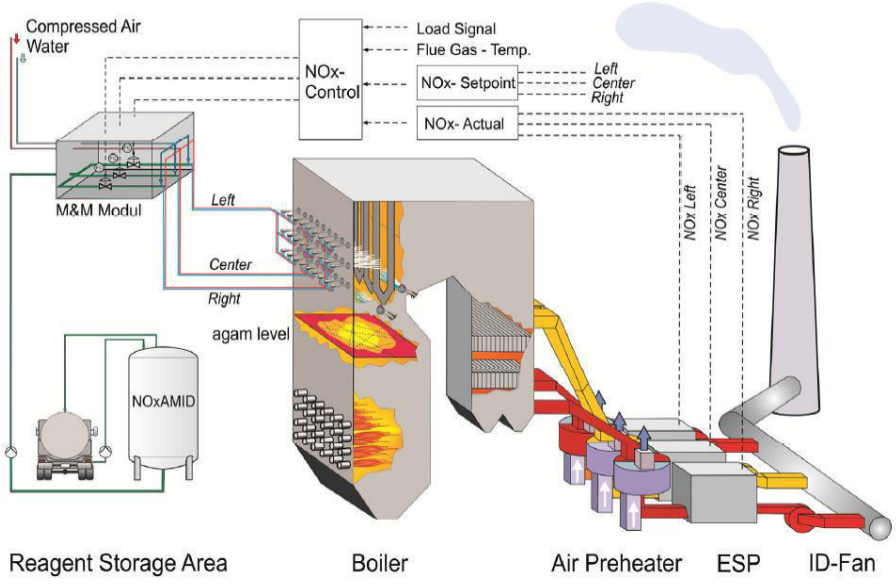

Figure 3.1.2-12 Flow chart of a boiler with SNCR system using AGAM (40)

Below the lower limit temperature the reaction slows which causes an increase of ammonia slip (ammonia does not have enough time for the reaction with NO_x). The ammonia excess may results in fouling and erosion of heat transfer surfaces and air heater. These damages are mainly caused by forming of ammonium salts at low temperatures (as is described in the text above).

Flue gas temperature can be too hot for the denitrification process, especially when the boiler is operated at full load. In this case it is not reasonable to inject the reagent due to the formation of NO_x. One possible alternative is to cool the flue gas by water injection. This solution is uncommon in real usage, because of its low efficiency. Cooling water can be injected by the same lances as used for the injection of the reagent (made by increasing the quantity of process water) or by some extra injectors which are usually situated below the reagent injection lances (40 p. 20). These extra injectors spray cooling water into the hot flue gas area to cool the flue gas under the highest limiting temperature.

$$4NH_3 + 5O_2 \rightarrow 4NO + 6H_2O$$ *Equation 3.1.2-7*

For proper distribution of ammonia it is important to know the temperature range where the reactions occur. It is a very complicated task to measure the temperature in the furnace. The temperature varies along and also across the furnace. For measuring such a problematic task, Acoustic Gas temperatures Measurement system (AGAM) can be used. For less accurate measurements it is possible to use thermocouples (40 p. 4). AGAM operates on the principal that the speed of sound is proportional to the square root of the temperature (see Equation 3.1.2-8). Molecules at higher temperature have more energy, so they vibrate more, which allows sounds waves to travel faster. AGAM uses this principle for gas temperature measurement. The advantage is that the measurement is not affected by radiation from the flames or boiler walls. The system consists of transmitters and receivers, located on the boiler walls. These devices measure the speed of sound and then the information is transformed to create two-dimensional temperature distribution (40). The temperature distribution of a furnace can be seen in Figure 3.1.2-12. This measurement is usually made in several levels to make proper input data for combustion process and the NH_3 injection system optimization.

$$c = \sqrt{\frac{\kappa \cdot R}{M} \cdot T}$$ *Equation 3.1.2-8*

The most used reagent are urea (NH_2 CO NH_2) or ammonia water (NH_4OH). Both these substances are described above, so the following text is more focused on the dissimilarities in their usage. Both of the reagents are mixed with water and air before spraying into the flue gas. Both substances use different processes of release and mixing of particles which are used for denitrification. The processes are more closely described in Figure 3.1.2-13. The urea is enclosed in water, which serves as carrier medium for active NH_2-species. To decompose the active NH_2-species the water must be evaporated, which gives an opportunity to control where the reaction takes place by changing the water droplet size and the penetration depth accordingly (36). This enables to inject the active NH_2-species into proper place. Urea, due to its toxicity, can have a harmful impact on heating surfaces, so this interaction has to be avoided (36). Usage of urea causes higher N_2O emissions due to the reaction described in Equation 3.1.2-9 (25 p. 688). In the Figure 3.1.2-13 there is also demonstrated the use of ammonia water. We can see that in this case the reagent is released immediately after exiting the lance, so the reaction starts immediately after exiting the lances.

$$NCO + NO \rightarrow N_2O + CO$$ *Equation 3.1.2-9*

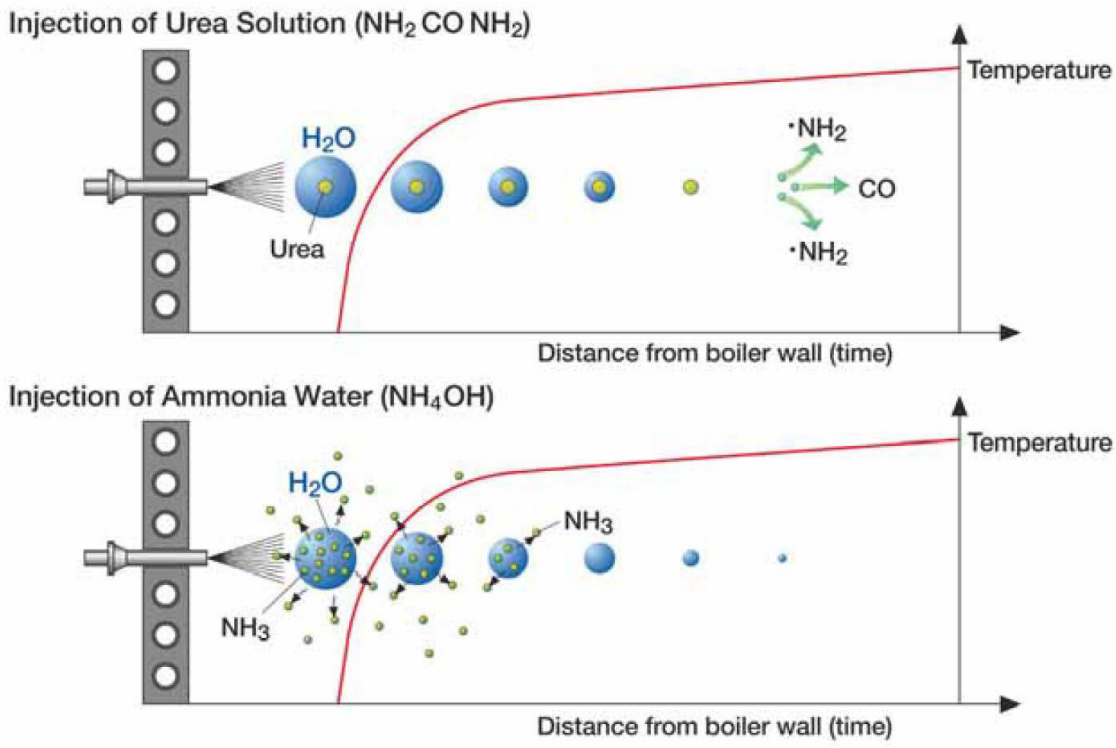

Figure 3.1.2-13 Process of denitrification using ammonia water or urea solution (36)

Nowadays, there exists a technology which uses urea simultaneously with ammonia water to achieve higher efficiency of the denitrification process. The technology is registered under trademark TWIN-NO_x® and provides other additional advantages, such as wider temperature range, lower ammonia slip etc. (40).

Before injecting into the flue gas stream, the reagent is pumped from the storage tank (usually stainless steel) and mixed with water and air in mixing and metering modules (M&M Module

– see Figure 3.1.2-12). M&M modules measure flow rate of reagent, water and air and provide mixing of these substances to ensure the best consistence for following denitrification (36).

The problematic task is to keep minimal ammonia slip which causes the same problems as in SCR method. The amount of unreacted ammonia depends mainly on proper distribution of the reagent into the flue gas stream. Common value for NH_3 slip is under 10 mg/Nm^3 (36). It is also important to assure a low NH_3 content in bottom ash, especially when the ash is further used. Bottom ash is often used as structural fill or when making concrete blocks.

The main reactions which are important for SNCR are the same as for SCR, namely Equation 3.1.2-1 and Equation 3.1.2-3, while in the case of using urea the denitrification process can be described by Equation 3.1.2-10 (10).

$$2NO + (NH_2)_2CO + \frac{1}{2}\,O_2 \rightarrow 2N_2 + 2H_2O + CO_2$$ *Equation 3.1.2-10*

The SNCR method alone is suitable for applications which do not require high degrees of denitrification. Low investment costs (in comparison with SCR – the absence of the catalytic bed) and relatively less troublesome retrofitting make this method very feasible for many power plants (25 p. 688) (35)). Nowadays an increasing number of companies are investigating the feasibility of the SNCR technology even for large boilers (40 p. 2).

3.2 Considered variants for denitrification of the boiler

3.2.1 Boiler description

PG 640 is a 640 t·h^{-1} once-through water tube boiler used in the Počerady power plant since 1970 (the boiler is shown in Appendix B). The power plant is situated in the north-west part of the Czech Republic. Nowadays the power plant uses five PG 640 boilers with installed capacity of 5×200 MW. PG 640 is a two pass boiler with a special position of an in-plant storage silo, which is situated between a combustion chamber and the second pass. The boiler uses brown coal transported via railway from opencast mines (mostly Hrabák) (41). The coal is fed into the combustion chamber using eight beater wheel mills. The shape of the combustion chamber is shown in Figure 3.3.1-2. The profile of the combustion chamber is not entirely rectangular, but two edges are chamfered to provide additional place for burners. The boiler uses total amount of 8 burners (4 on the chamfered edges, 2 in the middle of the rear wall and 2 on the side walls). Each burner feeds the combustion process by 12 nozzles. Under the burners (except burners on the side walls) there is one natural gas-fired start-up and stabilization burner. (42)

The boiler was modified in 1997-1998 to meet newly implemented NO_x emission limits of 500 mg/Nm^3 by using of air staging method. Since then the boilers have been equipped with over-fire air admission with 10 circular nozzles. Air staging control was implemented in dependence on the steam output of the boiler and air excess in flue gas. Burners were also able to control the amount of the secondary combustion air to provide correct air excess ratio. The air control was modified in order to improve combustion process in 2004 on one boiler. The rest of the boilers were modified the same way between 2009 and 2010. The air fan controls the air pressure in dependence on steam output. After these denitrification techniques the boiler is able to achieve the required NO_x limit that id valid until 31. 12. 2015 (500 mg/Nm^3). (42)

3.2.2 Denitrification requirements

From 1st January 2016 the boiler must achieve NO_x limit of 200 mg/Nm^3. NH_3 slip is required to be under 10 mg/Nm^3. The suggested denitrification technique must ensure this requirements within given fuel range and boiler operational range.

3.2.3 Possible variants of denitrification methods

The study takes into account two possible variants of denitrification of the boiler. The first variant (variant 1) uses SCR method while the second variant (variant 2) combines primary and secondary denitrification methods when using SNCR together with additional modification of burners and over-fire air (OFA) supply.

Variant 1: using only SCR method only

This variant studies the possibility and feasibility of SCR applied on the boiler. The SCR method consists mainly of an area with a catalyst and injecting lances. The position of the SCR reactor ensures the right temperature range for the SCR reaction (laying between 320 and 400°C (10)). In this particular boiler the temperature range lies between the economizer bundles, upstream from the air heater (this boiler uses the German LUVO (Luftvorwärmer) type of air heater). The possible space for a proper installation of SCR technology between the economizer bundles and the air heater is not sufficient, so another flue-gas pass with the SCR reactor should be built. A typical SCR reactor consists of injection lances, a modulating area of flue gas stream and an area with catalyst modules. The modulating area is needed for modulation of the flue gas stream with the reagent to ensure straight flow through the catalyzer. A design of the possible SCR reactor is shown in Figure 3.2.3-1. In the design one part of an economizer is placed after the catalyst elements – this layout is made to the fact that the duct system of the boiler does not have enough space for a turning chamber. The suggested design of the SCR reactor is only a rough lay-out to provide data for following economic analysis – for proper design of the reactor it is necessary to determine the proper position for SCR installation. The reactor has outer insulation and is supported by the supporting structure. The reagent supply technology consists of a storage tank for reagent, mixing module, metering module and reagent distribution module. The reagent pipes are from stainless steel and insulated.

Variant 2: using SNCR plus primary denitrification methods

With the SNCR method, it is usually necessary to also simultaneously use other primary denitrification methods. It is assumed that SNCR consists of two injecting levels, located near the area of the platen superheater and reagent supply technology. Primary denitrification is ensured by installation of new low-NOx burners and system of over-fire air supply (OFA). The reagent supply technology is similar to the technology applied on the variant using only SCR method.

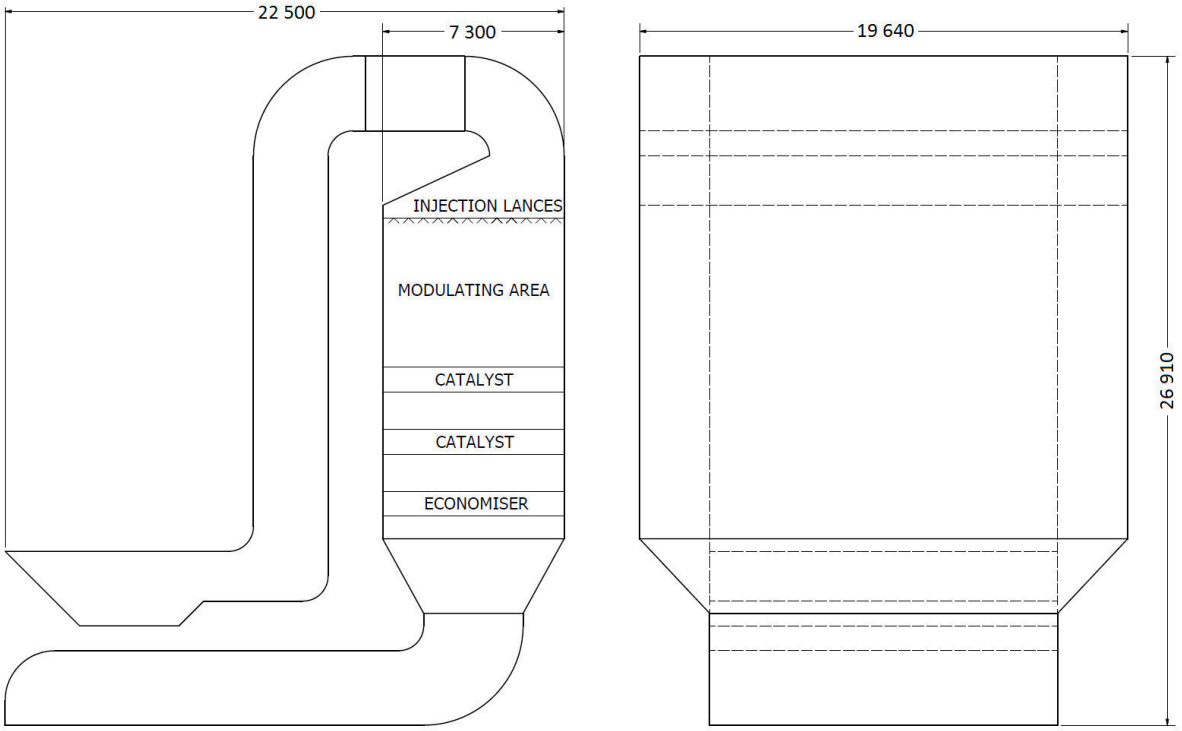

Figure 3.2.3-1 SCR reactor lay-out

3.2.4 Economic analysis of secondary denitrification methods

The investment costs analysis studies secondary denitrification methods (SCR and SNCR) in terms of their investment cost. The study calculates with predicted costs which are relative to the particular boiler placed in the Počerady powerplant. The analysis is made only as a rough estimation of the investment costs and contains only the main costs of material and work. It is possible that in a real realization there can be some additional aspects which are not considered in the calculation, so the real final investment costs can be different.

Due to the fact that SCR and SNCR method have different denitrification effectiveness, the SNCR method is supported by some primary methods - installation of low NO_x burners and reformation of over-fire air ducting. It is assumed that both of these variants reach the same denitrification effectiveness.

Unit prices of the components, material and work are the same for both variants to ensure the comparability of the costs. The prices are taken from Alstom purchasing department and represent the approximate value, so the real price can vary according to specific conditions.

The economic analysis of SCR assumes following expectations:

- The catalyst consists of 2 layers with overall volume of 260 m^3. The catalyst consists of 66 elements with size 1880×946×1006 mm and weight of 540 kg/element.
- The costs of technology for reagent injection and storage (injection module, compressed air station, storage tank and tank for mixing) include all the costs of installation etc.
- The carbon steel ducting for the SCR reactor is insulated. It is assumed that additional 60% of the ducting weight is used for reinforcement (strengthening of the ducting).
- The SCR reactor is surrounded by a 2 level platform (2 m wide) for service usage.

- It is assumed that weight of the supporting construction of the reactor is 25 kg·m^3 of the reactor.
- The reagent supply piping is made of stainless steel with inner diameter of 40 mm and thickness of 5 mm. The overall length of the pipes is considered 1000 m.
- The surface of the ducting and the reagent pipes are insulated.
- The last part of the economizer is placed after the catalysts in the SCR reactor. The weight of the last part of the economizer is estimated to be 1/3 of the whole economizer. The weight of the economizer is estimated to be 846 239 kg (this value calculated by assuming heat surface area of 12 410 m^2 and tubes of outer diameter 28 mm and thickness 4.5 mm – these data are taken from the design documentation of the economizer – and an additional +15% of the weight is added to estimate the weight of additional material used for supporting of the economizer)

The economic analysis of SNCR assumes following expectations:

- Original burner are replaced by low NO_x burners
- The SNCR system is supposed to use two injecting levels. Each level consists of 38 injecting lances
- The costs of technology for reagent injection and storage (injection module, compressor station, storage tank and tank for mixing) includes all the costs of installation etc.
- Electronics and measurement devices are modified (cabling, pressure sensors, temperature sensors, flow indicators, upgrade of existing control system, installation of AGAM etc.)
- New over-fire air ducting is used (60% of the ducting weight is assumed for reinforcement)
- Installation of the injecting lances requires modification of the evaporator tubes in the furnace – it is assumed that for each injecting lance, 0.3 m^2 of evaporator is reshaped.
- The reagent supply piping is made of stainless steel with inner diameter of 40 mm and thickness of 5 mm. The overall length of the pipes is 1000 m.
- The over-fire air ducting and the reagent supply piping are insulated.
- When calculating the investment cost of SNCR-only technology, the calculation uses following items: injecting lances, technology for reagent injection and storage, electronics and measurements, material and work for evaporator tubes replacement, material and work for reactant pipes and engineering.

The investment costs of the variants are shown in Table 3.2.4-1 and Table 3.2.4-2. The overall investment costs of variant 1 are **193 155 129 CZK** and for variant 2 are **155 647 695 CZK**. The investment costs for SNCR method are **38 728 718 CZK**.

Table 3.2.4-1 Investment costs of variant 1

Investment costs - Variant 1						
	Unit price		**Amount**		**Final price**	
Components						
Catalyser	156 750	CZK/m^3	260	m^3	40 717 315	CZK
Soot blower	33 814	CZK/m^2	235	m^2	7 941 588	CZK
Injection module					1 700 000	CZK
Compressor station					3 000 000	CZK
Storage tank 100 m^3	1 625 000	CZK/pc	1	pc	1 625 000	CZK
Tank for mixing 50 m^3	6 500 000	CZK/pc	1	pc	6 500 000	CZK
Material						
Ducting (+60% strengthening)	114	CZK/kg	192 399	kg	21 933 521	CZK
Platforms	86	CZK/kg	49 504	kg	4 232 592	CZK
Supporting construction	86	CZK/kg	297 116	kg	25 403 450	CZK
Piping - reactant pipes	200	CZK/kg	21 771	kg	4 354 247	CZK
Isolation - ducting+reactor	1 830	CZK/m^2	3 064	m^2	5 606 540	CZK
Isolation - reactant pipes	1 100	CZK/m^2	157	m^2	172 788	CZK
Work						
Engineering					2 000 000	CZK
Installation (throttling, measuring)					142 500	CZK
Economiser modification					1 000 000	CZK
Disassembling economiser	5	CZK/kg	282 079	kg	1 410 394	CZK
Disassembling- walls	5	CZK/kg	35 811	kg	179 054	CZK
Assembling - supporting construction	25	CZK/kg	346 620	kg	8 665 509	CZK
Assembling - steel duct	86	CZK/kg	192 399	kg	16 450 141	CZK
Assembling - economiser	25	CZK/kg	282 079	kg	7 051 969	CZK
Assembling - catalyser	25	CZK/kg	35 656	kg	891 397	CZK
Assembling - stainless steel piping	100	CZK/kg	21 771	kg	2 177 124	CZK
Construction work					30 000 000	CZK
Overall investment costs for variant 1					**193 155 129**	**CZK**

Table 3.2.4-2 Investment costs for the variant 2

Invesment costs - Variant 2						
	Unit price		**Amount**		**Final price**	
Components						
Low NO_x burners					65 000 000	CZK
Injecting lances	30 000	CZK/pc	76	pc	2 280 000	CZK
Compressor station					3 000 000	CZK
Storage tank 130 m^3	1 920 455	CZK/pc	1	pc	1 920 455	CZK
Tank for mixing 50 m^3	6 500 000	CZK/pc	1	pc	6 500 000	CZK
Electronics and measurements					14 000 000	CZK
Materials						
Over-fire air ducting (+60% strenghtening)	114	CZK/kg	332 372	kg	37 890 464	CZK
Evaporator tubes	170	CZK/kg	4 469	kg	759 804	CZK
Piping - reactant pipes	200	CZK/kg	21 771	kg	4 354 247	CZK
Isolation - reactant pipes	1 100	CZK/m^2	157	m^2	172 788	CZK
Isolation - over-fire air ducting	1 830	CZK/m^2	666	m^2	1 219 200	CZK
Work						
Engineering					2 000 000	CZK
Disassembling - tubes of evaporator	175	CZK/kg	4 469	kg	782 151	CZK
Assembling - stainless steel piping	100	CZK/kg	21 771	kg	2 177 124	CZK
Assembling - tubes of evaporator	175	CZK/kg	4 469	kg	782 151	CZK
Assembling - over-fire air ducting	25	CZK/kg	332 372	kg	8 309 312	CZK
Construction work					4 500 000	CZK
Overall investment costs for variant 2					**155 647 695**	**CZK**
Investment costs of SNCR technology					38 728 718	CZK

3.2.5 Selection of suitable denitrification method for the boiler

The selection of a suitable denitrification method considers investment costs, boiler dispositions and installation difficulties. Investment costs of variant 2 are by 19.4% lower than of variant 1. The installation of variant 1 has higher disposition requirements due to the need of catalyst, which needs to be placed in a new flue-gas pass. Installation difficulties of variant 1 include an installation and connection of the catalyst with the flue gas duct and economizer modifications. The installation of variant 2 brings changes into combustion process since new burners and OFA ducting is proposed to be replaced. According to these aspects **variant 2 is chosen as the more suitable solution**.

3.3 Detailed design of chosen denitrification method

When dealing with variant 2 it is essential to determine a proper area in the furnace where the flue gas has the right temperature for the SNCR denitrification process. This task is further solved and it is the fundamental part of the work.

To find the proper area, it is necessary to perform a thermal calculation of the furnace, determine temperatures there, and then determine the proper area where the denitrification process (reaction between reactant and flue gas) should take place. One the proper area has been identified, then the position for the injecting lances (chapter 3.3.3), which mix the reagent with flue gas, is designed. Proper mixing of the reagent with flue gas, together with the right temperature of the resulting denitrification process, is essential for high denitrification rate and low ammonia slip.

3.3.1 Determination of suitable area in the furnace for denitrification process

The suitable area for SNCR in the flue gas temperature range between 870-1150°C (35). The aim of this subchapter is to find the area in the boiler where the flue gas stream achieves these temperatures. The boiler is supposed to operate mainly between 60-100% BMCR with the fuel defined by two limit fuel compositions. Due to these aspects it is necessary to ensure that the suitable area for SNCR is suitable within all these conditions, therefore the following thermal calculation is performed for four different boiler conditions according to different boiler load (60% and 100%) and fuel composition (two types).

The following thermal calculations are made according to the normative method used for thermal calculation of boilers written by Budaj (15). This method is written in Czech and uses symbols according to Czech nomenclature. Due to this fact the calculation uses derived nomenclature mostly retrieved from the book *Boilers and Burners: Design and Theory* (19).

At the beginning of the calculation fuel characteristics (chapter 3.3.1.1), enthalpies of air and flue gas (chapter 3.3.1.2) and boiler heat balance (chapter 3.3.1.3) are determined. Then a thermal calculation of the furnace (chapter 3.3.1.4) and a zonal calculation of the furnace (chapter 3.3.1.5) is made to find out flue gas temperature above the platen superheater inlet. Finally a calculation of the platen superheater (chapter 3.3.1.6) is carried out.

The following equations contain only values for an upper limit coal (ULC) and the boiler load of 100% BMCR. Important results of other coal compositions and boiler loads are then shown in chapter 3.3.2.

3.3.1.1 Fuel characteristics

For a proper calculation of the temperature range for the SNCR method it is important to calculate the combustion process for different coal composition. The fuel range is described in Table 3.3.1-1. A wide range of coal compositions is substituted by two limit coals - an upper limit coal (ULC) and a lower limit coal (LLC). These two fuels represent the best coal and the worst coal, to be used as the fuel for the boiler. ULC is considered as the coal with minimal water content (minimal M_r) and LLC as the coal with maximal water content (maximal M_r).

Table 3.3.1-1 Fuel range of used coal

Parameter	Symbol	Min	Max	Unit
Lower heating value (LHV)	Q_i^r	10500	12700	kJ·kg^{-1}
Water	W^r	23.8	32	%
Ash (dry basis)	A^d	35	45	%
Sulfur (raw basis)	S^r	0.8	1.8	%
Heating value of volatiles	Q_i^{daf}	25.5	26.4	GJ·t^{-1}
Volatiles (Dry and ash-free basis)	V^{daf}	55	55	%
Granularity		0	40	mm

The composition of ULC and LLC is calculated from the design coal (DC) dry ash-free (DAF) content and from fuel range properties. The calculation assumes that the ULC and LLC have the same DAF composition as DC. Detailed compositions are calculated in accordance with the ash and water range to achieve limit values of LHV. For ULC the water content is 23.8% and for LLC the water content is 32%. The ash content is calculated to result in LHV specified in fuel range (without getting over fuel range limits). For the fuel composition calculation, factors are used which are shown in Table 3.3.1-2. More detailed results from the fuel characteristic are shown in Appendix C.

Table 3.3.1-2 Factors for basis conversion (15 p. 19)

From	To		
	Raw basis	Dry basis	Dry and ash-free basis
Raw basis	1	$\frac{100}{100 - W_t^r}$	$\frac{100}{100 - W_t^r - A^r}$
Dry basis	$\frac{100 - W_t^r}{100}$	1	$\frac{100}{100 - A^d}$
Dry and ash-free basis	$\frac{100 - W_t^r - A^r}{100}$	$\frac{100 - A^d}{100}$	1

The calculation considers that the sulfur content in the fuel consists of two constituent parts – a volatile part (S_{vol}^r) and a sulfurous part (S_{sulf}^r). It is considered that the volatile part contains 70% of S^r(sulfur in raw basis) and the sulfurous part 30% of S^r (see Equation 3.3.1-1 and Equation 3.3.1-2). For the following calculations the sulfurous part is added to the ash (see Equation 3.3.1-3). Another presumption is that the raw water content (W^r) is equal to the total raw water content (W_t^r). The composition of limit coal used is shown in Table 3.3.1-3.

$$S_{vol}^r = 0.7 \cdot S^r = 0.7 \cdot 0.893 = 0.625\ \%$$ *Equation 3.3.1-1*

$$S_{sulf}^r = 0.3 \cdot S^r = 0.3 \cdot 0.893 = 0.268\ \%$$ *Equation 3.3.1-2*

$$A^r = 26.67 + S_{sulf}^r = 26.67 + 0.268 = 26.938\ \%$$ *Equation 3.3.1-3*

Table 3.3.1-3 Composition of used limit coal

Parameter	Symbol	Unit	LLC	ULC
Water	W^r	%	32.00	23.80
Ash	A^r	%	26.11	26.94
Sulfur	S^r	%	0.53	0.63
Carbon	C^r	%	28.30	33.28
Hydrogen	H^r	%	2.53	2.97
Nitrogen	N^r	%	0.46	0.54
Oxygen	O^r	%	10.07	11.84
Volatiles	V^{daf}	%	55.00	55.00
Lover heating value	Q_i^r	kJ·kg^{-1}	10 500	12 687

3.3.1.2 Amount and enthalpies of air and flue gas

Theoretical air requirement

Some of the following calculations are in m^3·kgf^{-1} (normal cubic meters per kilogram of fuel burnt). 1 m^3 is volume at 0°C (273.15 K) and 0.101 MPa.

Minimal volume of oxygen required to burn 1 kg of fuel, $V_{O_{2_{min}}}$:

$$V_{O_{2_{min}}} = \frac{22.39}{100} \cdot \left(\frac{C^r}{12.01} + \frac{H^r}{4.032} + \frac{S^r_{vol}}{32.06} - \frac{O^r}{32} \right) \quad \textit{Equation 3.3.1-4}$$

$$V_{O_{2_{min}}} = \frac{22.39}{100} \cdot \left(\frac{33.28}{12.01} + \frac{2.97}{4.032} + \frac{0.625}{32.06} - \frac{11.84}{32} \right) = 0.707 \text{ m}^3 \cdot \text{kgf}^{-1}$$

Minimal volume of dry air required to burn 1 kg of fuel, $V^d_{air_{min}}$:

$$V^d_{air_{min}} = \frac{100}{21} \cdot V_{O_{2_{min}}} \quad \textit{Equation 3.3.1-5}$$

$$V^d_{air_{min}} = \frac{100}{21} \cdot 0.707 = 3.37 \text{ m}^3 \cdot \text{kgf}^{-1}$$

Volume of water vapor for 1 m^3 of dry air, V_{H_2O}:

$$V_{H_2O} = \varphi \cdot \frac{p''}{p_c - p''} \quad \textit{Equation 3.3.1-6}$$

$$V_{H_2O} = 0.7 \cdot 0.044 = 0.031 \text{ [-]}$$

φ - relative humidity of air [-], $\varphi = 0.7$ [−]

$\frac{p''}{p_c - p''} = 0.044$ [−] - value of this expression is valid for 30°C (15 p. 44)

Coefficient f:

$f = 1.03$ [−] – for air temperature 30°C and relative air humidity of 0.7 [-] (15 p. 44)

Minimal volume of humid air required to burn 1 kg of fuel, $V_{air_{min}}$:

$$V_{air_{min}} = f \cdot V^d_{air_{min}} \qquad \textit{Equation 3.3.1-7}$$

$$V_{air_{min}} = 1.03 \cdot 3.37 = 3.47\ \mathrm{m^3 \cdot kgf^{-1}}$$

Minimal volume of dry flue gas, $V^d_{fg_{min}}$:

$$V^d_{fg_{min}} = V_{CO_2} + V_{SO_2} + V_{N_2} + V_{Ar} \qquad \textit{Equation 3.3.1-8}$$

$$V^d_{fg_{min}} = 0.62 + 0.0043 + 2.63 + 0.031 = 3.29\ \mathrm{m^3 \cdot kgf^{-1}}$$

Gas volume of CO_2, V_{CO_2}:

$$V_{CO_2} = \frac{22.26}{100} \cdot \frac{C^r}{12.01} + 0.0003 \cdot V^d_{air_{min}} \qquad \textit{Equation 3.3.1-9}$$

$$V_{CO_2} = \frac{22.26}{100} \cdot \frac{33.28}{12.01} + 0.0003 \cdot 3.37 = 0.62\ \mathrm{m^3 \cdot kgf^{-1}}$$

Gas volume of SO_2, V_{SO_2}:

$$V_{SO_2} = \frac{21.89}{100} \cdot \frac{S^r_{vol}}{32.06} \qquad \textit{Equation 3.3.1-10}$$

$$V_{SO_2} = \frac{21.89}{100} \cdot \frac{0.625}{32.06} = 0.0043\ \mathrm{m^3 \cdot kgf^{-1}}$$

Gas volume of N_2, V_{N_2}:

$$V_{N_2} = \frac{22.4}{100} \cdot \frac{N^r}{28.016} + 0.7805 \cdot V^d_{air_{min}} \qquad \textit{Equation 3.3.1-11}$$

$$V_{N_2} = \frac{22.4}{100} \cdot \frac{0.54}{28.016} + 0.7805 \cdot 3.37 = 2.63\ \mathrm{m^3 \cdot kgf^{-1}}$$

Gas volume of A_r in flue gas, V_{Ar}:

$$V_{Ar} = 0.0092 \cdot V^d_{air_{min}} \qquad \textit{Equation 3.3.1-12}$$

$$V_{Ar} = 0.0092 \cdot 3.37 = 0.031\ \mathrm{m^3 \cdot kgf^{-1}}$$

Maximal amount of CO_2 in the flue gas, $CO_{2_{max}}$:

$$CO_{2_{max}} = \frac{V_{CO_2}}{V^d_{fg_{min}}} \cdot 100 \qquad \textit{Equation 3.3.1-13}$$

$$CO_{2_{max}} = \frac{0.62}{3.29} \cdot 100 = 18.8\%$$

Minimal volume of water vapor in the flue gas, $V_{H_2O_{min}}$:

$$V_{H_2O_{min}} = \frac{44.8}{100} \cdot \frac{H^r}{4.032} + \frac{22.4}{100} \cdot \frac{W^r_t}{18.016} + (f-1) \cdot V^d_{fg_{min}} \qquad \textit{Equation 3.3.1-14}$$

$$V_{H_2O_{min}} = \frac{44.8}{100} \cdot \frac{2.97}{4.032} + \frac{22.4}{100} \cdot \frac{23.8}{18.016} + (1.03-1) \cdot 3.29$$

$$V_{H_2O_{min}} = 0.73\ \mathrm{m^3 \cdot kgf^{-1}}$$

Minimal volume of the humid flue gas, $V_{fg_{\min}}$:

$$V_{fg_{\min}} = V_{fg_{min}}^{d} + V_{H_2O_{min}} \qquad \textit{Equation 3.3.1-15}$$
$$V_{fg_{\min}} = 3.29 + 0.73 = 4.01 \text{ m}^3 \cdot \text{kgf}^{-1}$$

Determination of excess-air coefficient

Excess-air coefficient at the furnace exit, α_{fu}:

$\alpha_{fu} = 1.15\ [-]$

Excess-air coefficient downstream LUVO, α_{LUVO}:

$\alpha_{LUVO} = 1.348\ [-]$

Leakage air coefficient of the pulverization system, $\Delta\alpha_{pul}$:

$\Delta\alpha_{pul} = 0.2\ [-]$

Combustion chamber false air ratio, $\Delta\alpha_{fu}$:

$\Delta\alpha_{fu} = 0.15\ [-]$

Amount of infiltrated air, $\Delta\alpha_{\text{inf}}$:

$\Delta\alpha_{\text{inf}} = 0.125\ [-]$ – according to (15 p. 51)

Excess-air coefficient at air heater outlet, β''_{ah}:

$$\beta''_{ah} = \alpha_{fu} - \Delta\alpha_{fu} - \Delta\alpha_{pul} \qquad \textit{Equation 3.3.1-16}$$
$$\beta''_{ah} = 1.15 - 0.15 - 0.2 = 0.8\ [-]$$

Excess-air coefficient at air heater inlet, β'_{ah}:

$$\beta'_{ah} = \beta''_{ah} + \Delta\alpha_{inf} \qquad \textit{Equation 3.3.1-17}$$
$$\beta'_{ah} = 0.8 + 0.125 = 0.925\ [-]$$

Volume of air and flue gas

Real amount of air (with air excess), V_{air}:

$$V_{air} = \beta''_{ah} \cdot V_{air_{min}} \qquad \textit{Equation 3.3.1-18}$$
$$V_{air} = 0.8 \cdot 3.47 = 2.77 \text{ m}^3 \cdot \text{kgf}^{-1}$$

Real amount of the flue gas (with air excess $\alpha_f = 1.15[-]$),V_{fg}:

$$V_{fg} = V_{fg_{\min}} + (\alpha_{fu} - 1) \cdot V_{air_{min}} \qquad \textit{Equation 3.3.1-19}$$
$$V_{fg} = 4.01 + (1.15 - 1) \cdot 3.47 = 4.53 \text{ m}^3 \cdot \text{kgf}^{-1}$$

Real amount of water vapor (with air excess $\alpha_f = 1.15[-]$), V_{H_2O}:

$$V_{H_2O} = V_{H_2O_{min}} + (f-1)\cdot(\alpha_{fu}-1)\cdot V^d_{air_{min}}$$ *Equation 3.3.1-20*

$$V_{H_2O} = 0.73 + (1.03-1)\cdot(1.15-1)\cdot 3.37 = 0.74\ \mathrm{m^3\cdot kgf^{-1}}$$

Volume fraction of CO_2 and SO_2, r_{RO_2}:

$$r_{RO_2} = \frac{V_{SO_2}+V_{CO_2}}{V_{fg}} = \frac{0.004+0.62}{4.53} = 0.14\ [-]$$ *Equation 3.3.1-21*

Volume fraction of water vapor, r_{H_2O}:

$$r_{H_2O} = \frac{V_{H_2O}}{V_{fg}} = \frac{0.74}{4.53} = 0.16\ [-]$$ *Equation 3.3.1-22*

Sum of volume fraction of tri-atomic gases, r_{fg}:

$$r_{fg} = r_{RO_2} + r_{H_2O} = 0.14 + 0.16 = 0.3\ [-]$$ *Equation 3.3.1-23*

Nondimensional mass concentration of fly ash, μ:

$$\mu = \frac{10\cdot A^r}{V_{fg}}\cdot\frac{x_{fa}}{100}$$ *Equation 3.3.1-24*

$$\mu = \frac{10\cdot 26.94}{4.53}\cdot\frac{85}{100} = 50.5\ \mathrm{g\cdot m^{-3}}$$

x_{fa} - fraction of total ash in the fly ash [%], $x_{fa} = 85\%$ (15 p. 62)

Table 3.3.1-4 Mean values of combustion product for ULC

Parameter	Unit	α =1.150	α =1.348
V_{H_2O}	$Nm^3\cdot kgf^{-1}$	0.74	0.76
V_{fg}	$Nm^3\cdot kgf^{-1}$	4.53	5.22
r_{RO_2}	-	0.14	0.12
r_{H_2O}	-	0.16	0.15
r_{fg}	-	0.30	0.27
μ	$g\cdot m^{-3}$	50.51	43.87

Mass of air and flue gas

Minimal mass of combustion oxygen, $G_{O_{2_{min}}}$:

$$G_{O_{2_{min}}} = \frac{32}{100}\cdot\left(\frac{C^r}{12.01}+\frac{H^r}{4.032}+\frac{S^r_{vol}}{32.06}-\frac{O^r}{32}\right)$$ *Equation 3.3.1-25*

$$G_{O_{2_{min}}} = \frac{32}{100}\cdot\left(\frac{33.28}{12.01}+\frac{2.97}{4.032}+\frac{0.63}{32.06}-\frac{11.84}{32}\right) = 1.01\ \mathrm{kg\cdot kgf^{-1}}$$

Minimal mass of dry combustion air for 1 kg of burned fuel, $G^{d}{}_{air_{min}}$:

$$G^{d}{}_{air_{min}} = \frac{1}{0.2331} \cdot G_{O_{2min}} \qquad \textit{Equation 3.3.1-26}$$

$$G^{d}{}_{air_{min}} = \frac{1}{0.2331} \cdot 1.01 = 4.36 \text{ kg} \cdot \text{kgf}^{-1}$$

- 0.2331 is a relative mass of oxygen in dry air.

Minimal mass of humid combustion air for 1 kg of burned fuel, $G_{air_{min}}$:

$$G_{air_{min}} = G^{d}_{air_{min}} + (f-1) \cdot \frac{1}{0.21} \cdot 0.804 \cdot V_{O_{2min}} \qquad \textit{Equation 3.3.1-27}$$

$$G_{air_{min}} = 4.36 + (1.03-1) \cdot \frac{1}{0.21} \cdot 0.804 \cdot 0.707 = 4.42 \text{ kg} \cdot \text{kgf}^{-1}$$

Mass of humid air with excess of β''_{ah}, G_{air}:

$$G_{air} = \beta''_{ah} \cdot G_{air_{min}} \qquad \textit{Equation 3.3.1-28}$$

$$G_{air} = 0.8 \cdot 4.42 = 3.53 \text{ kg} \cdot \text{kgf}^{-1}$$

Mass of the humid flue gas for using of humid air with excess of α, G_{fg}:

$$G_{fg} = 1 + \alpha_{fu} \cdot G_{air_{min}} \qquad \textit{Equation 3.3.1-29}$$

$$G_{fg} = 1 + 1.15 \cdot 4.42 = 6.08 \text{ kg} \cdot \text{kgf}^{-1}$$

Mass of the humid flue gas for using of humid air with excess of α_{fu} for exact amount of ash in fuel, G^{ash}_{fg}:

$$G^{ash}_{fg} = 1 - \frac{A^r}{100} + \alpha_{fu} \cdot G_{air_{min}} \qquad \textit{Equation 3.3.1-30}$$

$$G^{ash}_{fg} = 1 - \frac{26.94}{100} + 1.15 \cdot 4.42 = 5.81 \text{ kg} \cdot \text{kgf}^{-1}$$

Enthalpy calculation of air and combustion products

The calculation of enthalpies is made for a wide temperature range (see Table 3.3.1-5). The following sample calculation is made for temperature of 1000°C. Enthalpies of particular constituents of flue gas are taken from the table in (15 p. 25).

Enthalpy of flue gas for $\alpha = 1$ [-], $H_{fg_{\min}}$:

$$H_{fg_{\min}} = V_{CO_2} \cdot h_{CO_2} + V_{SO_2} \cdot h_{SO_2} + V_{N_2} \cdot h_{N_2} + V_{H_2O_{min}} \cdot h_{H_2O} + V_{Ar} \cdot h_{Ar} \qquad \textit{Equation 3.3.1-31}$$

$$H_{fg_{\min}} = 0.62 \cdot 2204 + 0.004 \cdot 2305 + 2.63 \cdot 1392 + 0.73 \cdot 1723 + 0.031 \cdot 928$$

$$H_{fg_{\min}} = 6318.3 \text{ kJ} \cdot \text{kgf}^{-1}$$

h_{CO_2} – enthalpy of CO_2 [kJ·m^{-3}]

h_{SO_2} – enthalpy of SO_2 [kJ·m^{-3}]

h_{N_2} – enthalpy of N_2 [kJ·m^{-3}]

h_{H_2O} – enthalpy of H_2O [kJ·m^{-3}]

h_{Ar} – enthalpy of Ar [kJ·m^{-3}]

Theoretical cold air enthalpy entering boiler (for $\alpha = 1$), $H_{air_{min}}$:

$$H_{air_{min}} = V^d_{air_{min}} \cdot (c \cdot t)_{air}$$ *Equation 3.3.1-32*

$$H_{air_{min}} = 3.37 \cdot 1.46 \cdot 1000 = 4922 \text{ kJ} \cdot \text{kgf}^{-1}$$

$$c = c_s + 0.0016 \cdot d \cdot c_{H_20}$$ *Equation 3.3.1-33*

$$c = 1.41 + 0.0016 \cdot 18.65 \cdot 1.72 = 1.46 \text{ kJ} \cdot \text{m}^{-3} \cdot \text{K}^{-1}$$

c_s - specific heat capacity of dry air [kJ·m^{-3}·K^{-1}]

c_{H_2O} - specific heat capacity of water [kJ·m^{-3}·K^{-1}]

c - specific heat capacity of wet air [kJ·m^{-3}·K^{-1}]

d - amount of water in 1 kg of dry air [g·kg^{-1}]:

$$d = (f - 1) \cdot \frac{\rho_{H2O_o}}{\rho_{air_o}} \cdot 10^3$$ *Equation 3.3.1-34*

$$d = (1.03 - 1) \cdot \frac{0.804}{1.293} \cdot 10^3 = 18.65 \text{ g} \cdot \text{kg}^{-1}$$

Values of expression $\frac{\rho_{H2O_o}}{\rho_{air_o}}$ is taken from (15 p. 57).

Enthalpy of fly ash:

The enthalpy of fly ash should be used in the calculation if the following equation (Equation 3.3.1-35) is valid:

$$A^r > \frac{6 \cdot Q_i^r}{41.8} \cdot x_{fa} = \frac{6 \cdot 12687}{41.8} \cdot 85$$ *Equation 3.3.1-35*

$$A^r (= 26.94) > 21.43$$

The enthalpy of fly ash should be used in the following calculation.

$$H_{fa} = \frac{A^r}{100} \cdot \frac{x_{fa}}{100} \cdot h_{fa}$$ *Equation 3.3.1-36*

$$H_{fa} = \frac{26.94}{100} \cdot \frac{85}{100} \cdot 984 = 225.3 \text{ kJ} \cdot \text{kgf}^{-1}$$

Flue gas enthalpy originated from burning of 1 kg of fuel, H_{fg}:

$$H_{fg} = H_{fg_{min}} + (\alpha_{fu} - 1) \cdot H_{air_{min}} + H_{fa}$$ *Equation 3.3.1-37*

$$H_{fg} = 6\,318 + (1.15 - 1) \cdot 4\,922 + 225 = 7\,282 \text{ kJ} \cdot \text{kgf}^{-1}$$

Results from the calculations of enthalpies are shown Table 3.3.1-5 and Figure 3.3.1-1.

Table 3.3.1-5 Flue gas and air enthalpies in dependence on temperature for ULC

$t\ [°C]$	$H_{fg_{min}}\ [\mathrm{kJ \cdot kg^{-1}}]$	$H_{air_{min}}\ [\mathrm{kJ \cdot kg^{-1}}]$	$H_{fa}\ [\mathrm{kJ \cdot kg^{-1}}]$	$H_{fg}\ [\mathrm{kJ \cdot kg^{-1}}]\ \alpha_{fu} = 1.15$
100	560	453	18	646
200	1 134	911	39	1 309
300	1 726	1 377	60	1 992
400	2 335	1 853	82	2 696
500	2 962	2 340	105	3 418
600	3 604	2 838	128	4 158
700	4 262	3 346	152	4 915
800	4 934	3 864	176	5 689
900	5 620	4 389	200	6 478
1000	6 318	4 922	225	7 282
1500	9 933	7 665	395	11 478
1600	10 682	8 224	430	12 346
1800	12 199	9 354	502	14 104
2000	13 735	10 497	577	15 887

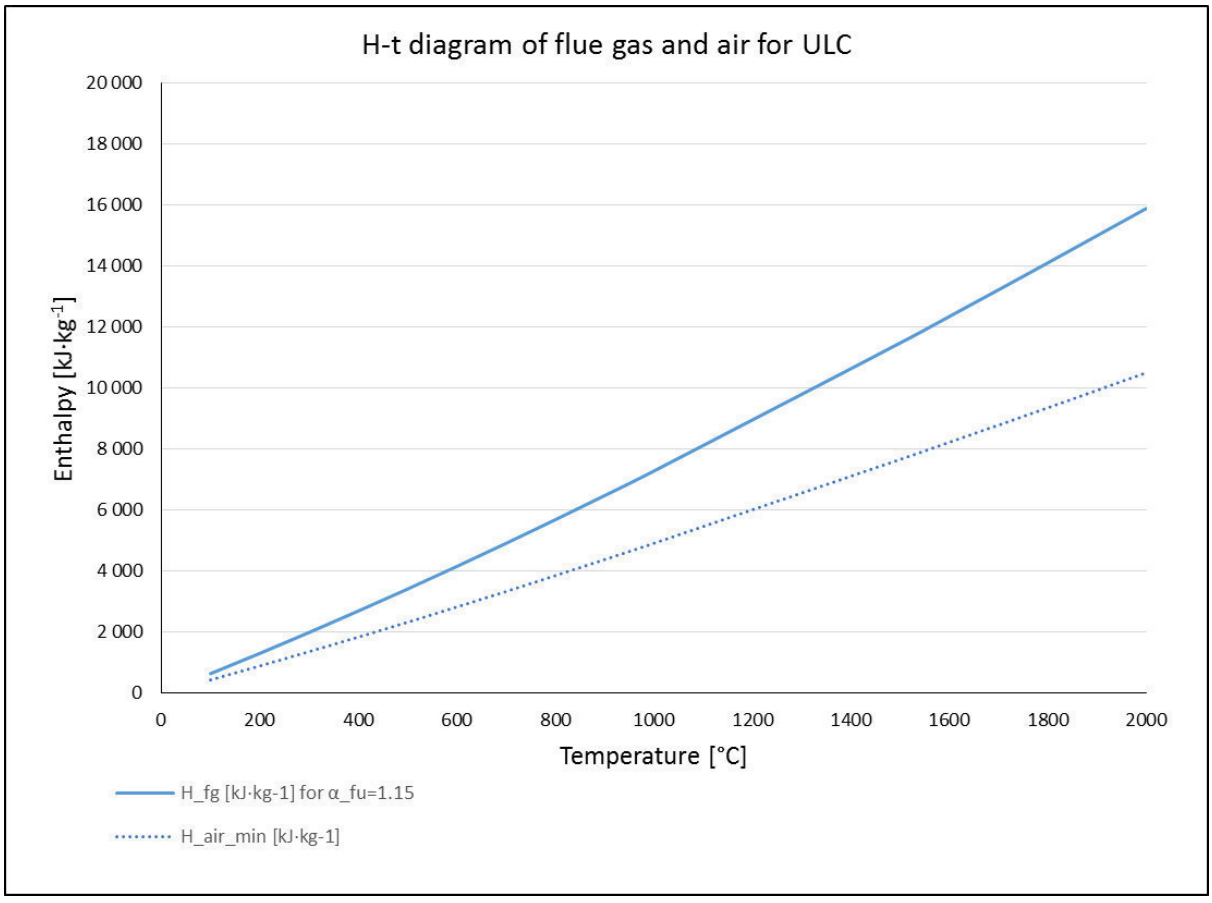

Figure 3.3.1-1 H-t diagram of flue gas and air for ULC

Results from the calculation of stoichiometry for LLC can be found in Appendix D.

3.3.1.3 Boiler heat balance

The heat balance of the boiler is given by Equation 3.3.1-38.

$$Q = Q_1 + Q_2 + Q_3 + Q_4 + Q_5 + Q_6 \qquad \textit{Equation 3.3.1-38}$$

Q – available heat of fuel fired [kJ·kg^{-1}]

Q_1 – heat absorbed by water and steam [kJ·kgf^{-1}]

Q_2 – heat loss through stack gas [kJ·kgf^{-1}]

Q_3 – heat loss by incomplete combustion [kJ·kgf^{-1}]

Q_4 – heat loss owing to unburned carbon in refuse [kJ·kgf^{-1}]

Q_5 – heat loss owing to convection and radiation from the furnace exterior [kJ·kgf^{-1}]

Q_6 – heat loss through the sensible heat of ash and slag [kJ·kgf^{-1}]

By dividing both sides of Equation 3.3.1-38 with Q, we get the heat losses in percentage:

$$100 = q_1 + q_2 + q_3 + q_4 + q_5 + q_6 \qquad \textit{Equation 3.3.1-39}$$

Where $q_i = \frac{Q_i}{Q} \cdot 100$ represents the percentage heat which is available.

Input heat to boiler

The total heat input to the coal-fired boiler is given by Equation 3.3.1-40.

$$Q = Q_i^r + H_f \qquad \textit{Equation 3.3.1-40}$$

$$Q = 12\,687.46 + 27.87 = 12\,715.34 \text{ kJ} \cdot \text{kg}^{-1}$$

H_f – sensible heat of fuel [kJ·kg^{-1}]

$$H_f = c_{pf} \cdot t_f = 1.86 \cdot 15 = 27.87 \text{ kJ} \cdot \text{kg}^{-1} \qquad \textit{Equation 3.3.1-41}$$

t_f – fuel temperature at burner or feeder exit [°C]; $t_f = 15°\text{C}$

c_{pf} – specific heat of fuel, as received basis [kJ·kg^{-1}·K^{-1}]

$$c_{pf} = c_w \cdot \frac{W_t^r}{100} + c_{pf}^g \cdot \frac{100 - W_r^t}{100} \qquad \textit{Equation 3.3.1-42}$$

$$c_{pf} = 4.19 \cdot \frac{23.8}{100} + 1.13 \cdot \frac{100 - 23.8}{100} = 1.86 \text{ kJ} \cdot \text{kg}^{-1} \cdot \text{K}^{-1}$$

c_w – specific heat of water [kJ·kg^{-1}·K^{-1}]; $c_w = 4.19 \text{ kJ} \cdot \text{kg}^{-1} \cdot \text{K}^{-1}$

c_{pf}^g – specific heat, as dry basis [kJ·kg^{-1}·K^{-1}]; $c_{pf}^g = 1.13 \text{ kJ} \cdot \text{kg}^{-1}$

Heat losses

Heat loss through stack gas, q_2:

$$q_2 = (100 - q_4) \cdot \frac{H_{fg} - H_{air}}{Q_1}$$ *Equation 3.3.1-43*

$$q_2 = (100 - 1.67) \cdot \frac{1\,215.24 - 135.03}{12\,715.34} = 8.35\%$$

H_{fg} – flue gas enthalpy at the furnace exit [kJ·kg^{-1}]

H_{air} – enthalpy of cold air with excess-air coefficient after the furnace [kJ·kg^{-1}]

$$H_{air} = \alpha_{LUVO} \cdot H_{air_{min}} = 1.348 \cdot 100.174 = 135.034\ \text{kJ} \cdot \text{kg}^{-1}$$ *Equation 3.3.1-44*

$$H_{fg} = H_{fg_{min}} + (\alpha_{f_{LUVO}} - 1) \cdot H_{air_{min}}$$ *Equation 3.3.1-45*

$$H_{fg} = 949.18 + (1.348 - 1) \cdot 764.54 = 1\,215.24\ \text{kJ} \cdot \text{kg}^{-1}$$

$H_{fg_{min}}$ – flue gas enthalpy for α=1, t=168.2°C [kJ·kg^{-1}]

$\alpha_{f_{LUVO}}$ – excess-air coefficient after the furnace [-]; $\alpha_{LUVO} = 1.348\ [-]$

$H_{air_{min}}$ – theoretical cold air enthalpy entering boiler (for 25°C) [kJ·kg^{-1}]

Heat loss by incomplete combustion of gaseous components, q_3:

$q_3 = 0.75\%$ - the value is taken from (15 p. 61) and respects the boiler size

Heat loss owing to unburned carbon in refuse, q_4:

$$q_4 = Q_{fa} + Q_{ba} = 0.59 + 1.09 = 1.67\%$$ *Equation 3.3.1-46*

Q_{fa} – heat loss owing to fly ash [%]

Q_{ba} – heat loss owing to bottom ash [%]

$$Q_{fa} = \frac{C_{fa}}{100 - C_{fa}} \cdot \frac{X_{fa}}{100} \cdot \frac{A^r}{Q} \cdot Q_{cfa}$$ *Equation 3.3.1-47*

$$Q_{fa} = \frac{1}{100 - 1} \cdot \frac{84}{100} \cdot \frac{26.94}{12\,715.34} \cdot 32\,600 = 0.59\%$$

C_{fa} – carbon content in fly ash [%]; $C_{fa} = 1\%$

X_{fa} – ash fraction in fly ash [%]; $X_{fa} = 84\%$ – the value is taken from (15 p. 62)

Q_{cfa} – calorific value of refuse [kJ·kg^{-1}]; $Q_{cfa} = 32\,600\ \text{kJ} \cdot \text{kg}^{-1}$ – the value is taken from (15 p. 60) as an average calorific value for combustible matters in refuse

$$Q_{ba} = \frac{C_{ba}}{100 - C_{ba}} \cdot \frac{X_{ba}}{100} \cdot \frac{A^r}{Q} \cdot Q_{cba}$$ *Equation 3.3.1-48*

$$Q_{ba} = \frac{12.5}{100 - 12.5} \cdot \frac{11}{100} \cdot \frac{26.94}{12\,715.34} \cdot 32\,600 = 1.09\%$$

C_{ba} – carbon content in bottom ash [%]; $C_{ba} = 12.5\%$

X_{ba} – ash fraction in bottom ash [%]; $X_{ba} = 11\%$ – the value is taken from (15 p. 62)

Q_{cba} – calorific value of refuse [kJ·kg^{-1}]; $Q_{cba} = 32\,600\ \text{kJ} \cdot \text{kg}^{-1}$ – the value is taken from (15 p. 60) as an average calorific value for combustible matters in refuse

Heat loss owing to convection and radiation, q_5:

$q_5 = 0.3\%$ - the value is from (15 p. 63)

Heat loss through the sensible heat of ash and slag, q_6:

$$q_6 = \left(\frac{X_{ba}}{100 - C_{ba}} \cdot c_{ba} \cdot t_{ba} + \frac{X_{fa}}{100 - C_{fa}} \cdot c_{fa} \cdot t_{fa}\right) \cdot \frac{A^r}{Q}$$ *Equation 3.3.1-49*

$$q_6 = \left(\frac{11}{100 - 12.5} \cdot 0.93 \cdot 600 + \frac{84}{100 - 1} \cdot 0.84 \cdot 168.2\right) \cdot \frac{26.94}{12\,715.34}$$

$$q_6 = 0.40\%$$

c_{ba} – specific heat of slag [kJ·kg^{-1}·K^{-1}]; $c_{ba} = 0.93\ \text{kJ} \cdot \text{kg}^{-1} \cdot \text{K}^{-1}$ – the value is taken from (15 p. 23) for t_{ba}

t_{ba} – temperature of slag [°C]; $t_{ba} = 600°\text{C}$ – the value is taken from (15 p. 61)

c_{fa} – specific heat of fly ash [kJ·kg^{-1}·K^{-1}]; $c_{fa} = 0.84\ \text{kJ} \cdot \text{kg}^{-1} \cdot \text{K}^{-1}$ – the value is taken from (15 p. 23) for t_{fa}

t_{fa} – temperature of fly ash [°C] ; $t_{fa} = 168.2°C$

Boiler thermal efficiency

$$\eta_{bo} = 100 - q_2 - q_3 - q_4 - q_5 - q_6$$ *Equation 3.3.1-50*

$$\eta_{bo} = 100 - 8.35 - 0.75 - 1.67 - 0.3 - 0.4 = 88.52\%$$

Boiler fuel consumption

Combustion heat absorbed by the water and steam, Q_1:

$$Q_1 = D_{sup} \cdot \left(H''_{sup} - H_{fw}\right) + D_{rh} \cdot \left(H''_{rh} - H'_{rh}\right) \qquad \textit{Equation 3.3.1-51}$$

$$Q_1 = 177.78 \cdot \left(3\,395.25 - 1\,040.56\right) + 156.6 \cdot \left(3\,563.04 - 3082.82\right)$$

$$Q_1 = 493\,842.25 \text{ kJ} \cdot \text{kg}^{-1}$$

The flow rate of blow-down water is lower than 2%, so it is neglected in the calculation.

D_{sup} – superheated steam flow rate [kg·s^{-1}]; $D_{sup} = 177.78 \text{ kg} \cdot \text{s}^{-1}$

D_{rh} – reheated steam flow rate [kg·s^{-1}]; $D_{rh} = 156.67 \text{ kg} \cdot \text{s}^{-1}$

H''_{sup} – enthalpy of superheated steam [kJ·kg^{-1}]; $H''_{sup} = 3\,395.25 \text{ kJ} \cdot \text{kg}^{-1}$; for $t = 540°\text{C}$ and $p = 17.5 \text{ MPa}$

H_{fw} – enthalpy of feed water [kJ·kg^{-1}]; $H_{fw} = 1\,040.56 \text{ kJ} \cdot \text{kg}^{-1}$; for $t = 240°\text{C}$ and $p = 21.89 \text{ MPa}$

H''_{rh} – enthalpy of steam at reheater outlet[kJ·kg^{-1}]; $H''_{rh} = 3\,563.04 \text{ kJ} \cdot \text{kg}^{-1}$; for $t = 550°\text{C}$ and $p = 3.7 \text{ MPa}$

H'_{rh} – enthalpy of steam at reheater inlet [kJ·kg^{-1}]; $H'_{rh} = 3\,082.82 \text{ kJ} \cdot \text{kg}^{-1}$; for $t = 346°\text{C}$ and $p = 4.02 \text{ MPa}$

Amount of fuel fed into boiler, B_{fed}:

$$B_{fed} = \frac{Q_1}{Q \cdot \frac{\eta_{bo}}{100}} = \frac{493\,842.25}{12\,715.34 \cdot \frac{88.52}{100}} = 43.87 \text{ kg} \cdot \text{s}^{-1} \qquad \textit{Equation 3.3.1-52}$$

Amount of fuel burned in boiler, B:

$$B = B_{fed} \cdot \left(1 - \frac{q_4}{100}\right) = 43.87 \cdot \left(1 - \frac{1.67}{100}\right) = 43.14 \text{ kg} \cdot \text{s}^{-1} \qquad \textit{Equation 3.3.1-53}$$

3.3.1.4 Furnace calculation

Following calculations follow the method described by Budaj (15). It is a Russian method[1] introduced in 1973. The method is considered as the normative method and is often used for designing boiler equipment. This method uses some simplifications and many of the coefficients used are taken from similar realizations which do not describe real conditions. However the data (results) calculated according to this method are considered as sufficient for designing of boiler equipment.

The furnace calculation is carried out to determine flue outlet gas temperature. The calculation uses estimated value of the outlet temperature from the beginning of the calculation and this estimated value is compared with further calculated outlet temperature. The estimation is considered as sufficient when the calculated flue gas outlet temperature varies ±50°C from the estimated value. If this condition is not fulfilled the calculation will have to be recalculated with a new estimated value.

[1] Teplovoj rasčot kotelnych agregatov [TRKA]. Normativnyj metod. Moskva, Leningrad 1973

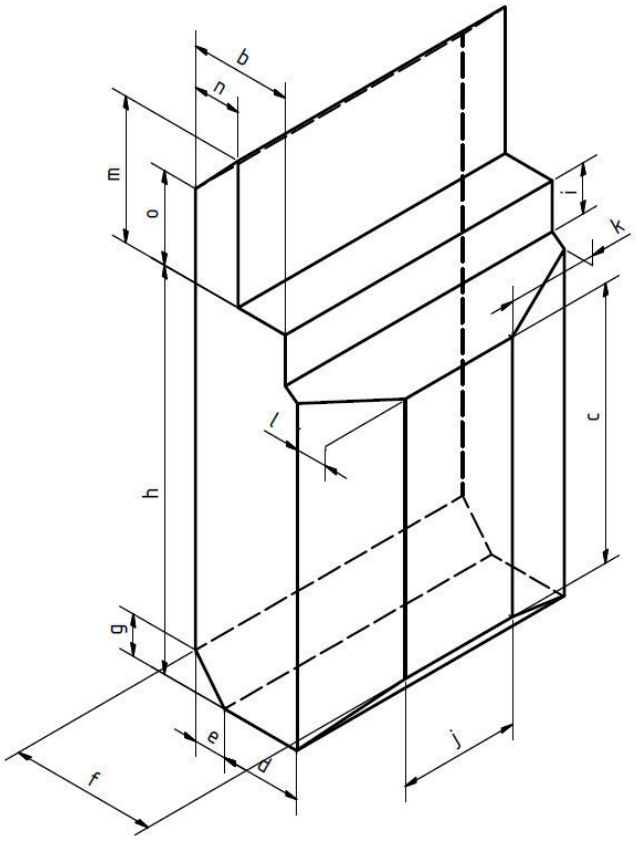

Parameter	Size [mm]
a	18940
b	6350
c	17182
d	5100
e	2050
f	9200
g	2589
h	25099
i	3132
j	7600
k	5670
l	2000
m	8645
n	2680
o	5804

Figure 3.3.1-2 Shape and proportions of the boiler furnace

The shape of the furnace (combustion chamber) and basic proportions is shown in Figure 3.3.1-2. The projected surface area of the furnace is 1 910.65 m^2. The active combustion chamber volume is 4 201.08 m^3. The furnace is enclosed by a water-cooled walls, known as the water wall. The water wall consists of many pipes. In this particular boiler there are three types of pipes. Due to this fact, the calculation of the furnace emissivity was calculated with three furnace sectors as is described in Table 3.3.1-6.

Table 3.3.1-6 Different water tubes used in the furnace and their parameters

Position	***D* [mm]**	***e* [mm]**	***s* [mm]**	x_i [-]	ξ_i [-]	F_i [m^2]
bottom	35	50	44	0.97	0.45	602.6
middle	38	50	46	0.98	0.45	396.2
top	45	50	63	0.94	0.45	516.8
D - outer diameter of water wall tubes						
e - distance from the refractory wall to the center of water wall tubes						
s - water wall tubes spacing						
x_i - angular coefficient of water wall tubes						
ξ_i - fouling factor for water wall tubes						
F_i - surface area						

Relative flue gas temperature, θ_{ou}:

$$\theta_{ou} = \frac{T_{ou}}{T_{th}} = \frac{1}{1 + M \cdot \left(\frac{a_{fu}}{B_0}\right)^{0.6}} = \frac{1}{1 + 0.45 \cdot \left(\frac{0.985}{1.21}\right)^{0.6}} = 0.71\ [-]$$ *Equation 3.3.1-54*

T_{ou} – absolute boiler-outlet flue gas temperature [K]

T_{th} – theoretical (adiabatic) flame temperature [K] – refers to Q_{fu}

M – temperature field coefficient [-]

B_o – Boltzmann number [-]

a_{fu} – overall emissivity of furnace [-]

Temperature field coefficient, *M*:

$$M = 0.59 - 0.5 \cdot (X_r + \Delta X) = 0.59 - 0.5 \cdot (0.224 + 0.05) = 0.453\ [-]$$ *Equation 3.3.1-55*

X_r – relative position of the highest temperature zone in the furnace [-]

ΔX – correction factor ($\Delta X = 0.05\ [-]$)

$$X_r = \frac{h_r}{h_{fu}} = \frac{6189}{27\,586} = 0.224\ [-]$$ *Equation 3.3.1-56*

h_r – relative position of the highest temperature zone in the furnace [*mm*]; $h_r = 6\,189$ mm

h_{fu} – height of the burner axis above the bottom of the furnace [*mm*]; $h_{fu} = 27\,586$ mm

Boltzmann number, B_o:

$$B_o = \frac{\varphi \cdot B \cdot \overline{V \cdot C_p}}{\sigma \cdot \bar{\psi} \cdot F \cdot T_{th}^3} = \frac{0.997 \cdot 43.14 \cdot 8.58}{5.7 \cdot 10^{-11} \cdot 0.34 \cdot 1910.65 \cdot 2013^3} = 1.21\ [-]$$ *Equation 3.3.1-57*

φ – coefficient of retention [-]

$\overline{V \cdot C_p}$ – average specific heat of combustion products formed by 1 kg of fuel within the temperature interval $T_{th} - T_{ou}$; [kJ·kg^{-1}·K^{-1}]

σ – Stefan-Boltzmann constant [kW·m^{-2}·K^{-4}]; σ=5.678·10^{-11} kW·m^{-2}·K^{-4}

$\bar{\psi}$ – thermal efficiency factor [-]

F – furnace overall wall surface [m^2], $F = 1910.65$ m^2

$$\varphi = 1 - \frac{q_5}{q_5 + \eta_{bo}} = 1 - \frac{0.3}{0.3 + 88.52} = 0.997\ [-]$$ *Equation 3.3.1-58*

$$\overline{V \cdot C_p} = \frac{Q_{fu} - H_{ou}}{T_{th} - T_{ou}} = \frac{13\,572.47 - 8\,629.27}{1\,739.8 - 1\,164} = 8.58\ \text{kJ} \cdot \text{kg}^{-1} \cdot \text{K}^{-1}$$ *Equation 3.3.1-59*

Q_{fu} – heat entering furnace through combustion and hot air [kJ·kg^{-1}]

H_{ou} – enthalpy of flue gas leaving the furnace [kJ·kg^{-1}]; for $t = 1\,164$°C

$$Q_{fu} = Q \cdot \frac{100 - q_3 - q_4 - q_6}{100 - q_4} + Q_{ai}$$ *Equation 3.3.1-60*

$$Q_{fu} = 12\,712.34 \cdot \frac{100 - 0.75 - 1.67 - 0.4}{100 - 1.67} + 1\,006.08$$

$$Q_{fu} = 13\,572.47\ \text{kJ} \cdot \text{kg}^{-1}$$

Q_{ai} – heat brought into the furnace by preheated and cold leakage air [kJ·kg^{-1}]

$$Q_{ai} = \left(\alpha_{fu} - \Delta\alpha_{fu} - \Delta\alpha_{pul}\right) \cdot H_{ha} + \left(\Delta\alpha_{fu} + \Delta\alpha_{pul}\right) \cdot H_{ca}$$ *Equation 3.3.1-61*

$$Q_{ai} = (1.15 - 0.15 - 0.2) \cdot 1\,208.18 + (0.2 + 0.15) \cdot 112.98$$

$$Q_{ai} = 1\,006.08\ \text{kJ} \cdot \text{kg}^{-1}$$

H_{ha} – enthalpy of preheated air [kJ·kg^{-1}], $H_{ha} = 1\,208.18\ \text{kJ} \cdot \text{kg}^{-1}$

H_{ca} – enthalpy of theoretical cold air [kJ·kg^{-1}], $H_{ca} = 112.98\ kJ \cdot kg^{-1}$

$$\bar{\psi} = \frac{\sum x_i \cdot \xi_i \cdot F_i}{F}$$ *Equation 3.3.1-62*

$$\bar{\psi} = \frac{0.97 \cdot 0.45 \cdot 602.2 + 0.98 \cdot 0.45 \cdot 396.2 + 0.94 \cdot 0.45 \cdot 516.8}{1\,910.45}$$

$$\bar{\psi} = 0.34\ [-]$$

Overall furnace emissivity, a_{fu}:

$$a_{fu} = \frac{a_{fl}}{a_{fl} + \left(1 - a_{fl}\right) \cdot \bar{\psi}} = \frac{0.96}{0.96 + (1 - 0.96) \cdot 0.34} = 0.985\ [-]$$ *Equation 3.3.1-63*

a_{fl} – flame emissivity [-]

$$a_{fl} = 1 - e^{-k \cdot P \cdot S} = 1 - e^{-3.997 \cdot 0.1 \cdot 7.92} = 0.96$$ *Equation 3.3.1-64*

k – coefficient of radiation absorption [$m^{-1} \cdot MPa^{-1}$]

P – pressure of gases in the furnace [MPa]; p=0.1 MPa

S – mean beam length of effective thickness of absorbing gas layer [m]

$$k = k_y \cdot r + k_h \cdot \mu + 10 \cdot c_1 \cdot c_2$$ *Equation 3.3.1-65*

$$k = 2.70 \cdot 0.30 + 0.053 \cdot 50.51 + 10 \cdot 0.5 \cdot 0.1 = 3.997 \text{ m}^{-1} \cdot \text{MPa}^{-1}$$

k_y – coefficient of radiant absorption owing to triatomic gases [$m^{-1} \cdot MPa^{-1}$]

r – total volume concentration of tri-atomic gases [-]

k_h – coefficient of radiant absorption owing to ash particles [-]

μ – concentration of ash particles in the furnace [$g \cdot m^{-3}$]

c_1 – coefficient determined by the type of fuel [-]; $c_1 = 0.5\ [-]$

c_2 – coefficient determined by the firing method [-]; $c_2 = 0.1\ [-]$

$$k_y = \left(\frac{7.8 + 16 \cdot r_{H_2O}}{3.16 \cdot \sqrt{r \cdot P \cdot S}} - 1\right) \cdot \left(1 - 0.37 \cdot \frac{T_{ou}}{1000}\right)$$ *Equation 3.3.1-66*

$$k_y = \left(\frac{7.8 + 16 \cdot 0.164}{3.16 \cdot \sqrt{0.3 \cdot 0.1 \cdot 7.92}} - 1\right) \cdot \left(1 - 0.37 \cdot \frac{1\,437.15}{1\,000}\right)$$

$$k_y = 2.70 \text{ m}^{-1} \cdot \text{MPa}^{-1}$$

r_{H_2O} – volume concentration of H_2O in flue gas [-]

$$S = 3.6 \cdot \frac{V}{F} = 3.6 \cdot \frac{4201.08}{1910.65} = 7.92 \text{ m}$$ *Equation 3.3.1-67*

V – furnace volume [m^3]

$$k_h = \frac{43}{\sqrt[3]{T_{ou}^2 \cdot d_h^2}} = \frac{43}{\sqrt[3]{1\,437.15^2 \cdot 16^2}} = 0.053 \text{ m}^{-1} \cdot \text{MPa}^{-1}$$ *Equation 3.3.1-68*

d_h – diameter of ash particles [μm]; $d_h = 16$ μm (15 p. 83))

3.3.1.5 Zonal calculation of the furnace

This part of the calculation is performed in order to determine the temperature profile along the furnace height. The calculation is necessary for proper determination of the injection levels of the reagent. The furnace is divided vertically into individual zones and then the outlet temperature of each zone is calculated.

The final outlet temperature from the furnace should be in the range of ±30°C of the furnace outlet temperature calculated in 3.3.1.4. When the calculated temperature exceeds the range, the fuel burn-out in particular zone should be corrected by changing of $\Delta\beta$ – amount of fuel burned in the zone. The calculation consists of areas above the burner zone (the zone with maximal heat release). It is not important to know the temperature profile below the burner zone.

The furnace is divided into six zones – the schematic model of the zones is shown in Figure 3.3.1-3. Zone 1 represents the zone with the maximal heat release and it is the area of the furnace where the burners are placed. The calculation of the zone with maximal heat release uses different equation than the calculation of other zones.

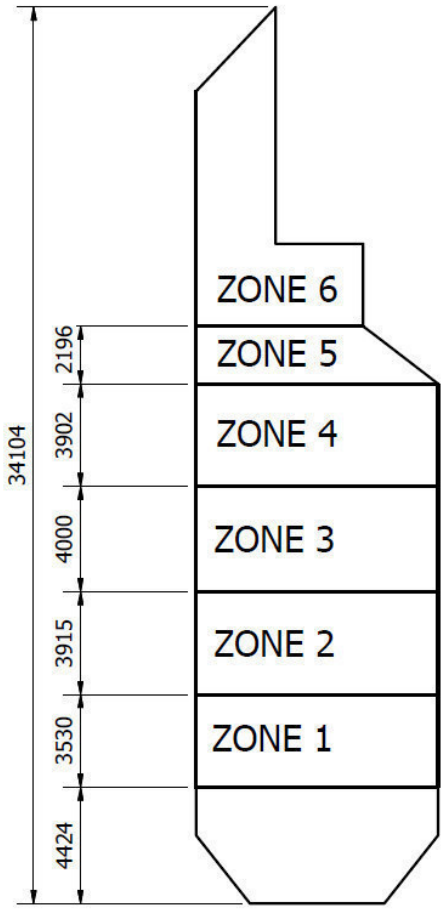

Figure 3.3.1-3 Furnace zones for zonal calculation of the furnace

Zone with maximal heat release

The flue gas temperature at the zone with maximal heat release (l_2^σ) is calculated by:

$$l_2^\sigma = \frac{100}{100 - q_4} \cdot \frac{\beta \cdot Q_i^r + Q_{ai} + c_{pf} \cdot t_f - Q_{slag}}{\overline{V \cdot C_p}} - \frac{a_{fu} \cdot \sigma \cdot T_2^4}{B \cdot \overline{V \cdot C_p}} \cdot \psi \cdot A_{zone}$$ *Equation 3.3.1-69*

$$l_2^\sigma = \frac{100}{100 - 1.67} \cdot \frac{0.75 \cdot 12\,687.46 + 1\,006.8 + 1.86 \cdot 15 - 18.96}{8.58} - \frac{0.997 \cdot 5.7 \cdot 10^{-11} \cdot 1\,434^4}{43.14 \cdot 8.58} \cdot 0.72 \cdot 186.96$$

$$l_2^\sigma = 1160.76\ °C$$

β – coefficient of heat release [-]; β=0.77 [-], the value is determined to observe final outlet temperature from the furnace calculated in 3.3.1.4 with the accuracy of ±30°C

Q_i^r – lower heating value [kJ·kg^{-1}]

Q_{ai} – heat brought into the furnace by preheated and cold leakage air [kJ·kg^{-1}]; $Q_{ai} = 1\,006.08\ kJ \cdot kg^{-1}$

c_{pf} – specific heat of fuel, as receives basis [kJ·kg^{-1}·K^{-1}]; $c_{pf} = 1.86\ kJ \cdot kg^{-1} \cdot K^{-1}$

t_f – fuel temperature at burner or feeder exit [°C]; $t_f = 15°C$

Q_{slag} – heat loss through the sensible heat of slag [kJ·kg^{-1}]

$\overline{V \cdot C_p}$ – average specific heat of combustion products formed by 1 kg of fuel within the temperature interval T_{th}– T_{ou}; [kJ·kg^{-1}·K^{-1}]

a_{fu} – overall emissivity of furnace [-]

σ – Stefan-Boltzmann constant; $\sigma = 5.678 \cdot 10^{-11}\ kW \cdot m^{-2} \cdot K^{-4}$

T_2 – flue gas outlet temperature from the zone [K]; the value is calculated through iteration calculation till $l_2^\sigma = t_2$

B - amount of fuel burned in boiler [kg·s^{-1}]; B=43.14 kg·s^{-1}

A_{zone} – area of the zone [m^2]; A_{zone}=186.97 m^2

ψ – thermal efficiency factor [-]

$$Q_{slag} = \frac{X_{ba}}{100 - C_{ba}} \cdot \frac{c_{ba} \cdot t_{ba} \cdot A_r}{100} = \frac{11}{100 - 12.5} \cdot \frac{0.93 \cdot 600 \cdot 26.94}{100}$$ *Equation 3.3.1-70*

$$Q_{slag} = 18.96\ \text{kJ} \cdot \text{kg}^{-1}$$

$$\overline{V \cdot C_p} = \frac{Q_{fu} - H_{ou}}{T_{th} - T_{ou}} = \frac{13\,572.47 - 8\,645.88}{1\,739.84 - 1\,161} = 8.58\ \text{kJ} \cdot \text{kg}^{-1} \cdot \text{K}^{-1}$$ *Equation 3.3.1-71*

Overall emissivity of furnace, zone 1:

$$a_{fu} = 1 - e^{-k \cdot P \cdot S} = 1 - e^{-5.35 \cdot 0.1 \cdot 11.07} = 0.997$$ *Equation 3.3.1-72*

k – coefficient of radiation absorption [$m^{-1} \cdot MPa^{-1}$]

P – pressure of gases in the furnace [MPa]; $p = 0.1\ MPa$

S – mean beam length of effective thickness of absorbing gas layer [m]

$$k = k_y \cdot r + k_h \cdot \mu + 10 \cdot c_1 \cdot c_2$$ *Equation 3.3.1-73*

$$k = 2.21 \cdot 0.30 + 0.053 \cdot 50.51 + 10 \cdot 0.5 \cdot 0.4 = 5.355\ \mathrm{m^{-1} \cdot MPa^{-1}}$$

k_y – coefficient of radiant absorption owing to triatomic gases [$m^{-1} \cdot MPa^{-1}$]

r – total volume concentration of tri-atomic gases [-]

k_h – coefficient of radiant absorption owing to ash particles [-]

μ_h – concentration of ash particles in the furnace [$g \cdot m^{-3}$]

c_1 – coefficient determined by the type of fuel [-]; $c_1 = 0.5$ [-]

c_2 – coefficient determined by the firing method [-]; $c_2 = 0.4$ [-]

$$k_y = \left(\frac{7.8 + 16 \cdot r_{H_2O}}{3.16 \cdot \sqrt{r \cdot P \cdot S}} - 1\right) \cdot \left(1 - 0.37 \cdot \frac{T_2}{1000}\right)$$ *Equation 3.3.1-74*

$$k_y = \left(\frac{7.8 + 16 \cdot 0.164}{3.16 \cdot \sqrt{0.3 \cdot 0.1 \cdot 11.07}} - 1\right) \cdot \left(1 - 0.37 \cdot \frac{1\,434}{1\,000}\right)$$

$$k_y = 2.21\ \mathrm{m^{-1} \cdot MPa^{-1}}$$

r_{H_2O} – volume concentration of H_2O in flue gas [-]; $r_{H_2O} = 0.146$ [-]

$$S = 3.6 \cdot \frac{V}{A_{zone}} = 3.6 \cdot \frac{575}{186.97} = 11.07\ \mathrm{m}$$ *Equation 3.3.1-75*

V – zone volume [m^3]; volume of zone 1 is 575 m^3

$$k_h = \frac{43}{\sqrt[3]{T_2^2 \cdot d_h^2}} = \frac{43}{\sqrt[3]{1\,434.15^2 \cdot 16^2}} = 0.053\ \mathrm{m^{-1} \cdot MPa^{-1}}$$ *Equation 3.3.1-76*

d_h – diameter of ash particles [μm]; $d_h = 16\ \mu m$ (15 p. 83))

T_2 - flue gas outlet temperature from the zone [K]

Thermal efficiency factor, ψ:

$$\psi = \frac{\bar{\psi} \cdot A_{zone} + \psi_1 \cdot A_{in} + \psi_2 \cdot A_{out}}{A_{zone}} \qquad \textit{Equation 3.3.1-77}$$

$$\psi = \frac{0.34 \cdot 186.97 + 0.34 \cdot 162.91 + 0.1 \cdot 162.91}{186.97} = 0.72\ [-]$$

$\bar{\psi}$ – mean thermal efficiency factor [-]

A_{zone} – zone side walls surface area [m^2]; $A_{zone} = 186.97$ m^2

ψ_1 – thermal efficiency factor for inlet cross-section of the zone [-], according to (15 p. 84) $\psi_1 = \bar{\psi}$

ψ_2 - thermal efficiency factor for outlet cross-section of the zone [-], according to (15 p. 84)

A_{in} – cross-section of the zone inlet [m^2], $A_{in} = 162.91\ m^2$

A_{out} – cross-section of the zone outlet [m^2], $A_{out} = A_{in} = 162.91\ m^2$

$\bar{\psi} = \frac{\sum x_i \cdot \xi_i \cdot A_i}{A_{zone}} = \frac{0.97 \cdot 0.45 \cdot 144.01}{186.97} = 0.34\ [-]$	*Equation 3.3.1-78*

ξ_i – fouling factor for water wall tubes [-];$\xi_i = 0.45\ [-]$

x_i – angular coefficient of water wall tubes [-]; $x_i = 0.97\ [-]$

A_i – surface area [m^2], for zone 1 $A_i = 144.01\ m^2$ (= zone side wall surface area – surface of the burners)

Other zones

Flue gas outlet temperatures from particular zones are calculated by using Equation 3.3.1-79. Following equations shows the calculation of zone 2. Other parameters used for calculation of other zones are described in Table 3.3.1-7.

The flue gas temperature at the outlet of zone 2, t_2 [°C]:

$$t_2 = \frac{\Delta\beta \cdot Q_i^r}{V_{fg} \cdot c_2} + \frac{c_1}{c_2} \cdot t_1 - \left[1 + \left(\frac{T_2}{T_1}\right)^4\right] \cdot \frac{\sigma \cdot a_{fu} \cdot T_1^4 \cdot \left[A_{1,2} \cdot (\psi_2 - \psi_1) + \bar{\psi} \cdot A_{zone}\right]}{2 \cdot B \cdot V_{fg} \cdot c_2} \qquad \textit{Equation 3.3.1-79}$$

$$t_2 = \frac{0.22 \cdot 12\,687.46}{4.53 \cdot 7.47} + \frac{7.54}{7.47} \cdot 1\,161 - \left[1 + \left(\frac{1\,511}{1\,434}\right)^4\right] \cdot \frac{5.7 \cdot 10^{-11} \cdot 0.9873 \cdot 1\,434^4 \cdot [163 \cdot 0 + 0.437 \cdot 207]}{2 \cdot 43.14 \cdot 4.53 \cdot 7.47}$$

$t_2 = 1\,237$ °C

$\Delta\beta$ – amount of fuel burned in the zone [%]

t_1 – flue gas temperature at the inlet of the zone [°C]

T_1 - flue gas temperature at the inlet of the zone [K]

t_2 – flue gas temperature at the outlet of the zone [°C]

T_2 - flue gas temperature at the outlet of the zone [K]

c_1 – flue gas specific heat for the temperature t_1 [kJ·m^{-3}·K^{-1}]

c_2 – flue gas specific heat for the temperature t_2 [kJ·m^{-3}·K^{-1}]

V_{fg} – real amount of flue gas [m^3·kgf^{-1}]

σ – Stefan-Boltzmann constant; $\sigma = 5.678 \cdot 10^{-11}\ kW \cdot m^{-2} \cdot K^{-4}$

a_{fu} – overall emissivity of furnace [-]; for zonal calculation it is calculated by interpolation between the zone 1 and zone 6

$A_{1,2}$ – mean value of the zone cross-section [m^2]

ψ_1 - thermal efficiency factor of the inlet cross-section of the zone [-]

ψ_2 - thermal efficiency factor of the outlet cross-section of the zone [-]

($\psi_1 - \psi_2$) – according to (15 p. 85) this value is equal to 0 for this type of boiler

$\bar{\psi}$ - thermal efficiency factor of the outlet cross-section of the zone [-]

Overall furnace emissivity – zone 6:

$$a_{fu} = 1 - e^{-k \cdot P \cdot S} = 1 - e^{-3.46 \cdot 0.1 \cdot 8.56} = 0.947 \text{ [-]} \qquad \textit{Equation 3.3.1-80}$$

k – coefficient of radiation absorption [m^{-1}·MPa^{-1}]

P – pressure of gases in the furnace [MPa]; $p = 0.1$ MPa

S – mean beam length of effective thickness of absorbing gas layer [m]

$$k = k_y \cdot r + k_h \cdot \mu + 10 \cdot c_1 \cdot c_2 \qquad \textit{Equation 3.3.1-81}$$
$$k = 2.57 \cdot 0.30 + 0.053 \cdot 50.51 + 10 \cdot 0.5 \cdot 0 = 3.46\ \text{m}^{-1} \cdot \text{MPa}^{-1}$$

k_y – coefficient of radiant absorption owing to triatomic gases [m^{-1}·MPa^{-1}]

r – total volume concentration of tri-atomic gases [-]

k_h – coefficient of radiant absorption owing to ash particles [-]

μ – concentration of ash particles in the furnace [g·m^{-3}]

c_1 – coefficient determined by the type of fuel [-]; $c_1 = 0.5$ [−]

c_2 – coefficient determined by the firing method [-]; $c_2 = 0.4$ [−]

$$k_y = \left(\frac{7.8 + 16 \cdot r_{H_2O}}{3.16 \cdot \sqrt{r \cdot P \cdot S}} - 1\right) \cdot \left(1 - 0.37 \cdot \frac{T_2}{1000}\right)$$ *Equation 3.3.1-82*

$$k_y = \left(\frac{7.8 + 16 \cdot 0.164}{3.16 \cdot \sqrt{0.3 \cdot 0.1 \cdot 8.56}} - 1\right) \cdot \left(1 - 0.37 \cdot \frac{1\,454}{1\,000}\right)$$

$$k_y = 2.54\ \mathrm{m^{-1} \cdot MPa^{-1}}$$

r_{H_2O} – volume concentration of H_2O in flue gas [-]; $r_{H_2O} = 0.163$ [–]

$$S = 3.6 \cdot \frac{V}{A_{zone}} = 3.6 \cdot \frac{376}{158.4} = 8.56\ \mathrm{m}$$ *Equation 3.3.1-83*

V – zone volume [m^3]; volume of zone 6 is 376 m^3

$$k_h = \frac{43}{\sqrt[3]{T_2^2 \cdot d_h^2}} = \frac{43}{\sqrt[3]{1\,454^2 \cdot 16^2}} = 0.053\ \mathrm{m^{-1} \cdot MPa^{-1}}$$ *Equation 3.3.1-84*

d_h – diameter of ash particles [μm]; $d_h = 16$ μm (15 p. 83))

T_2 - flue gas outlet temperature from the zone [K]

Table 3.3.1-7 Parameters used for the zonal calculation

Parameter	Unit	Zone 2	Zone 3	Zone 4	Zone 5	Zone 6
$\Delta\beta$	-	0.22	0.02	0.01	0.00	0.00
Q_i^r	kJ·kg^{-1}	12 687.46	12 687.46	12 687.46	12 687.46	12 687.46
$V_{fg} \cdot c_2$	kJ·kg-1·K^{-1}	33.86	33.82	33.78	33.75	33.66
c_1	kJ·kg-1·K^{-1}	7.54	7.47	7.46	7.45	7.45
c_2	kJ·kg-1·K^{-1}	7.47	7.46	7.45	7.45	7.43
t_1	°C	1 161	1 237	1 228	1 216	1 207
T_1	K	1 434	1 511	1 501	1 489	1 480
t_2	°C	1 237	1 228	1 216	1 207	1 181
T_2	K	1 511	1 501	1 489	1 480	1 454
a_{fu}	-	0.9873	0.9772	0.9671	0.9570	0.9469
$\bar{\psi}$	-	0.4365	0.4410	0.4410	0.4230	0.4188
A_{zone}	m^2	207.36	211.86	206.67	135.75	396.42
B	kg·s^{-1}	43.14	43.14	43.14	43.14	43.14

3.3.1.6 Calculation of outlet flue gas temperature from platen superheater area

The platen superheater area is directly downstream the furnace. This area contains radiant heat surfaces (platen superheater SH3, platen superheater SH2, part of the roof superheater and part of evaporator). The goal of this calculation is to determine the amount of heat transferred from flue gas stream in the platen superheater and to determine flue gas temperature at platen superheater outlet.

Calculation of platen superheater SH3

The design of the platen superheater SH3 is described in Table 3.3.1-8. Steam parameters are shown in Table 3.3.1-9.

Table 3.3.1-8 Parameters of the platen superheater SH3

Parameter	Symbol	Value	Unit
number of platens	n_p	10	-
number of tubes in one plate	x	40	-
outside diameter of tubes	D_{out}	0.035	m
thickness of tubes	t	0.005	m
inside diameter of tubes	D_{in}	0.025	m
number of parallel tubes	n_t	400	-
platens spacing	s_1	0.9	m
spacing of tubes within the platen	s_2	0.039	m
depth of the platen	c	3.371	m
mean platen height	h	9.85	m

Table 3.3.1-9 Steam parameters of the SH3

Parameter	Symbol	Value	Unit
Steam inlet temperature	$t_{SH\,3_{in}}$	401.6	°C
Steam outlet temperature	$t_{SH\,3_{out}}$	455	°C
Steam inlet pressure	$p_{SH\,3_{in}}$	19.35	MPa
Steam outlet pressure	$p_{SH\,3_{out}}$	19.23	MPa
Steam flow rate	D_{SH3}	154.56	kg·s^{-1}

$$t_{fg_m} = \frac{t_{fg_{in}} - t_{fg_{out}}}{2} = \frac{1164-986}{2} = 1\,075°C$$ *Equation 3.3.1-85*

t_{fg_m} – mean flue gas temperature in platen superheater [°C]

$t_{fg_{in}}$ – flue gas temperature at the platen superheater inlet [°C] (is equal to furnace outlet temperature)

$t_{fg_{out}}$ – flue gas temperature at the platen superheater outlet (guessed value) [°C]

Heat transfer for platen superheater SH3, Q_{SH3}:

$$Q_{SH3} = \frac{k_{SH3} \cdot A \cdot \Delta t}{B} \cdot 10^{-3} = \frac{66.65 \cdot 644.14 \cdot 646.7}{43.14} \cdot 10^{-3} \qquad \textit{Equation 3.3.1-86}$$

$$Q_{SH3} = 643.55 \text{ kJ} \cdot \text{kg}^{-1}$$

k_{SH3} – overall heat transfer coefficient for SH3 [W·m^{-2}·K^{-1}]

A – area of heat transfer [m^2]

Δt – average temperature difference between flue gas and steam [°C]

B – fuel consumption [kg·s^{-1}]

$$\Delta t = t_{fg_m} - t_{SH3_m} = 1\,075 - 428.3 = 646.7°\text{C} \qquad \textit{Equation 3.3.1-87}$$

Overall heat transfer coefficient of SH3, k_{SH3}:

$$k_{SH3} = \frac{1}{\frac{1}{\alpha_1} + \frac{1}{\alpha_2} + \varepsilon} = \frac{1}{\frac{1}{208.96} + \frac{1}{4569.29} + 0.01} = 66.65 \text{ W} \cdot \text{m}^2 \cdot \text{K}^{-1} \qquad \textit{Equation 3.3.1-88}$$

α_1 – gas side heat transfer coefficient [W·m^{-2}·K^{-1}]

α_2 – steam side heat transfer coefficient [W·m^{-2}·K^{-1}]

ε – ash deposit coefficient [m^2·K·W^{-1}]; $\varepsilon = 0.01\ m^2 \cdot K \cdot W^{-1}$ (15 p. 148)

Area of heat transfer, A:

$$A = 2 \cdot (c + D_{out}) \cdot h \cdot x_p \cdot n_p = 2 \cdot (3.371 + 0.035) \cdot 9.85 \cdot 0.96 \cdot 10 \qquad \textit{Equation 3.3.1-89}$$

$$A = 644.14 \text{ m}^2$$

x_p – angular coefficient of the platen [-]; $x_p = 0.96\ [-]$

Overall gas side heat transfer coefficient, α_1:

$$\alpha_1 = \omega \cdot (\alpha_{co} + \alpha_{ra}) = 0.9 \cdot (29.93 + 202.249) \qquad \textit{Equation 3.3.1-90}$$

$$\alpha_1 = 208.96 \text{ W} \cdot \text{m}^2 \cdot \text{K}^{-1}$$

ω – correction coefficient for cross-flow over platen superheater [-]; $\omega = 0.9\ [-]$ (15 p. 140)

α_{co} – convective heat transfer coefficient [W·m^{-2}·K^{-1}]

α_{ra} – radiative heat transfer coefficient [W·m^{-2}·K^{-1}]

Convective heat transfer coefficient, α_{co}:

Equation 3.3.1-91

$$\alpha_{co} = 0.2 \cdot C_z \cdot C_s \cdot \frac{\lambda}{d} \cdot \left(\frac{w_{fg} \cdot d}{\nu}\right)^{0.65} \cdot Pr^{0.33}$$

$$\alpha_{co} = 0.2 \cdot 1 \cdot 0.629 \cdot \frac{0.1198}{0.035} \cdot \left(\frac{5.0 \cdot 0.035}{0.0002}\right)^{0.65} \cdot 0.5825^{0.33}$$

$$\alpha_{co} = 29.93\ \mathrm{W \cdot m^2 \cdot K^{-1}}$$

C_z – correction factor for the tube row number n_p along the direction of gas flow [-]; for $n_p \geq 10$ $C_z = 1\ [-]$ (15 p. 97)

C_s – correction factor of the geometric arrangement of the tube bank [-]

λ – thermal conductivity of flue gas at mean temperature of flue gas flow [$\mathrm{W \cdot m^{-1} \cdot K^{-1}}$]

ν – kinematic viscosity of flue gas at mean temperature of the flue gas flow [$\mathrm{m^2 \cdot s^{-1}}$]

d – tube diameter [m]

w_{fg} – flue gas flow velocity [$\mathrm{m \cdot s^{-1}}$]

Pr – Prandlt number [-]

Equation 3.3.1-92

$$C_s = \left[1 + (2 \cdot \sigma_1 - 3) \cdot \left(1 - \frac{\sigma_2}{2}\right)^3\right]^{-2}$$

$$C_s = \left[1 + (2 \cdot 3 - 3) \cdot \left(1 - \frac{1.11}{2}\right)^3\right]^{-2} = 0.629\ [-]$$

According to the (15 p. 98) the Equation 3.3.1-92 uses σ_1=3 (valid if $\sigma_2 < 2$ and $\sigma_1 > 3$)

σ_1 – transverse pitch [-]

σ_2 – longitudinal pitch [-]

$$\sigma_1 = \frac{s_1}{D_{out}} = \frac{0.9}{0.035} = 25.71\ [-]$$

$$\sigma_2 = \frac{s_2}{D_{out}} = \frac{0.039}{0.035} = 1.11\ [-]$$

Properties of flue gas for t_{fg_m}:

$\lambda_{fg} = 0.1198\ \mathrm{W \cdot m^{-1} \cdot K^{-1}}$ (from (15 p. 24) for 1075°C and $x_{H_2O} = 15\%$)

$\nu = 0.0002\ \mathrm{m^2 \cdot s^{-1}}$ (from (15 p. 24) for 1075°C and $x_{H_2O} = 15\%$)

Pr = 0.5825 (from (15 p. 25) for 1075°C and x_{H2O} = 15%)

Flue gas velocity, w:

$$w_{fg} = \frac{B \cdot V_{fg}}{A_{fg}} \cdot \left(1 + \frac{t_{fg_m}}{273}\right) = \frac{43.14 \cdot 4.53}{193.16} \cdot \left(1 + \frac{1\,075}{273}\right) = 5.0 \text{ m} \cdot \text{s}^{-1}$$ *Equation 3.3.1-93*

A_{fg} – flow area of gases [m^2]

$$A_{fl} = a \cdot b - Z \cdot a \cdot d = 10.59 \cdot 18.94 - 20 \cdot 10.59 \cdot 0.035$$ *Equation 3.3.1-94*

$$A_{fl} = 193.16 \text{ m}^2$$

a – length of the passage section [m]; $a = 10.59$ m

b – width of the passage section [m]; $b = 18.94$ m

Z – total number of tubes in platen superheater area [-]; $Z = 20$

d – outside diameter of tubes [m]; $d = 0.035$ m

Radiative heat transfer coefficient, α_{ra}:

$$\alpha_{ra} = \sigma_o \cdot \frac{a_w + 1}{2} \cdot a \cdot T_{fg_{out}}^3 \cdot \frac{1 - \left(\frac{T_{as}}{T_{fg_{out}}}\right)^4}{1 - \left(\frac{T_{as}}{T_{fg_{out}}}\right)}$$ *Equation 3.3.1-95*

$$\alpha_{ra} = 5.7 \cdot 10^{-8} \cdot \frac{0.8 + 1}{2} \cdot 0.47 \cdot 1\,259^3 \cdot \frac{1 - \left(\frac{1\,306}{1\,259}\right)^4}{1 - \left(\frac{1\,306}{1\,259}\right)}$$

$$\alpha_{ra} = 202.25 \text{ W} \cdot \text{m}^{-2} \cdot \text{K}^{-1}$$

a_w – emissivity of walls [-], $a_w = 0.8$ [-] according to (15 p. 118)

a – flue gas stream emissivity [-]

T_{as} – temperature of fouled surface [K]

$$a = 1 - e^{-k \cdot P \cdot S} = 1 - e^{-5.28 \cdot 0.1 \cdot 1.19} = 0.47\ [-]$$ *Equation 3.3.1-96*

$$k = k_y \cdot r + k_h \cdot \mu_h = 8.22 \cdot 0.3 + 0.055 \cdot 50.5 = 5.28 \text{ m}^{-1} \cdot \text{MPa}^{-1}$$ *Equation 3.3.1-97*

$$k_y = \left(\frac{7.8 + 16 \cdot r_{H_2O}}{3.16 \cdot \sqrt{r \cdot P \cdot S}} - 1\right) \cdot \left(1 - 0.37 \cdot \frac{T_{ou}}{1\,000}\right)$$ *Equation 3.3.1-98*

$$k_y = \left(\frac{7.8 + 16 \cdot 0.16}{3.16 \cdot \sqrt{0.3 \cdot 0.1 \cdot .19}} - 1\right) \cdot \left(1 - 0.37 \cdot \frac{1\,348}{1\,000}\right)$$

$$k_y = 8.22\ \mathrm{m^{-1} \cdot MPa^{-1}}$$

$$k_h = \frac{43}{\sqrt[3]{T_{ou}^2 \cdot d_h^2}} = \frac{43}{\sqrt[3]{1\,348^2 \cdot 16^2}} = 0.055\ \mathrm{m^{-1} \cdot MPa^{-1}}$$ *Equation 3.3.1-99*

$$S = \frac{1.8}{\frac{1}{h} + \frac{1}{s_1} + \frac{1}{c}} = \frac{1.8}{\frac{1}{9.85} + \frac{1}{0.9} + \frac{1}{3.371}} = 1.19\ \mathrm{m}$$ *Equation 3.3.1-100*

$$t_{as} = t_{SH3_m} + \left(\varepsilon + \frac{1}{\alpha_2}\right) \cdot \frac{B \cdot Q_{SH3}}{A}$$ *Equation 3.3.1-101*

$$t_{as} = 428.3 + \left(0.01 + \frac{1}{4\,569}\right) \cdot \frac{43.14 \cdot 883}{644}$$

$$t_{as} = 1\,032\ ^\circ\mathrm{C}$$

Q_{SH3} – heat absorbed by SH3 [kJ·kg^{-1}]

$$Q_{SH3} = D_{SH3} \cdot \left(\frac{h_{SH3_{out}} - h_{SH3_{in}}}{B}\right) = 154.56 \cdot \left(\frac{3\,096 - 2\,850}{43.14}\right)$$ *Equation 3.3.1-102*

$$Q_{SH3} = 883\ \mathrm{kJ \cdot kg^{-1}}$$

$h_{SH3_{out}}$ – enthaply of steam at SH3 outlet [kJ·kg^{-1}], enthalpy for $t_{SH3_{out}}$, $p_{SH3_{out}}$

$h_{SH3_{in}}$ – enthaply of steam at SH3 inlet [kJ·kg^{-1}], enthalpy for $t_{SH3_{in}}$, $p_{SH3_{in}}$

Steam side heat transfer coefficient, α_2:

$$\alpha_2 = \alpha_{co} = 4\,569.29\ \mathrm{W \cdot m^{-2} \cdot K^{-1}}$$ *Equation 3.3.1-103*

α_{co} – coefficient of convective heat transfer [W·m^{-2}·K^{-1}]

Equation 3.3.1-104

$$\alpha_{co} = 0.023 \cdot \frac{\lambda}{d_{eq}} \cdot \left(\frac{w \cdot d_{eq}}{\nu}\right)^{0.8} \cdot Pr^{0.4} \cdot C_l \cdot C_t$$

$$\alpha_{co} = 0.023 \cdot \frac{0.0902}{0.025} \cdot \left(\frac{9.68 \cdot 0.025}{3.297 \cdot 10^{-7}}\right)^{0.8} \cdot 1.323^{0.4} \cdot 1 \cdot 1$$

$$\alpha_{co} = 4\,569.29\ \mathrm{W \cdot m^{-2} \cdot K^{-1}}$$

λ – thermal conductivity at mean temperature of steam flow [W·m^{-1}·K^{-1}]

d_{eq} – equivalent diameter [m]; $d_{eq} = D_{in} = 0.025$ m

ν – kinematic viscosity under the mean temperature of the steam flow [m^2·s^{-1}]

w – steam flow velocity [m·s^{-1}]

Pr – Prandlt number [-]

C_t – correction factor for the temperature difference between the medium and the wall [-]; $C_t = 1\ [-]$ when gases are cooled (15 p. 100)

C_l – correction factor of tube length [-] (for platen superheaters $C_l = 1$ [-] (15 p. 100))

Equation 3.3.1-105

$$t_{SH3_m} = \frac{t_{SH3_{out}} - t_{SH3_{in}}}{2} = \frac{455.0 - 401.6}{2} = 428.3°\mathrm{C}$$

Equation 3.3.1-106

$$p_{SH3_m} = \frac{p_{SH3_{in}} - p_{SH3_{out}}}{2} = \frac{19.35 - 19.23}{2} = 19.29\ \mathrm{MPa}$$

Properties of steam for t_{SH3_m} and p_{SH3_m}:

ν_o=0.01223 m^3·kg^{-1} - specific volume

λ=0.0902 W·m^{-1}·K^{-1}

$\mu = 2.683 \cdot 10^{-5}$ Pa · s - dynamic viscosity

Pr=1.323

Equation 3.3.1-107

$$\nu = \nu_o \cdot \mu = 0.01223 \cdot 2.683 \cdot 10^{-5} = 3.297 \cdot 10^{-7}\ \mathrm{m \cdot s^{-1}}$$

Steam flow velocity, w:

Equation 3.3.1-108

$$w = \frac{D_{SH3} \cdot \nu_o}{A_{flow}} = \frac{154.56 \cdot 0.01223}{0.1963} = 9.68\ \mathrm{m \cdot s^{-1}}$$

A_{flow} – cross section area of flow passage [m^2]

Equation 3.3.1-109

$$A_{flow} = n_t \cdot \frac{\pi \cdot D_{in}^2}{4} = 400 \cdot \frac{\pi \cdot 0.025^2}{4} = 0.1963\ \mathrm{m^2}$$

Calculation of platen superheater SH2

The design of the platen superheater SH2 is the same as the design of SH3, which is described in Table 3.3.1-8. The steam inlet and outlet parameters are shown in Table 3.3.1-10.

Table 3.3.1-10 Steam parameters of the SH2

Parameter	Symbol	Value	Unit
Steam inlet temperature	$t_{SH\,2_{in}}$	405.5	°C
Steam outlet temperature	$t_{SH\,2_{out}}$	480	°C
Steam inlet pressure	$p_{SH\,2_{in}}$	18.58	MPa
Steam outlet pressure	$p_{SH\,2_{out}}$	18.35	MPa
Steam flow rate	D_{SH2}	154.56	kg·s^{-1}

Heat transfer for plate superheater SH2, Q_{SH2}:

$$Q_{SH2} = \frac{k_{SH2} \cdot A \cdot \Delta t}{B} \cdot 10^{-3} = \frac{69.85 \cdot 644.14 \cdot 632.25}{43.14} \cdot 10^{-3} \qquad \textit{Equation 3.3.1-110}$$

$$Q_{SH2} = 659.46\ \text{kJ} \cdot \text{kg}^{-1}$$

k_{SH2} – overall heat transfer coefficient of SH2 [W·m^{-2}·K^{-1}]

A – area of heat transfer [m^2]; same value as for SH3

Δt – average temperature difference between flue gas and steam [°C]

B – fuel consumption [kg·s^{-1}]

$$\Delta t = t_{fg_m} - t_{SH2_m} = 1\,075 - 442.75 = 632.25°\text{C} \qquad \textit{Equation 3.3.1-111}$$

Overall heat transfer coefficient, k_{SH2}:

$$k_{SH2} = \frac{1}{\frac{1}{\alpha_1} + \frac{1}{\alpha_2} + \varepsilon} = \frac{1}{\frac{1}{245.30} + \frac{1}{4\,189.26} + 0.01} \qquad \textit{Equation 3.3.1-112}$$

$$k_{SH2} = 69.86\ \text{W} \cdot \text{m}^2 \cdot \text{K}^{-1}$$

α_1 – gas side heat transfer coefficient [W·m^{-2}·K^{-1}]

α_2 – steam side heat transfer coefficient [W·m^{-2}·K^{-1}]

ε – ash deposit coefficient [m^2·K·W^{-1}]; $\varepsilon = 0.01\ \text{m}^2 \cdot \text{K} \cdot \text{W}^{-1}$ (15 p. 148)

Gas side overall heat transfer coefficient, α_1:

$$\alpha_1 = \omega \cdot (\alpha_{co} + \alpha_{ra}) = 0.9 \cdot (29.93 + 242.63) \qquad \textit{Equation 3.3.1-113}$$

$$\alpha_1 = 245.30\ \text{W} \cdot \text{m}^2 \cdot \text{K}^{-1}$$

ω – correction coefficient for cross-flow over platen superheater [-]; $\omega = 0.9\ [-]$ (15 p. 140))

α_{co} – convective heat transfer coefficient [W·m^{-2}·K^{-1}]; the same value as for SH3,

$$\alpha_{co} = 29.93\ W \cdot m^{-2} \cdot K^{-1}$$

α_{ra} – radiative heat transfer coefficient [W·m^{-2}·K^{-1}];

Radiative heat transfer coefficient, α_{ra}:

Equation 3.3.1-114

$$\alpha_{ra} = \sigma_o \cdot \frac{a_w + 1}{2} \cdot a \cdot T_{fg_{out}}^3 \cdot \frac{1 - \left(\frac{T_{as}}{T_{fg_{out}}}\right)^4}{1 - \left(\frac{T_{as}}{T_{fg_{out}}}\right)}$$

$$\alpha_{ra} = 5.7 \cdot 10^{-8} \cdot \frac{0.8 + 1}{2} \cdot 0.47 \cdot 1\,259^3 \cdot \frac{1 - \left(\frac{1\,461}{1\,259}\right)^4}{1 - \left(\frac{1\,461}{1\,259}\right)}$$

$$\alpha_{ra} = 242.48\ \mathrm{W \cdot m^{-2} \cdot K^{-1}}$$

a_w – emissivity of walls [-], $a_w = 0.8\ [-]$ according to (15 p. 118)

a – flue gas stream emissivity [-]

T_{as} – temperature of fouled surface [K]

Equation 3.3.1-115

$$a = 1 - e^{-k \cdot P \cdot S} = 1 - e^{-5.28 \cdot 0.1 \cdot 1.19} = 0.47\ [-]$$

Equation 3.3.1-116

$$k = k_y \cdot r + k_h \cdot \mu_h = 8.22 \cdot 0.3 + 0.055 \cdot 50.5 = 5.28\ \mathrm{m^{-1} \cdot MPa^{-1}}$$

Equation 3.3.1-117

$$k_y = \left(\frac{7.8 + 16 \cdot r_{H_2O}}{3.16 \cdot \sqrt{r \cdot P \cdot S}} - 1\right) \cdot \left(1 - 0.37 \cdot \frac{T_{ou}}{1\,000}\right)$$

$$k_y = \left(\frac{7.8 + 16 \cdot 0.16}{3.16 \cdot \sqrt{0.3 \cdot 0.1 \cdot .19}} - 1\right) \cdot \left(1 - 0.37 \cdot \frac{1\,348}{1\,000}\right)$$

$$k_y = 8.22\ \mathrm{m^{-1} \cdot MPa^{-1}}$$

Equation 3.3.1-118

$$k_h = \frac{43}{\sqrt[3]{T_{ou}^2 \cdot d_h^2}} = \frac{43}{\sqrt[3]{1\,348^2 \cdot 16^2}} = 0.055\ \mathrm{m^{-1} \cdot MPa^{-1}}$$

$$S = \frac{1.8}{\frac{1}{h} + \frac{1}{s_1} + \frac{1}{c}} = \frac{1.8}{\frac{1}{9.85} + \frac{1}{0.9} + \frac{1}{3.371}} = 1.19 \text{ m}$$ *Equation 3.3.1-119*

$$t_{as} = t_{SH3_m} + \left(\varepsilon + \frac{1}{\alpha_2}\right) \cdot \frac{B \cdot Q_{SH2}}{A}$$ *Equation 3.3.1-120*

$$t_{as} = 442.75 + \left(0.01 + \frac{1}{4\,323}\right) \cdot \frac{43.14 \cdot 1\,087}{644}$$

$$t_{as} = 1\,188\ ^{\circ}\text{C}$$

Q_{SH2} – heat absorbed by SH2 [kJ·kg^{-1}]

$$Q_{SH2} = D_{SH2} \cdot \left(\frac{h_{SH2_{out}} - h_{SH2_{in}}}{B}\right) = 154.56 \cdot \left(\frac{3\,096 - 2\,850}{43.14}\right)$$ *Equation 3.3.1-121*

$$Q_{SH2} = 883 \text{ kJ} \cdot \text{kg}^{-1}$$

$h_{SH2_{out}}$ – enthaply of steam at SH2 outlet [kJ·kg^{-1}], enthalpy for $t_{SH2_{out}}$, $p_{SH2_{out}}$

$h_{SH2_{in}}$ – enthaply of steam at SH2 inlet [kJ·kg^{-1}], enthalpy for $t_{SH2_{in}}$, $p_{SH2_{in}}$

Steam side heat transfer coefficient, α_2:

The calculation of α_1 assumes that the flue gases flow along the SH3 longitudinally.

$$\alpha_2 = \alpha_{co} = 4\,189.26 \text{ W} \cdot \text{m}^{-2} \cdot \text{K}^{-1}$$ *Equation 3.3.1-122*

α_{co} – coefficient of convective heat transfer for longitudinal sweeping [W·m^{-2}·K^{-1}]

$$\alpha_{co} = 0.023 \cdot \frac{\lambda}{d_{eq}} \cdot \left(\frac{w \cdot d_{eq}}{\nu}\right)^{0.8} \cdot Pr^{0.4} \cdot C_l \cdot C_t$$ *Equation 3.3.1-123*

$$\alpha_{co} = 0.023 \cdot \frac{0.0562}{0.025} \cdot \left(\frac{10.88 \cdot 0.025}{3.768 \cdot 10^{-7}}\right)^{0.8} \cdot 1.231^{0.4} \cdot 1 \cdot 1$$

$$\alpha_{co} = 4\,189.26 \text{ W} \cdot \text{m}^{-2} \cdot \text{K}^{-1}$$

λ – thermal conductivity at mean temperature of steam flow [W·m^{-1}·K^{-1}]

d_{eq} – equivalent diameter [m]; $d_{eq} = D_{in} = 0.025$ m

ν – kinematic viscosity under the mean temperature of the steam flow [m^2·s^{-1}]

w – steam flow velocity [m·s^{-1}]

Pr – Prandlt number [-]

C_t – correction factor for the temperature difference between the steam and the wall [-]; $C_t = 1\ [-]$ when gases are cooled (15 p. 100)

C_l – correction factor of tube length [-]; for platen superheaters: $C_l = 1\ [-]$ (15 p. 100)

$$t_{SH2_m} = \frac{t_{SH2_{out}} - t_{SH2_{in}}}{2} = \frac{480.0 - 405.5}{2} = 442.3\ °C$$ *Equation 3.3.1-124*

$$p_{SH3_m} = \frac{p_{SH2_{in}} - p_{SH2_{out}}}{2} = \frac{18.58 - 18.35}{2} = 18.47\ \text{MPa}$$ *Equation 3.3.1-125*

Properties of steam for t_{SH2_m} and p_{SH2_m}:

$\nu_o = 0.01382\ \text{m}^3 \cdot \text{kg}^{-1}$ - specific volume

$\lambda = 0.0862\ \text{W} \cdot \text{m}^{-1} \cdot \text{K}^{-1}$

$\mu = 2.726 \cdot 10^{-5}\ \text{Pa} \cdot \text{s}$ - dynamic viscosity

$Pr = 1.231\ [-]$

$$\nu = \nu_o \cdot \mu = 0.01382 \cdot 2.726 \cdot 10^{-5} = 3.768 \cdot 10^{-7}\ \text{m}^2 \cdot \text{s}^{-1}$$ *Equation 3.3.1-126*

Steam flow velocity, w:

$$w = \frac{D_{SH2} \cdot \nu_o}{A_{flow}} = \frac{160.76 \cdot 0.01382}{0.1963} = 11.31\ \text{m} \cdot \text{s}^{-1}$$ *Equation 3.3.1-127*

A_{flow} – cross section area of flow passage [m^2]; the same value as for SH3

Calculation of additional surfaces

In the area of platen superheater there are additional surfaces which also transfer heat from flue gas. These surfaces are the roof superheater and the evaporator membrane walls, which create furnace walls. The following calculation uses simplification according to (15 p. 42) where it is possible to take the value of the overall heat transfer coefficient *k* from the main surfaces (in this case SH3 and SH2). The surface area of additional surfaces should be between 5-10% from the surface area of the main surfaces. I this case the surface area of additional surfaces is 12.8%. The following calculation uses the above mentioned simplification because the error made due to the simplified calculation of the heat transfer coefficient is negligible.

Heat transfer for roof superheater, Q_{SHr}:

$$Q_{SHr} = \frac{k_{add} \cdot A \cdot \Delta t}{B} \cdot 10^{-3} = \frac{68.26 \cdot 97.82 \cdot 619}{43.14} \cdot 10^{-3} \qquad \textit{Equation 3.3.1-128}$$

$$Q_{SHr} = 95.81 \text{ kJ} \cdot \text{kg}^{-1}$$

k_{add} – overall heat transfer coefficient of additional surfaces [W·m^{-2}·K^{-1}]

A – area of heat transfer [m^2], $A = 97.82\ m^2$

Δt – average temperature difference between flue gas and steam [°C]

B – fuel consumption [kg·s^{-1}]

Overall heat transfer coefficient of additional surfaces, k_{add}:

The overall heat transfer coefficient for additional surfaces is the same as for the main surfaces. Due to the fact that the main surfaces (SH3 and SH2) consist of two different overall heat transfer coefficients the k_{add} is determined as a mean value of these two coefficients. Because the heat transfer area of SH3 is the same as of SH4 the overall heat transfer coefficient can be determined by Equation 3.3.1-129.

$$k_{add} = \frac{k_{SH3} + k_{SH2}}{2} = \frac{66.65 + 69.88}{2} = 68.26 \text{ W} \cdot \text{m}^{-2} \cdot \text{K}^{-1} \qquad \textit{Equation 3.3.1-129}$$

Average temperature difference between flue gas and steam, Δt:

$$\Delta t = t_{fg_m} - t_{SHr_m} = 1\,075 - 456 = 619°\text{C} \qquad \textit{Equation 3.3.1-130}$$

t_{SHc_m} – mean steam temperature of ceiling superheater [°C], $t_{SHc_m} = 456°\text{C}$ (given by Alstom)

Heat transfer for evaporating part of the boiler in the platen superheater area, Q_{ev}:

$$Q_{ev} = \frac{k_{add} \cdot A \cdot \Delta t}{B} \cdot 10^{-3} = \frac{68.26 \cdot 97.82 \cdot 701}{43.14} \cdot 10^{-3} \qquad \textit{Equation 3.3.1-131}$$

$$Q_{ev} = 74.43 \text{ kJ} \cdot \text{kg}^{-1}$$

k_{add} – overall heat transfer coefficient of additional surfaces [W·m^{-2}·K^{-1}]

A – area of heat transfer [m^2]

Δt – average temperature difference between flue gas and steam [°C]

B – fuel consumption [kg·s^{-1}]

Average temperature difference between flue gas and steam, Δt:

$$\Delta t = t_{fg_m} - t_{ev_m} = 1\,075 - 374 = 701°\text{C} \qquad \textit{Equation 3.3.1-132}$$

t_{ev_m} – mean steam temperature of evaporator part in the area of platen superheaters [°*C*];
$t_{ev_m} = 374°C$ (given by Alstom)

Heat balance in the area of platen superheaters

To check expected flue gas outlet temperature from the platen superheater it is necessary to calculate the heat balance in the area of the platen superheater.

Energy transferred to the heating surfaces in the platen superheater area by flue gas, Q_{SH}:

$$Q_{SH} = Q_{SH3} + Q_{SH2} + Q_{SHr} + Q_{ev} \qquad \textit{Equation 3.3.1-133}$$
$$Q_{SH} = 643.55 + 659.70 + 95.81 + 74.42 = 1\,473.49\ \text{kJ} \cdot \text{kg}^{-1}$$

Energy transferred from flue gas in the platen superheater area, Q_{SH}^{fg}:

$$Q_{SH}^{fg} = \varphi \cdot \left(H_{fg_{in}} - H_{fg_{out}} + \Delta\alpha \cdot H_e\right) \qquad \textit{Equation 3.3.1-134}$$
$$Q_{SH}^{fg} = 0.997 \cdot \left(8\,629.27 - 7\,168.56 + 0\right) = 1\,455.78\ \text{kJ} \cdot \text{kg}^{-1}$$

φ – coefficient of reheat retention [-]; φ=0.997 [-]

$\Delta\alpha \cdot H_e$ – heat carried by leakage air into the boiler [kJ·kg^{-1}]; the air leakage into the area around the platen superheaters is small, so it is neglected in the calculation ($\Delta\alpha \cdot H_e = 0$)

$H_{fg_{in}}$- flue gas enthalpy at the platen superheater area entrance [kJ·kg^{-1}];

$$H_{fg_{in}} = 8\,629.27\ \text{kJ} \cdot \text{kg}^{-1}$$

$H_{fg_{out}}$- flue gas enthalpy at the platen superheater area exit [kJ·kg^{-1}];

$$H_{fg_{out}} = 7\,168.56\ \text{kJ} \cdot \text{kg}^{-1}$$

The difference between the energy taken away from flue gas, Q_{SH}, and the energy transferred to the heating surfaces in the platen superheater area by flue gas, Q_{SH}^{fg}, should not get over ±2%.

$$\frac{(Q_{SH}^{fg} - Q_{SH})}{Q_{SH}^{fg}} \cdot 100 = \frac{(1\,455.78 - 1\,473.49)}{1\,455.78} \cdot 100 = -1.22\% \qquad \textit{Equation 3.3.1-135}$$

According to the fact that the difference is in the range, the expected flue gas temperature at the platen superheater outlet ($t_{fg_{out}} = 986°\text{C}$) is considered correct.

3.3.2 Main results from thermal calculation

The final flue gas outlet temperatures from the furnace (calculated in 3.3.1.4 and 3.3.1.5) and the platen superheater (calculated in chapter 3.3.1.6) for all considered conditions are shown in Figure 3.3.2-2 and Figure 3.3.2-1.

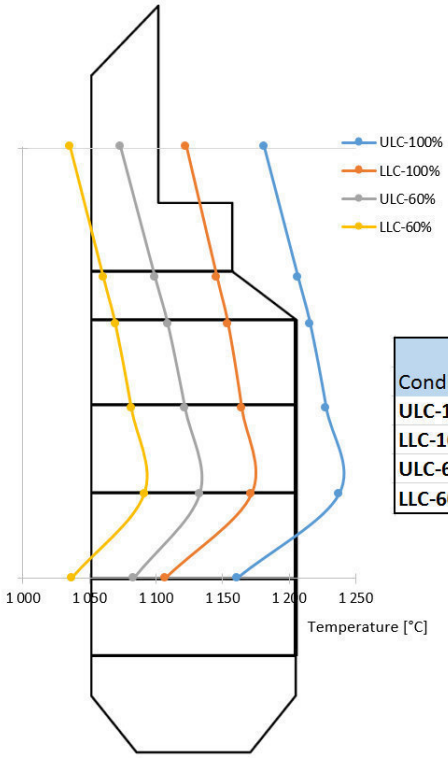

	Flue gas outlet temperature [°C]					
Conditions	Zone 1	Zone 2	Zone 3	Zone 4	Zone 5	Zone 6
ULC-100% BMCR	1 161	1 237	1 228	1 216	1 207	1 181
LLC-100% BMCR	1 107	1 172	1 164	1 154	1 146	1 123
ULC-60% BMCR	1 083	1 133	1 122	1 109	1 099	1 073
LLC-60% BMCR	1 037	1 091	1 082	1 070	1 061	1 035

Figure 3.3.2-1 Results from zonal calculation of the furnace

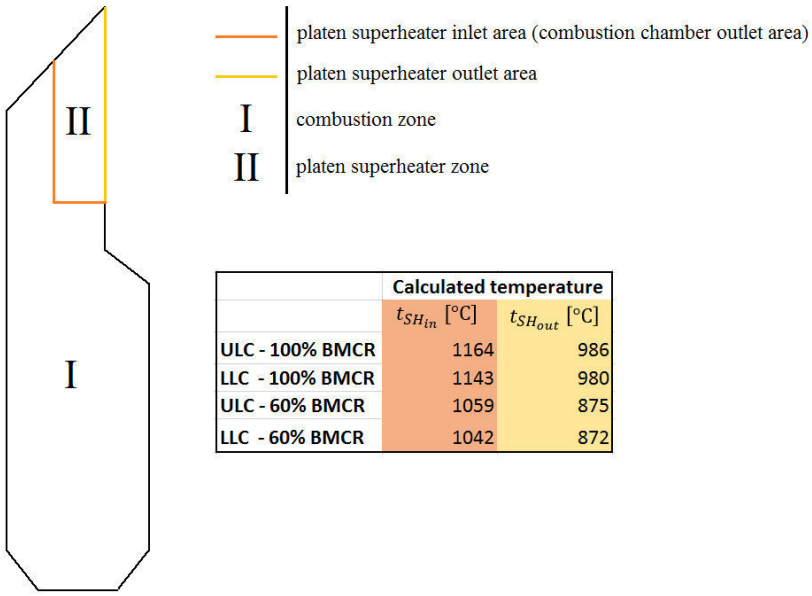

	Calculated temperature	
	$t_{SH_{in}}$ [°C]	$t_{SH_{out}}$ [°C]
ULC - 100% BMCR	1164	986
LLC - 100% BMCR	1143	980
ULC - 60% BMCR	1059	875
LLC - 60% BMCR	1042	872

Figure 3.3.2-2 Final results from the platen superheater area calculation

3.3.3 Selection of suitable position for reagent injection

The selection process assumes that the optimal temperature range for reagent injecting for SNCR method is 870-1150°C (35). This temperature range has to be ensured within the considered boiler conditions. The results given in 3.3.2 are taken as the main data for positioning of lances (injection nozzles). The first injection level (level 1) is designed to inject the reagent directly under the platen superheater area (horizontally) while the second (level 2) is designed to inject the reagent in the area of the platen superheater to create the denitrification area between the platen superheater exit and superheater 5 (SH5) inlet. Only one of the injection levels is in operation during the process – in dependence on boiler load. The position of the injection levels is shown in Appendix B.

Level 1 (horizontal direction) is situated directly upstream from the platen superheater at 32.20 m (above the ground). The injection lances are located on the front and back side of the duct (the lances must ensure proper penetration and reagent distribution across the duct cross-section). This injection level consists of 38 lances (19 in each side) which are placed along the furnace width.

Level 2 is situated in the area of platen superheater and the direction of the injection is determined to create the denitrification zone between the platen superheater and the next convective surface (SH5). It is necessary to ensure that the denitrification reactions take place before entering SH5 to protect bundle material against undesired interaction. Due to the duct height, the injection lances are placed on the duct roof and also on the bottom surface of the duct to ensure the proper mixing and necessary penetration. This level consists also of 38 lances (19 placed on the duct roof and 19 on the bottom surface of the duct) distributed along the furnace width.

To determine the range of boiler loads where the individual injection level should work, it is necessary to determine the temperatures at each of the positions for the whole boiler load range. Assuming that the flue gas temperature grows linearly with the boiler load, it is possible to calculate flue gas temperature in each of the positions for different boiler load. The results from this calculation are shown in Table 3.3.3-1. Taking into account these results, the lances of level 1 are used in the range of 60-70% BMCR while the lances of level 2 are used in the range of 70-100% BMCR (the boiler is expected to work mostly at this boiler load range). In the Table 3.3.3-1 are highlighted (green background) the temperatures in which the reagent is injected. All of these temperatures are in the required temperature range for SNCR reactions (870-1150°C).

Table 3.3.3-1 Flue gas temperature in injection layers under the different value of BMCR

	Boiler maximum continuous rating (BMCR)				
	100%	**90%**	**80%**	**70%**	**60%**
Level 1 - temperature for ULC [°C]	1164	1138	1112	1085	1059
Level 1 - temperature for LLC [°C]	1143	1118	1093	1067	1042
Level 2 - temperature for ULC [°C]	986	958	931	903	875
Level 2 - temperature for LLC [°C]	980	953	926	899	872

3.4 General comparison of SCR and SNCR

3.4.1 Advantages and disadvantages of SCR and SNCR

- The investment costs of SNCR for the selected unit are 5 times lower that of SCR. According to Bernd von der Heide (43 p. 10) the investment costs of SNCR system can be even 10 times higher than of SCR.
- SNCR achieves NO_x-reduction rates up to 50 to 60% (43 p. 7) whereas SCR can achieve NO_x-reduction higher that 90% (44) (34). The SNCR method alone is in most cases (high NO_x reduction requirements) not able to achieve the required NO_x emissions for coal-fired boilers, so additional denitrification techniques have to be used simultaneously. In these cases, when using SNCR method, it is unavoidable to make modifications to the combustion process (installation of OFA ducting, low NO_x burners etc.).
- Installation of SNCR is not as problematic as of SCR, but it is essential to select proper position (specific temperature range) and adjustment of the injecting lances (35). It is also important to avoid reactions of the reagent with heating surfaces (especially with superheaters).
- SNCR requires proper mixing and penetration of reagent with flue gas which is difficult to achieve in large boilers, so it is usually used for boilers with less than 200 MW_{th} output (45).
- SCR has much higher space demands due to the need for a catalyst reactor (and a supporting construction). It is often necessary to build a new flue-gas-pass due to the lack of space between the economizer and the air heater.
- When using SCR, increased pressure drop due to the catalyst has to be taken into account – and existing Induce Draft (ID) fans have to be checked and if needed replaced, which results in higher electricity consumption.
- Catalysts must be regularly be exchanged or regenerated which reduces boiler operating hours. (43 pp. 4,11)
- According to the US Environmental Protection Agency (35) SNCR is more suitable for applications with high levels of PM (firing of high ash content coals) in the flue gas stream than SCR.

3.4.2 General applicability of SNCR/SCR installation in existing coal-fired boilers

SNCR is a suitable solution especially when the boiler does not offer enough space for installation of additional devices and when the denitrification rate is not high. When it is necessary to achieve high NO_x reduction, other denitrification methods have to be used simultaneously. Installation of SNCR technology is not as complicated as of SCR. SNCR does not affect the overall availability of the plant (36 p. 24). Complications can occur when conditions are not suitable for the denitrification process (difficulties with mixing of the reagent, lack of space and time for denitrification process etc.) (10 p. 303).

SCR is especially suitable for applications where high NO_x reduction and low NH_3 slip is required. High NO_x reduction effectivity is outweighed by the high investment costs, space requirements and difficulty of the installation.

Both SCR and SNCR should be investigated when denitrification of an existing boiler is required. All the advantages and disadvantages of the methods should be taken into account

when selecting a denitrification technique. Denitrification by SNCR method often leads to lower investment costs but it can be problematic to ensure proper reagent distribution in flue gas due to the fact that flue gas flow and temperature varies in the high temperature area. Temperature and flow distribution is also dependent on combination of mills in operation. Suitable conditions for SCR are easier to determine because flue gas is more uniform in convictive part of the boiler.

SNCR technology is nowadays considered as the 'best available technology' (BAT) for small and medium sized boilers, where it is possible to mix the reagent with flue gas stream easily, but it is also often investigated for the usage in large boilers (36 p. 4).

4 DISCUSSION

The economic analysis studies only investment costs of the variants (rough estimation of investment costs) and does not include operational costs. The unit prices are equivalent for the both variants and their values are estimated so it is possible that real unit prices could differ. Depending on the specific conditions, which can occur during project execution, the final investment costs could differ. The calculated difference of investment costs of SCR and SNCR (the fact that SNCR is 5 times less expensive) agrees with the results published by Spliethoff (10 p. 307).

Chapter 3.3.2 assumes that the temperature is constant over the furnace cross-section. In reality the temperature varies over the furnace cross-section and usually the lowest temperature appears close to furnace walls and increases towards the center of the flue gas stream. To find out the temperature distribution over the boiler cross-section area it is necessary to make experimental measurements or computer fluid dynamic (CFD) simulations to determine the temperature and velocity profile across the duct cross-section in order to optimize the injection positions.

The suitable locations of injection lances are chosen by taking into account the results in chapter 3.3.2. The injection lances of level 2 should be further investigated to ensure that the denitrification process takes place between the platen superheater exit and SH5 inlet. It is considered that the flue gas temperature decrease between the platen superheater exit and SH5 inlet is not significant due to the fact that there are only evaporator pipes which transfer heat and no other convective heating surfaces.

When designing the injection levels it is important to consider the undesirable effect of the reaction between the reagent and the surface of the superheaters (and other surfaces in the duct). Due to this fact it is important to properly adjust the injection lances to avoid this reaction. The suggested injection level 2 injects the reagent in the area of the platen superheater where increased possibility of undesirable reactions occurs. Therefore proper adjustment based on more detailed calculations, measurements or modelling should be carried out.

5 CONCLUSIONS

The aim of the thesis was to investigate modern denitrification methods of coal-fired boilers and to determine a suitable denitrification method for 640 $t \cdot h^{-1}$ coal-fired boiler (PG 640) placed in the Počerady power plant, Czech Republic.

From the brief study of nitrogen oxides (chapter 3.1.1) emerges that significant amount of NO_x is emitted from combustion processes and that these particles contribute to climate change and have unfavorable effect on human health. Large emitters of NO_x have to fulfill strict emission limits, which forces them to implement and use various denitrification methods. Nowadays large coal-fired power plants have to reduce their NO_x emissions under 200 $mg \cdot Nm^{-3}$. **The background research about modern denitrification methods** (chapter 3.1.2) summarizes the most used denitrification techniques and focuses deeply on secondary denitrification.

The selection process of a suitable denitrification method for particular boiler (chapter 3.2) studies two variants – variant 1 uses only SCR method while variant 2 utilizes SNCR simultaneously with low NO_x burners and over-fire air staging. To choose the more suitable variant, **an economic analysis of investment costs** (chapter 3.2.4) was carried out. **Variant 2 was selected as the more suitable solution for denitrification of the boiler** due to its lower investment costs 1 (CZK 155 647 695 instead of CZK 193 155 129) and additional advantages concerning less construction difficulties and size requirements.

The main purpose of the thesis was to prepare process data for technical specification of selected denitrification method, which **is in this case determining of the suitable position for SNCR injecting lances**. This principal part of the thesis contains a thermal calculation of the furnace (chapter 3.3.1.4 and 3.3.1.5) and the platen superheater (chapter 3.3.1.6) for four different boiler conditions to find the proper position with suitable temperature for denitrification process (870-1150°C (35)). The calculation is made for two fuel compositions within the boiler load of 60% and 100% of BMCR. Giving the results from the calculations together, suggested SNCR technology uses two injecting levels – level 1 injects the reagent into the area below the platen superheater inlet (in the height of 32.20 m) and is used for the BMCR of 60-70% while level 2 is used for the BMCR of 70-100% and injects the reagent into the platen superheater area to ensure that the denitrification process takes place between the platen superheater outlet and the superheater 5 inlet.

The general comparison of the SCR and SNCR methods (chapter 3.4) revealed that both of the methods can be used for denitrification of existing power plants. When choosing the suitable deNO_x method it is appropriate to investigate both of the methods. SNCR is often used for small and medium sized boilers usually with simultaneous usage of other deNOx methods and can be also suitable for larger boilers, while SCR method is usually used for large boilers where high denitrification rate with low NH_3 slip is required.

In my opinion it is important to consider if the savings of SNCR investment costs (in this case 19.4%) overweight disadvantages of the solution. Especially in large coal-fired boilers it is problematic to determine the proper position for SNCR reagent injection lances and to ensure proper reagent distribution due to unstable and variable flue gas stream parameters in the denitrification area. Where it is problematic to ensure proper reagent distribution or important to observe low NH_3 slip I would recomment to use SCR method, while this solution ensures required demands with less risks.

LIST OF SOURCES

(1) International Energy Agency. *World Energy Outlook 2014* [online]. Paris: OECD/IEA, November 2014. [Accessed 14 May 2015]. Retrieved from: https://www.iea.org/Textbase/npsum/ WEO2014SUM.pdf

(2) LUKÁČ, Petr, RŮŽIČKOVÁ, Blanka and ZELENKA, Robert. *Energy outlook 2013* [online]. Prague: Economia a.s., 2013. [Accessed 26 April 2015]. Retrieved from: http://www.cez.cz/edee/content/file/pro-media-2013/12-prosinec/energy-outlook-2013.pdf

(3) VEJVODA, Josef. *Technologie ochrany ovzduší a čištění odpadních plynů* [Air protection technology and waste gas purification]. Praha: VŠCHT, 2003. ISBN 80-708-0517-X.

(4) EUROPEAN ENVIRONMENT AGENCY. *Air quality in Europe - 2013 report*. Luxembourg: Publications Office of the European Union, 2013. ISBN 978-929-2134-068.

(5) EUROPEAN ENVIRONMENT AGENCY (EEA). *Sector share of nitrogen oxides emissions* [online]. 2014. [Accessed 26 April 2015]. Retrieved from: http://www.eea.europa.eu/data-and-maps/daviz/sector-share-of-nitrogen-oxides-emissions#tab-based-on-data

(6) SKÁLA, Zdeněk. *Ekologie v energetice* [Ecology in energetics]. Brno: PC DIR, 1994. ISBN 80-214-0477-9.

(7) MORETTI, A. L. and JONES, C. S. *Advanced Emissions Control Technologies for Coal-Fired Power Plants* [Technical paper BR-1886] [online]. Bangkok: Babcock & Wilcox Power Generation Group, 2012. [Accessed 26 April 2015]. Retrieved from: http://www.babcock.com/library/documents/br-1886.pdf

(8) FLAGAN, Richard C. and SEINFELD, John H., *Fundamentals of air pollution engineering*. Englewood Cliffs, N.J.: Prentice Hall, c1988. p. 167-225. ISBN 0133325377.

(9) Pollutant control techniques. In: ISHIGAI, edited by Seikan, *Steam power engineering: thermal and hydraulic design principles*. Cambridge: Cambridge University Press, 2010. p. 126-150. ISBN 9780521135184.

(10) Methods for NOx reduction. In: SPLIETHOFF, Hartmut, *Power generation from solid fuels*. New York: Springer, c2010. p. 277-306. ISBN 978-3-642-02855-7.

(11) DVOŘÁKOVÁ, I., et al. *ZNEČIŠTĚNÍ OVZDUŠÍ NA ÚZEMÍ ČESKÉ REPUBLIKY V ROCE 2012: Emise do ovzduší v České republice: Tab.I.1.3. Vývoj emisí ze spalovacích zařízení LCP* [Air pollution in the Czech republic in 2012: Air emissions in the Czech Republic: Table I.1.3. Emissions from large combustion plants] [online]. Prague, 2013. [Accessed 26 April 2015]. Retrieved from: http://www.chmi.cz/files/portal/docs/uoco/isko/grafroc/groc/gr12cz/tab/t113.html

(12) Grafická ročenka 2013 [Graphic year-book 2013]. *Portal.chmi.cz* [online]. 2014. [Accessed 26 April 2015]. Retrieved from: http://portal.chmi.cz/files/portal/docs/uoco/isko/grafroc/13groc/gr13cz/II_ovzd_CZ.html

(13) The Czech Republic. Government Regulation No. 352/2002 Coll from 14. 8. 2012 [orig. in Czech: 352/2002 Sb., Nařízení vlády, kterým se stanoví emisní limity a další podmínky provozování spalovacích stacionárních zdrojů znečišťování ovzduší; účinnost od 14. 8. 2012]. In: *Sbírka zákonů České republiky* [Collection of Laws of the Czech Republic]. 2002.

(14) The Czech Republic. Decree No. 415/2012 Coll. from 21st November 2012. [orig. in Czech: Předpis č. 415/2012 Sb.: Vyhláška o přípustné úrovni znečišťování a jejím zjišťování a o provedení některých dalších ustanovení zákona o ochraně ovzduší; 21. listopadu 2012]. In: *Sbírka zákonů České republiky* [Collection of Laws of the Czech Republic]. 2012.

(15) BUDAJ, Florian. *Parní kotle: podklady pro tepelný výpočet [Steam boilers: supporting documents for thermal calculation]*. 4. vyd. Brno: Nakladatelství VUT Brno, 1992. ISBN 80-214-0426-4.

(16) CLEAVER-BROOKS, INC. *Boiler emission guide* [CB-7435]. [online]. 2015. [Accessed 26 April 2015]. Retrieved from: http://www.cleaverbrooks.com/uploadedFiles/Internet_Content/Reference_Center/Insights/Boiler%20Emissions%20Guide.pdf

(17) BURGE, A. M., KING, B. M. and NITSCH, B. *Reducing NOx via Replacement Burners, Overfire Air & Optimized Combustion* [Technical paper]. [online]. 2006. [Accessed 26 April 2015]. Retrieved from: http://www.burnsmcd.com/Resource_/PressRelease/1560/FileUpload/ReducingNOxviaReplacementBurnersOverfireAirandOptimizedC.pdf

(18) IEA Clean Coal Centre. *Low NOx burners*. [online]. *iea-coal.org.uk* [Accessed 26 April 2015]. Retrieved from: http://www.iea-coal.org.uk/site/ieacoal/databases/ccts/low-nox-burners

(19) BASU, Prabir. *Boilers and burners: design and theory*. New York: Springer, 2000. ISBN 03-879-8703-7.

(20) OCHI, K., KIYAMA, K., YOSHIZAKO, H., OKAZAKI, H. and TANIGUCHI, M. *Latest Low-NOx Combustion Technology for Pulverized-coal-fired Boilers* [online]. p. 187-193, 2009. [Accessed 26 April 2015]. Retrieved from: http://www.hitachi.com/rev/pdf/2009/r2009_05_102.pdf

(21) LIU, Changchun, HUI, Shien, PAN, Su, WANG, Denghui, SHANG, Tong and LIANG, Ling. The influence of air distribution on gas-fired coal preheating method for NO emissions reduction. *Fuel* [online]. 2015. Vol. 139, p. 206-212. DOI 10.1016/j.fuel.2014.08.068. [Accessed 26 April 2015]. Retrieved from: http://linkinghub.elsevier.com/retrieve/pii/S0016236114008552

(22) FORZATTI, Pio. *Applied Catalysis A: General* [online]. Vol. 222, no. 1-2. DOI 10.1016/S0926-860X(01)00832-8. [Accessed 26 April 2015]. Retrieved from: http://linkinghub.elsevier.com/retrieve/pii/S0926860X01008328

(23) CHENG, Xingxing and BI, Xiaotao T. A review of recent advances in selective catalytic NOx reduction reactor technologies. *Particuology* [online]. 2014. Vol. 16, p. 1-18. DOI 10.1016/j.partic.2014.01.006. Retrieved from: http://linkinghub.elsevier.com/retrieve/pii/S1674200114000558

(24) NORMANN, Fredrik, ANDERSSON, Klas, LECKNER, Bo and JOHNSSON, Filip. Emission control of nitrogen oxides in the oxy-fuel process. *Progress in Energy and Combustion Science* [online]. 2009. Vol. 35, No. 5, p. 385-397. DOI 10.1016/j.pecs.2009.04.002. [Accessed 26 April 2015]. Retrieved from: http://linkinghub.elsevier.com/retrieve/pii/S0360128509000185

(25) RADOJEVIC, Miroslav. Reduction of nitrogen oxides in flue gases. *Environmental Pollution* [online]. 1998. Vol. 102, No. 1. p. 685-689. DOI 10.1016/S0269-7491(98)80099-7. [Accessed 26 April 2015]. Retrieved from: http://linkinghub.elsevier.com/retrieve/pii/S0269749198800997

(26) IEA GREENHOUSE GAS R&D PROGRAMME (IEA GHG). *Biomass CCS Study*. [online]. IEA Environmental Projects Ltd., 2009/09. Section C: 7-9. [Accessed 26 April 2015]. Retrieved from: http://ieaghg.org/docs/General_Docs/Reports/2009-9.pdf

(27) FISHER, J. E. *Comparison of Urea-Based Ammonia to Liquid Ammonia Systems for NOx Reduction Applications* [online]. Electric Energy Online. 2002. [Accessed 26 April 2015]. Retrieved from: http://www.electricenergyonline.com/show_article.php?mag=&article=70

(28) WILSON, Chu. *NSCR, SCR Systems Reduce Emissions* [online]. 2007. [Accessed 26 April 2015]. Retrieved from: http://www.environmental-expert.com/Files%5C1069%5Carticles%5C18106%5C7.pdf

(29) LIU, Zhiming and IHL WOO, Seong. Recent Advances in Catalytic DeNO X Science and Technology. *Catalysis Reviews* [online]. 2006. Vol. 48, No. 1, p. 43-89. DOI 10.1080/01614940500439891. [Accessed 26 April 2015]. Retrieved from: http://www.tandfonline.com/doi/abs/10.1080/01614940500439891

(30) PACYNA, E.G., PACYNA, J.M., SUNDSETH, K., MUNTHE, J., KINDBOM, K., WILSON, S., STEENHUISEN, F. and MAXSON, P. Global emission of mercury to the atmosphere from anthropogenic sources in 2005 and projections to 2020. *Atmospheric Environment* [online]. 2010. Vol. 44, No. 20, p. 2487-2499. DOI 10.1016/j.atmosenv.2009.06.009. [Accessed 26 April 2015]. Retrieved from: http://linkinghub.elsevier.com/retrieve/pii/S1352231009005007

(31) PUDASAINEE, Deepak, LEE, Sung Jun, LEE, Sang-Hyeob, KIM, Jeong-Hun, JANG, Ha-Na, CHO, Sung-Jin and SEO, Yong-Chil. Effect of selective catalytic reactor on oxidation and enhanced removal of mercury in coal-fired power plants. *Fuel* [online]. 2010. Vol. 89, no. 4, p. 804-809. DOI 10.1016/j.fuel.2009.06.022. [Accessed 26 April 2015]. Retrieved from: http://linkinghub.elsevier.com/retrieve/pii/S0016236109002944

(32) BENSON, Steven A., LAUMB, Jason D., CROCKER, Charlene R. and PAVLISH, John H. SCR catalyst performance in flue gases derived from subbituminous and lignite coals. *Fuel Processing Technology* [online]. 2005. Vol. 86, No. 5, p. 577-613. DOI 10.1016/j.fuproc.2004.07.004. [Accessed 26 April 2015]. Retrieved from: http://linkinghub.elsevier.com/retrieve/pii/S0378382004001870

(33) RODDY, D. *Advanced Power Plant Materials*. Cambridge : Woodhead Pub, 2010. p. 203-215. ISBN 978-184-5695-156.

(34) Alstom. *AQCS PRODUCT SOLUTIONS: Selective Catalytic Reduction (SCR) of Nitrogen Oxides (NOx)* [informative brochure] [online] 2014. [Accessed 12 December 2014]. Retrieved from: http://www.alstom.com/Global/Power/Resources/Documents/Brochures/selective-catalytic-reduction-of-nox.pdf?epslanguage=en-GB.

(35) Environmental Protection Agency. *Air Polution Control Technology Fact Sheet [EPA452/03-032]*. Environmental Protection Agency. 2003. [Accessed 26 April 2015]. Retrieved from: http://www.epa.gov/ttncatc1/dir1/fscr.pdf

(36) BENRD, von der Heide. *NOx Reduction for the Future with the SNCR Technology for Medium and Large Combustion Plants [presented at Power engineerging and environment]* [online]. Essen : Mehldau & Steinfath Umwelttechnik GmbH, 2010. [Accessed 26 April 2015]. Retrieved from: http://www.ms-umwelt.de/english/downloads/Advanced%20SNCR%20Technology%20for%20the%20Future.pdf

(37) MILLER, Bruce G and TILLMAN, David A. *Combustion engineering issues for solid fuel systems*. Boston, MA: Academic Press, c2008. ISBN 978-012-3736-116.

(38) Alstom. *AQCS PRODUCT SOLUTIONS: SCR IsoSwirl™ Mixer And High Efficiency Ammonia Injection* [informative brochure] [online] 2014. [Accessed 26 April 2015]. Retrieved from: http://www.alstom.com/Global/Power/Resources/Documents/Brochures/aqcs-scr-isoswirl-mixer-ammonia-injection.pdf?epslanguage=en-GB

(39) ZANDARYAA, Sarantuyaa, GAVASCI, Renato, LOMBARDI, Francesco and FIORE, Antonella. Nitrogen oxides from waste incineration: control by selective non-catalytic reduction. *Chemosphere* [online]. 2001. Vol. 42, No. 5-7, p. 491-497. DOI 10.1016/S0045-6535(00)00221-6. [Accessed 26 April 2015]. Retrieved from: http://linkinghub.elsevier.com/retrieve/pii/S0045653500002216

(40) VON DER HEIDE, Bernd J. *SNCR Process for Coal fired Boilers: Experiences and Potential for the future* [online]. Essen: Meldhau & Steinfath Umwelttechnik GmbH, 2013. [Accessed 26 April 2015]. Retrieved from: http://pennwell.websds.net/2013/vienna/pge/papers/T4S6O4-paper.pdf

(41) ČEZ, a.s. Elektrárna Počerady. *cez.cz.* [online] 2015. [Accessed 5 April 2015]. Retrieved from: http://www.cez.cz/cs/vyroba-elektriny/uhelne-elektrarny/cr/ pocerady.html

(42) SÝKORA, J. and TYRPEKL, P. *Řešení regulace spalování na kotlích elektrárny Počerady* [Combustion regulation on boilers placed in Počerady power plant] [online]. [published in conference Kotle 2011]. allforpower.cz. 2011. [Accessed 26 April 2015]. Retrieved from: http://www.allforpower.cz/UserFiles/files/2011/Alstom_Kotle_2011_2.pdf

(43) von der Heide, Benrd. *Advanced SNCR technology for Power Plants* [Presented at POWER-GEN International Las Vegas, 13-15 December 2011]. Essen: Meldhau & Steinfath Umwelttechnik GmbH. 2011. 34 p.

(44) XUAN, Xiaoping, YUE, Changtao, LI, Shuyuan and YAO, Qiang. Selective catalytic reduction of NO by ammonia with fly ash catalyst. *Fuel*. 2003. Vol. 82, no. 5. p. 575-579. DOI 10.1016/s0016-2361(02)00321-6.

(45) Nalbandian, H. *Air pollution control technologies and their interactions.* London: IEA Clean Control Centre, CCC/111, 2004.

(46) CAMARILLO, Mary Kay, STRINGFELLOW, William T., HANLON, Jeremy S. and WATSON, Kyle A. Investigation of selective catalytic reduction for control of nitrogen oxides in full-scale dairy energy production. *Applied Energy* [online]. 2013. Vol. 106, p. 328-336. DOI 10.1016/j.apenergy.2013.01.066. [Accessed 22 April 2015]. Retrieved from: http://linkinghub.elsevier.com/retrieve/pii/S0306261913000779

(47) BARENDREGT, Simon, RISSEEUW, Iek and WATERREUS, Frank. *Applying ultra-low-NOx burners* [paper presented in ARTC in Kuala Lumpur] [online]. 2006, March. [Accessed 10 April 2015]. Retrieved from: http://www.johnzink.com/wp-content/uploads/ultra-low-nox-burners.pdf

(48) *DIRECTIVE 2001/80/EC OF THE EUROPEAN PARLIAMENT AND OF THE COUNCIL of 23 October 2001 on the limitation of emissions of certain pollutants into the air from large combustion plants [L 309].* 27. November 2001. p. 20.

(49) Grandjean, Alain. *Energy transition Series – A new Grail: the quest for an ideal energy mix* [online]. Paris Tech Review. June 29th, 2014. [Accessed 15 May 2015]. Retrieved from: http://www.paristechreview.com/2014/06/29/ideal-energy-mix/

LIST OF SYMBOLS AND ABBREVIATIONS

Symbols

A	%	ash content
A	m^2	area of heat transfer
a	m	length of the passage section
a	-	flue gas stream emissivity
$A_{1,2}$	m^2	mean value of the zone cross-section
A_{fg}	m^2	flow area of gases
a_{fl}	-	flame emissivity
A_{flow}	m^2	cross section area of flow passage
a_{fu}	-	overall emissivity of furnace
A_{in}	m^2	cross-section of the zone inlet
A_{out}	m^2	cross-section of the zone outlet
a_w	-	emissivity of the walls
A_{zone}	m^2	zone side walls surface area
B	$kg \cdot s^{-1}$	amount of fuel burned in boiler
b	m	width of the passage section
B_{fed}	$kg \cdot s^{-1}$	amount of fuel fed into boiler
B_0	-	Boltzmann number
C	%	carbon content
c	$kJ \cdot m^{-3} \cdot K^{-1}$	specific heat capacity of wet air
c	m	depth of the platen
c_1	-	coefficient determined by the type of fuel
c_1	$kJ \cdot m^{-3} \cdot K^{-1}$	flue gas specific heat for temperature t_1
c_2	-	coefficient determined by the firing method
c_2	$kJ \cdot m^{-3} \cdot K^{-1}$	flue gas specific heat for temperature t_2
C_{ba}	%	carbon content in bottom ash
c_{ba}	$kJ \cdot kg^{-1} \cdot K^{-1}$	specific heat of slag
C_{fa}	%	carbon content in fly ash
c_{fa}	$kJ \cdot kg^{-1} \cdot K^{-1}$	specific heat of fly ash
c_{H2O}	$kJ \cdot m^{-3} \cdot K^{-1}$	specific heat capacity of water/steam
C_l	-	correction factor of tube length
$CO_{2_{max}}$	%	maximal amount of CO_2 in flue gas
c_{pf}	$kJ \cdot kg^{-1} \cdot K^{-1}$	specific heat of fuel, as receives basis
c_{pf}^{g}	$kJ \cdot kg^{-1} \cdot K^{-1}$	specific heat, as dry basis
c_s	$kJ \cdot m^{-3} \cdot K^{-1}$	specific heat capacity of dry air
C_s	-	correction factor of the geometric arrangement of the tube bank
C_t	-	correction factor for the temperature difference between the medium and the wall
$(c \cdot t)_{air}$	$kg \cdot kgf^{-1}$	enthalpy of vet air per standard cubic meter at temperature t [°C]
c_w	$kJ \cdot kg^{-1} \cdot K^{-1}$	specific heat of water

C_z	-	correction factor for the tube row number n_p along the direction of gas flow
d	g·kg^{-1}	amount of water in 1 kg of dry air
d	m	tube diameter
D	mm	outer diameter of water wall tubes
d_{eq}	m	equivalent diameter
d_h	μm	diameter of ash particles
D_{in}	M	inside diameter of tubes
D_{out}	M	outside diameter of tubes
D_{rh}	kg·s^{-1}	reheated steam flow rate
D_{SH2}	kg·s^{-1}	steam flow rate in SH2
D_{SH3}	kg·s^{-1}	steam flow rate in SH3
D_{sup}	kg·s^{-1}	superheated steam flow rate
e	mm	distance from refractory wall to the center of water wall tubes
f	-	coefficient f
F	m^2	furnace overall wall surface
F_i	m^2	surface area
G_{air}	kg·kgf^{-1}	mass of humid air with excess of β''_{ah}
$G_{air_{min}}$	kg·kgf^{-1}	minimal mass of humid combustion air for 1 kg of burned fuel
$G^{d}{}_{air_{min}}$	kg·kgf^{-1}	minimal mass of dry combustion air for 1 kg of burned fuel
G_{fg}	kg·kgf^{-1}	mass of the humid flue gas for using of humid air with excess of α_{fu}
G_{fg}^{ash}	kg·kgf^{-1}	mass of the humid flue gas for using of humid air with excess of α_{fu} for exact amount of ash in fuel
$G_{O_{2_{min}}}$	kg·kgf^{-1}	minimal mass of combustion oxygen
h	m	mean platen height
H	%	hydrogen content
H_{air}	kJ·kg^{-1}	enthalpy of cold air with excess-air coefficient after the furnace
$H_{air_{min}}$	kJ·kgf^{-1}	theoretical cold air enthalpy entering boiler
h_{Ar}	kJ·m^{-3}	enthalpy of Ar
H_{ca}	kJ·kg^{-1}	enthalpy of theoretical cold air
h_{CO_2}	kJ·m^{-3}	enthalpy of CO_2
H_f	kJ·kg^{-1}	sensible heat of fuel
h_{fa}	kJ·m^{-3}	enthalpy of fly ash
H_{fa}	kJ·kgf^{-1}	enthalpy of fly ash
H_{fg}	kJ·kg^{-1}	flue gas enthalpy at the furnace exit
$H_{fg_{in}}$	kJ·kg^{-1}	flue gas enthalpy at the platen superheater area entrance
$H_{fg_{\min}}$	kJ·kgf^{-1}	enthalpy of flue gas for $\alpha = 1$
$H_{fg_{out}}$	kJ·kg^{-1}	flue gas enthalpy at the platen superheater area exit
h_{fu}	mm	height of the burner axis above the bottom of the furnace
H_{fw}	kJ·kg^{-1}	enthalpy of feed water

h_{H_2O}	kJ·m^{-3}	enthalpy of H_2O
H_{ha}	kJ·kg^{-1}	enthalpy of preheated air
h_{N_2}	kJ·m^{-3}	enthalpy of N_2
H_{ou}	kJ·kg^{-1}	enthalpy of flue gas leaving the furnace
h_r	mm	relative position of the highest temperature zone in the furnace
H'_{rh}	kJ·kg^{-1}	enthalpy of steam at reheater inlet
H''_{rh}	kJ·kg^{-1}	enthalpy of steam at reheater outlet
$h_{SH2_{in}}$	kJ·kg^{-1}	enthaply of steam at SH2 inlet
$h_{SH2_{out}}$	kJ·kg^{-1}	enthaply of steam at SH2 outlet
$h_{SH3_{in}}$	kJ·kg^{-1}	enthaply of steam at SH3 inlet
$h_{SH3_{out}}$	kJ·kg^{-1}	enthaply of steam at SH3 outlet
h_{SO_2}	kJ·m^{-3}	enthalpy of SO_2
H''_{sup}	kJ·kg^{-1}	enthalpy of superheated steam
k	m^{-1}·MPa^{-1}	coefficient of radiation absorption
k_{add}	W·m^{-2}·K^{-1}	overall heat transfer coefficient of additional surfaces
k_h	m^{-1}·MPa^{-1}	coefficient of radiant absorption owing to ash particles
k_{SH2}	W·m^{-2}·K^{-1}	overall heat transfer coefficient of SH2
k_{SH3}	W·m^{-2}·K^{-1}	overall heat transfer coefficient for SH3
k_y	m^{-1}·MPa^{-1}	coefficient of radiant absorption owing to triatomic gases
l_2^{σ}	°C	flue gas temperature at the zone with maximal heat release
M	-	temperature field coefficient
N	%	nitrogen content
n_p	-	number of platens
n_t	-	number of parallel tubes
O	%	oxygen content
P	MPa	pressure of gases in the furnace
Pr	-	Prandlt number
$p_{SH2_{in}}$	MPa	steam pressure at SH2 inlet
p_{SH2_m}	MPa	mean steam pressure in SH2
$p_{SH2_{out}}$	MPa	steam pressure at SH2 outlet
$p_{SH3_{in}}$	MPa	steam pressure at SH3 inlet
p_{SH3_m}	MPa	mean steam pressure in SH3
$p_{SH3_{out}}$	MPa	steam pressure at SH3 outlet
Q	kJ·kg^{-1}	available heat of fuel fired
Q_1	kJ·kgf^{-1}	heat absorbed by water and steam
q_1	%	heat absorbed by steam
Q_2	kJ·kgf^{-1}	heat loss through stack gas
q_2	%	heat loss through stack gas
Q_3	kJ·kgf^{-1}	heat loss by incomplete combustion
q_3	%	heat loss by incomplete combustion
Q_4	kJ·kgf^{-1}	heat loss owing to unburned carbon in refuse
q_4	%	heat loss owing to unburned carbon in refuse

Q_5	kJ·kgf^{-1}	heat loss owing to convection and radiation from the furnace exterior
q_5	%	heat loss owing to convection and radiation from the furnace exterior
Q_6	kJ·kgf^{-1}	heat loss through the sensible heat of ash and slag
q_6	%	heat loss through the sensible heat of ash and slag
Q_{ai}	kJ·kg^{-1}	heat brought into the furnace by preheated and cold leakage air
Q_{ba}	%	heat loss owing to bottom ash
Q_{cfa}	kJ·kg^{-1}	calorific value of refuse
Q_{ev}	kJ·kg^{-1}	heat transfer for evaporating part of the boiler in the platen superheater area
Q_{fa}	%	heat loss owing to fly ash
Q_{fu}	kJ·kg^{-1}	heat entering furnace through combustion and hot air
Q_i^{daf}	kJ·kg^{-1}	heating value of volatiles
Q_i^r	kJ·kg^{-1}	lower heating value of fuel as received basis (LHV)
Q_{SH}	kJ·kg^{-1}	energy transferred to the heating surfaces in the platen superheater area by flue gas
Q_{SH2}	kJ·kg^{-1}	heat transfer for plate superheater SH2
Q_{SH3}	kJ·kg^{-1}	heat transfer for platen superheater SH3
Q_{SH}^{fg}	kJ·kg^{-1}	energy transferred from flue gas in the platen superheater area
Q_{SHr}	kJ·kg^{-1}	heat transfer for roof superheater
Q_{slag}	kJ·kg^{-1}	heat loss through the sensible heat of slag
r	-	total volume concentration of tri-atomic gases
r_{fg}	-	sum of volume fraction of tri-atomic gases
r_{H_2O}	-	volume concentration of H_2O in flue gas
r_{RO_2}	-	volume fraction of CO_2 and SO_2
S	%	sulfur content
s	mm	water wall tubes spacing
S	m	mean beam length of effective thickness of absorbing gas layer
s_1	m	platens spacing
s_2	m	spacing of tubes within the platen
S_{sulf}	%	sulfurous part of sulfur content
S_{vol}	%	volatile part of sulfur content
t	m	thickness of tubes
t	°C	temperature
T	K	temperature
T_1	K	flue gas temperature at the inlet of the zone
T_2	K	flue gas outlet temperature from the zone
t_2	°C	flue gas temperature at the outlet of the zones
T_2	K	flue gas temperature at the outlet of the zone
T_{as}	K	temperature of fouled surface
t_{ba}	°C	temperature of slag

t_{ev_m}	°C	mean steam temperature of evaporator part in the area of platen superheaters
t_f	°C	fuel temperature at burner or feeder exit
t_{fa}	°C	temperature of fly ash
$t_{fg_{in}}$	°C	flue gas temperature at the platen superheater inlet
t_{fg_m}	°C	mean flue gas temperature in platen superheater
$t_{fg_{out}}$	°C	flue gas temperature at the platen superheater outlet (guessed value)
T_{ou}	K	absolute boiler-outlet flue gas temperature
$t_{SH2_{in}}$	°C	steam temperature at SH2 inlet
t_{SH2_m}	°C	mean steam temperature in SH2
$t_{SH2_{out}}$	°C	steam temperature at SH2 outlet
$t_{SH3_{in}}$	°C	steam temperature at SH3 inlet
t_{SH3_m}	°C	mean steam temperature in SH3
$t_{SH3_{out}}$	°C	steam temperature at SH3 outlet
t_{SHr_m}	°C	mean steam temperature of roof superheater
T_{th}	K	theoretical (adiabatic) flame temperature – refers to Q_{fu}
V	%	content of volatiles
V	m^3	overall furnace volume
ν	$m^2 \cdot s^{-1}$	kinematic viscosity of flue gas at mean temperature of the flue gas
V_{air}	$m^3 \cdot kgf^{-1}$	real amount of air (with air excess)
$V_{air_{min}}$	$m^3 \cdot kgf^{-1}$	minimal volume of humid air required to burn 1 kg of fuel
$V^d_{air_{min}}$	$m^3 \cdot kgf^{-1}$	minimal volume of dry air required to burn 1 kg of fuel
V_{Ar}	$m^3 \cdot kgf^{-1}$	gas volume of Ar
V_{CO_2}	$m^3 \cdot kgf^{-1}$	gas volume of CO_2
$\overline{V \cdot C_p}$	$kJ \cdot kg^{-1} \cdot K^{-1}$	average specific heat of combustion products formed by 1 kg of fuel within the temperature interval T_{th}–T_{ou}
V_{fg}	$m^3 \cdot kgf^{-1}$	real amount of flue gas
$V_{fg_{\min}}$	$m^3 \cdot kgf^{-1}$	minimal volume of the humid flue gas
$V^d_{fg_{min}}$	$m^3 \cdot kgf^{-1}$	minimal volume of dry flue gas
$V^{d\_air}_{H_2O}$	-	volume of water vapor for 1 m^3 of dry air
V_{H_2O}	$m^3 \cdot kgf^{-1}$	real amount of water vapor
$V_{H_2O_{min}}$	$m^3 \cdot kgf^{-1}$	minimal volume of water vapor in flue gas
V_{N_2}	$m^3 \cdot kgf^{-1}$	gas volume of N_2
v_o	$m^3 \cdot kg^{-1}$	specific volume of steam
$V_{O_{2_{min}}}$	$m^3 \cdot kgf^{-1}$	minimal volume of oxygen required to burn 1 kg of fuel
V_{SO_2}	$m^3 \cdot kgf^{-1}$	gas volume of SO_2
W	%	water content
w	$m \cdot s^{-1}$	steam flow velocity
w_{fg}	$m \cdot s^{-1}$	flue gas flow velocity
W_t	%	total water content
W^r_t	%	total raw water content

x	-	number of tubes in one plate
X_{ba}	%	ash fraction in bottom ash
x_{fa}	%	fraction of total ash in the fly ash
X_{fa}	%	ash fraction in fly ash
x_i	-	angular coefficient of water wall tubes
x_p	-	angular coefficient of the platen
X_r	-	relative position of the highest temperature zone in the furnace
Z	-	total number of tubes in platen superheater area

Superscripts

d	dry
daf	dry ash-free
r	raw
vol	volatile part

Greek Symbols

α_1	$W \cdot m^{-2} \cdot K^{-1}$	gas side heat transfer coefficient
λ	$W \cdot m^{-1} \cdot K^{-1}$	thermal conductivity of flue gas at mean temperature of flue gas flow
λ	$W \cdot m^{-1} \cdot K^{-1}$	thermal conductivity at mean temperature of air flow
α_2	$W \cdot m^{-2} \cdot K^{-1}$	steam side heat transfer coefficient
μ	$g \cdot m^{-3}$	nondimensional mass concentration of fly ash
ξ_i	-	fouling factor for water wall tubes
ρ_{air}	$kg \cdot m^{-3}$	density of air
ρ_{H2O}	$kg \cdot m^{-3}$	density of water
σ	$kW \cdot m^{-2} \cdot K^{-4}$	Stefan-Boltzmann constant
σ_1	-	transverse pitch
σ_2	-	longitudinal pitch
α_{co}	$W \cdot m^{-2} \cdot K^{-1}$	convective heat transfer coefficient
α_{fu}	-	excess-air coefficient at the furnace exit
α_{LUVO}	-	excess-air coefficient downstream LUVO
α_{ra}	$W \cdot m^{-2} \cdot K^{-1}$	radiative heat transfer coefficient
β	-	coefficient of heat release
φ	-	relative humidity of air
φ	-	coefficient of reheat retention
$\bar{\psi}$	-	thermal efficiency factor
ψ_1	-	thermal efficiency factor for inlet cross-section of the zone
ψ_2	-	thermal efficiency factor for outlet cross-section of the zone
ω	-	correction coefficient for cross-flow over platen superheater
β'_{ah}	-	excess-air coefficient at air heater inlet
β''_{ah}	-	excess-air coefficient at air heater outlet
$\Delta\alpha \cdot H_e$	$kJ \cdot kg^{-1}$	heat carried by leakage air into the boiler

$\Delta\alpha_{fu}$	-	combustion chamber false air ratio
$\Delta\alpha_{\mathrm{inf}}$	-	amount of infiltrated air
$\Delta\alpha_{pul}$	-	leakage air coefficient of the pulverization system
$\Delta\beta$	%	amount of fuel burned in the zone
Δt	°C	average temperature difference between flue gas and steam
ΔX	-	correction factor
ε	$m^2 \cdot K \cdot W^{-1}$	ash deposit coefficient
η_{bo}	%	boiler thermal efficiency
θ_{ou}	-	relative flue gas temperature

Abbreviations

AGAM	Acoustic Gas temperatures Measurement system
BAT	Best Available Technology
BMCR	Boiler Maximum Continuous Rating
CFD	Computer Fluid Dynamic
DC	Design Coal
deNO$_x$	Denitrification
EGR	Exhaust Gas Recirculation
EP	Electrostatic Precipitator
EU	European Union
GFCP	Gas-Fired Coal Preheating
ID	Induced Draft
IEA	International Energy Agency
LEA	Low Excess Air firing
LLC	Lower Limit Coal
LUVO	Luftvorwärmer
M&M	Mixing and Metering module
NO$_x$	Nitrogen oxides
OFA	Over-Fire Air
PM	Particulate Matter
SCR	Selective Catalytic Reduction
SH	Superheater
SNCR	Selective Non-Catalytic Reduction
ULC	Upper Limit Coal
VOC	Volatile Organic Compounds

LIST OF APPENDICES

APPENDICES

Appendix A: Detailed data for the thermal calculation of the furnace

Boiler design data:

1. Rated boiler parameters:

Steam output:	640 $t \cdot h^{-1}$
Steam outlet pressure:	17.5 MPa
Steam outlet temperature:	540°C
Feed-water temperature:	252°C
Operation range:	60-100% BMCR
Reheated steam output:	564 $t \cdot h^{-1}$
Steam outlet pressure:	3.7 MPa
Steam inlet pressure:	4.02 MPa
Steam outlet temperature:	550°C
Steam inlet temperature:	346°C

2. Fuel range:

Lower Heating Value:	10.5-12.7 $MJ \cdot kg^{-1}$
Water (raw):	25-32%
Ash (dry):	35-45%
Sulfur (raw):	0.8-1.8%
Volatiles (dry ash-free):	55%

Parameter	Symbol	Unit	Design Coal
Lower heating value	Q_i^r	$MJ \cdot kg^{-1}$	11.4
Water	W_r	%	28.2
Ash	A^r	%	28
Sulfur	S^r	%	0.79
Carbon	C^r	%	29.43
Hydrogen	H^r	%	2.63
Nitrogen	N^r	%	0.48
Oxygen	O^r	%	10.47
Volatiles	V^{daf}	%	55

3. Boiler parameters according to ALSTOM thermal calculation and baseline test measurement:

Parameter	Unit	Rated output		Minimal output	
		Fuel			
		ULC	LLC	ULC	LLC
Hot air temperature downstream LUVO	°C	264	268	271	272
False air temperature	°C	25	25	25	25
Combustion chamber false air ratio	-	0.15	0.15	0.15	0.15
Mills false air ratio	-	0.2	0.2	0.3	0.3
Air-excess coefficient at combustion chamber outlet	-	1.15	1.15	1.25	1.25
Water temperature upstream economizer	°C	240	240	220	220
Water temperature downstream economizer	°C	322	326	326	328
Water pressure upstream economizer	MPa	21.89	21.89	19.59	19.59
Flue gas temperature upstream economizer	°C	484	485	489	482
Air-excess coefficient upstream economizer	-	1.331	1.327	1.216	1.213
Economizer effectivity coefficient	-	0.627	0.627	0.604	0.604
Steam temperature upstream SH3	°C	401.6	401.8	415	415.1
Steam temperature downstream SH3	°C	455	455	455	455
Steam pressure upstream SH3	MPa	19.35	19.31	18.28	18.26
Steam pressure downstream SH3	MPa	19.23	19.20	18.22	18.21
Steam flow upstream SH3	$kg \cdot s^{-1}$	154.56	150.12	102.73	99.98
Steam temperature upstream SH4	°C	405.5	405.3	415.6	414.5
Steam temperature downstream SH4	°C	480	480	480	480
Steam pressure upstream SH4	MPa	18.58	18.57	17.94	17.93
Steam pressure downstream SH4	MPa	18.35	18.35	17.83	17.83
Steam flow upstream SH4	$t \cdot h^{-1}$	160.76	158.52	104.41	103.58
Air-excess coefficient downstream LUVO	-	1.348	1.339	1.543	1.529
Flue gas temperature downstream the boiler	°C	168.2	174.0	187.7	190.1

Appendix B: Boiler scheme with SNCR injecting levels lay-out

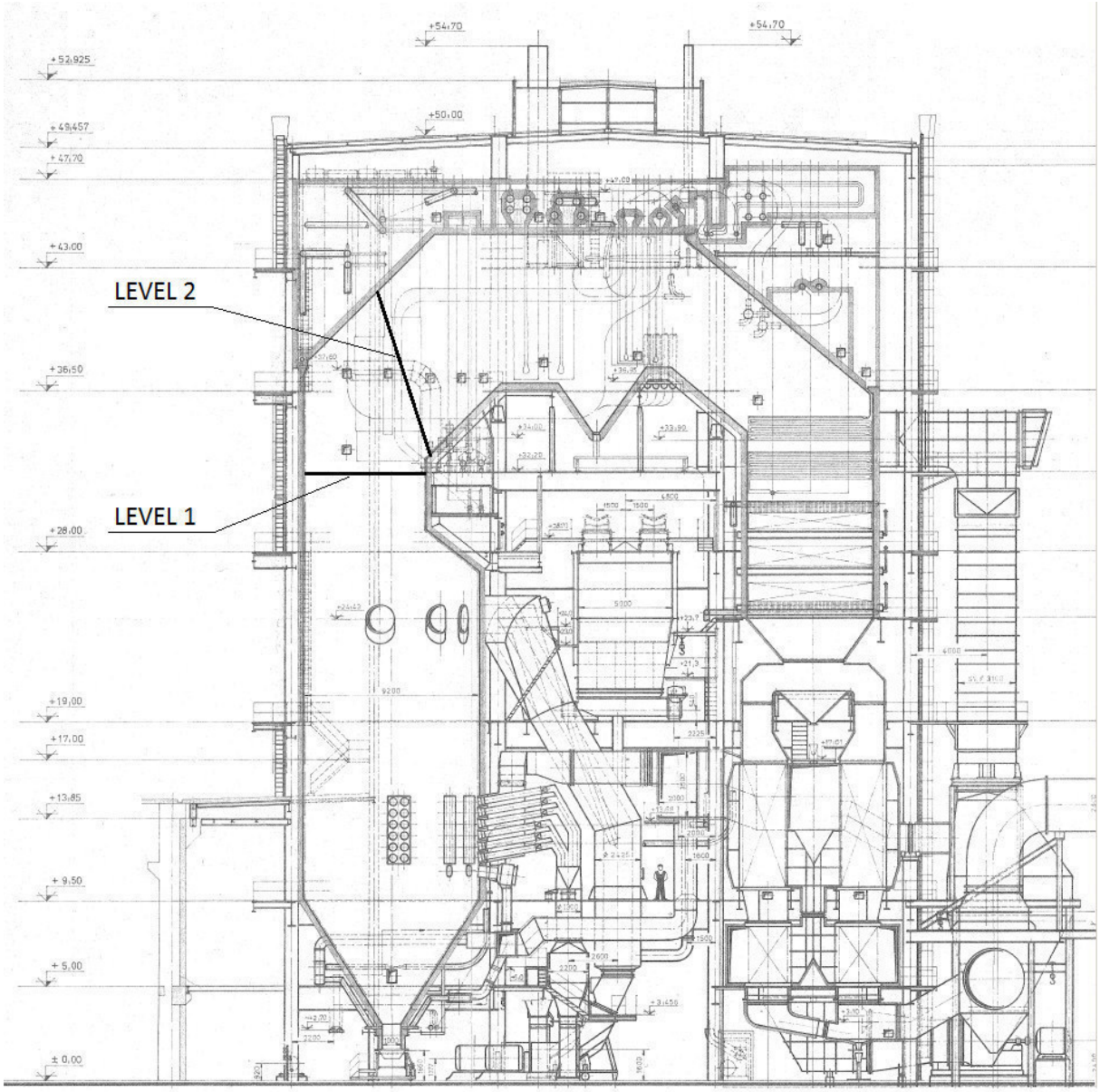

Figure I: Scheme of the 640 t·h^{-1} coal-fired boiler in the Počerady power plant

Appendix C: Coal composition

Table I: Considered coal composition

				WORST		BEST	
			Design Coal	**max A**	**max W (LLC)**	**min A**	**min W (ULC)**
Raw							
Water	W_r	%	28.20	24.65	32.00	23.80	23.80
Ash	A^r	%	28.00	33.91	25.88	26.67	26.67
Sulfur	S^r	%	0.79	0.75	0.76	0.89	0.89
Carbon	C^r	%	29.43	27.85	28.30	33.28	33.28
Hydrogen	H^r	%	2.63	2.49	2.53	2.97	2.97
Nitrogen	N^r	%	0.48	0.45	0.46	0.54	0.54
Oxygen	O^r	%	10.47	9.91	10.07	11.84	11.84
Dry							
Water	W^d	%	0.00	0.00	0.00	0.00	0.00
Ash	A^d	%	39.00	45.00	38.06	35.00	35.00
Sulfur	S^d	%	1.10	0.99	1.12	1.17	1.17
Carbon	C^d	%	40.99	36.96	41.62	43.67	43.67
Hydrogen	H^d	%	3.66	3.30	3.72	3.90	3.90
Nitrogen	N^d	%	0.67	0.60	0.68	0.71	0.71
Oxygen	O^d	%	14.58	13.15	14.81	15.54	15.54
Dry ash-free							
Water	W^{daf}	%	0.00	0.00	0.00	0.00	0.00
Ash	A^{daf}	%	0.00	0.00	0.00	0.00	0.00
Sulfur	S^{daf}	%	1.80	1.80	1.80	1.80	1.80
Carbon	C^{daf}	%	67.19	67.19	67.19	67.19	67.19
Hydrogen	H^{daf}	%	6.00	6.00	6.00	6.00	6.00
Nitrogen	N^{daf}	%	1.10	1.10	1.10	1.10	1.10
Oxygen	O^{daf}	%	23.90	23.90	23.90	23.90	23.90
Lover heating value	Q_i^r	kJ/kg	11044.43	10500.00	10500.13	12687.46	12687.46

Appendix D: Results from the stoichiometry calculation for LLC

Table II - Flue gas and air enthalpies in dependence on temperature for LLC

$t\ [°C]$	$H_{fg_{min}}\ [\mathrm{kJ \cdot kg^{-1}}]$	$H_{air_{min}}\ [\mathrm{kJ \cdot kg^{-1}}]$	$H_{fa}\ [\mathrm{kJ \cdot kg^{-1}}]$	$H_{fg}\ [\mathrm{kJ \cdot kg^{-1}}]\ \alpha_{fu} = 1.15$
100	498	385	18	574
200	1 008	775	38	1 162
300	1 535	1 171	58	1 769
400	2 077	1 576	80	2 393
500	2 634	1 990	102	3 035
600	3 206	2 413	124	3 692
700	3 792	2 845	147	4 365
800	4 390	3 285	170	5 053
900	5 001	3 732	194	5 755
1000	5 625	4 185	218	6 471
1500	8 854	6 517	383	10 214
1600	9 523	6 993	417	10 989
1800	10 880	7 953	487	12 559
2000	12 254	8 925	559	14 152

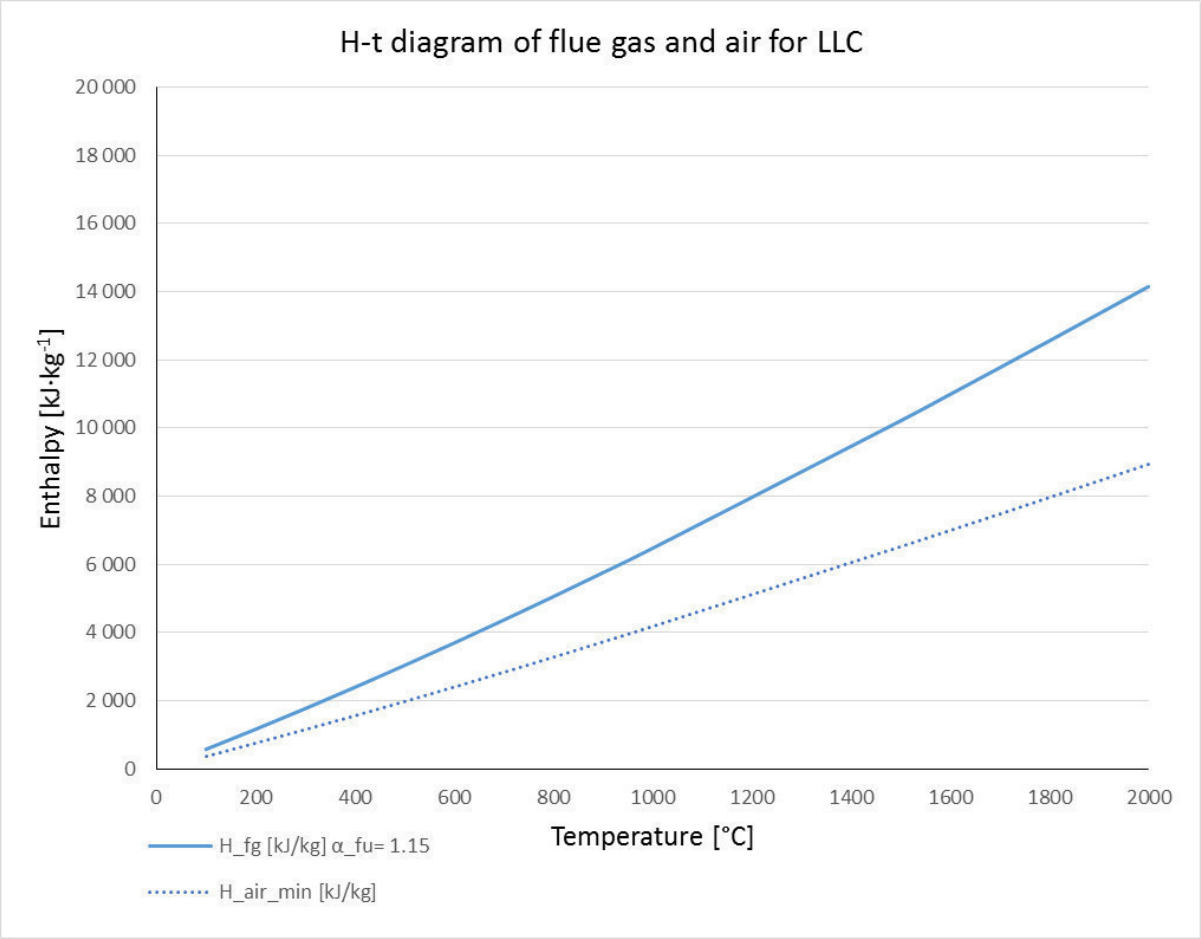

Figure II - H-t diagram of flue gas and air for ULC